Aus dem Institut für Herz- und Kreislaufphysiologie
(Prof. Dr. med. D. M. Katschinski)
im Zentrum Physiologie und Pathophysiologie
der Medizinischen Fakultät der Universität Göttingen

Hypoxia stimulates retrograde membrane trafficking to the *trans*-Golgi network via recruitment of T-plastin

INAUGURAL-DISSERTATION

zur Erlangung des Doktorgrades
der Medizinischen Fakultät der
Georg-August-Universität zu Göttingen

vorgelegt von

Stephanie Naas

aus

Hachenburg

Göttingen 2018

Dekan:	Prof. Dr. rer. nat. H. K. Kroemer
Referent/in	Prof. Dr. med. D. M. Katschinski
Ko-Referent/in:	Prof. Dr. rer. nat. P. Schu

Datum der mündlichen Prüfung: 25. Oktober 2018

Hiermit erkläre ich, die Dissertation mit dem Titel "Hypoxia stimulates retrograde membrane trafficking to the *trans*-Golgi network via recruitment of T-plastin" eigenständig angefertigt und keine anderen als die von mir angegebenen Quellen und Hilfsmittel verwendet zu haben.

Göttingen, den 23.10.2018

Publication

Data of this thesis have been published in the following article:

Wottawa M*, Naas S*, Bottger J, van Belle GJ, Mobius W, Revelo NH, Heidenreich D, von Ahlen M, Zieseniss A, Krohnert K, et al. (2017): Hypoxia-stimulated membrane trafficking requires T-plastin. Acta Physiol (Oxf) 221, 59-73

*Both authors contributed equally.

Table of Contents

List of Figures

List of Tables

List of Abbreviations

AEC	alveolar epithelial cell
AP2	adaptor protein 2
ARNT	aryl hydrocarbon receptor nuclear translocator
bHLH	basic helix-loop-helix
BSA	bovine serum albumin
cAMP	cyclic adenosine 3',5'monophosphate
cDNA	complementary DNA
CEB	CREB-binding protein
CLIC	clathrin-independent carriers
CME	clathrin-mediated endocytosis
CREB	cAMP response element-binding protein
C-TAD	*C-terminus* transactivation domain
DABCO	1,4-diazabicyclo-[2.2.2]-octane
DAPI	4',6-diamidino-2-phenylindole
DMEM	Dulbecco's Modified Eagle Medium
DMOG	dimethyloxalylglycine
EEA1	early endosome antigen 1
ECL	enhanced chemiluminescence
EDTA	ethylenediaminetetraacetic acid
EGF	epidermal growth factor
EGLN	egg-laying defective nine homolog
Endo	endocytosis
eNOS	endothelial nitric oxide synthase
ER	endoplasmic reticulum
et al.	*et alii*
Exo	exocytosis
FACS	fluorescence activated cell sorting
F-actin	filamentous actin
FCS	fetal calf serum
FIH	factor inhibiting HIF
FM	N-(3-triethylammoniumpropyl)-4-(4-(dibutylamino) styryl) pyridinium dibromide
G-actin	globular actin
GEEC	GPI-anchored proteins enriched early endosomal compartments
GPI	glycosylphosphatidylinositol
GM130	Golgi matrix protein of 130 kDa
GTPase	guanosine triphosphatase
HIF	hypoxia-inducible factor

HIFα	hypoxia-inducible factor α-subunit
HIFβ	hypoxia-inducible factor β-subunit
HRE	hypoxia-responsive element
HRP	horeseradish peroxidase
hrs	hours
mCLING	membrane-binding fluorophore-cysteine-lysine-palmitoyl group
MEF	mouse embryonal fibroblasts
MHC	major histocompatibility complex
N-TAD	*N-terminus* transactivation domain
ODD	oxygen-dependent degradation
PAS	Per-ARNT-Sim
PBS	phosphate-buffered saline
PCR	polymerase chain reaction
Pen/Strep	penicillin/streptomycin
PFA	paraformaldehyde
PHD	prolyl 4-hydroxylase
pVHL	von Hippel-Lindau tumor suppressor protein
qRT PCR	quantitative real-time polymerase chain reaction
Reox	reoxygenation
RT	room temperature
SDS	sodium dodecylsulfate
SDS-PAGE	sodium dodecylsulfate polyacrylamide gel electrophoresis
SEM	standard error
sh	small hairpin
TGN	*trans*-Golgi network
TGN38	*trans*-Golgi network protein 38
Trf	transferrin
WGA	wheat germ agglutinin

1 Introduction

1.1 Hypoxia

Oxygen is essential for the physiological cellular function of most complex organisms since it operates as an electron acceptor in mitochondria to yield adenosine triphosphate through aerobic metabolism. In the human body, oxygen is absorbed in the lungs, distributed throughout the body via the blood flow through the cardiovascular system and ultimately delivered to the oxygen-consuming cells via diffusion. The state of adequate oxygen supply of cells in the body is termed tissue normoxia whereas the state of lower oxygen availability, in which the oxygen demand of the respective tissue is not met, is called hypoxia. Normoxia in the ambient air is defined as the oxygen partial pressure (pO_2) that is measured at sea level and amounts to 20.9% O_2, hence 159 mmHg or 21.2 kPa. Within the body, the values of the pO_2, and thus the limits of tissue normoxia, are considerably lower and vary significantly between different organs, e.g. ranging between a pO_2 of 100 mmHg in the arterial blood to a pO_2 of approximately 30 mmHg in the muscle (Carreau et al. 2011).

Hypoxia is an important physiological stimulus. *In vivo*, hypoxic microenvironments affect cellular survival, proliferation and differentiation in all states of development from the embryo to the adult organism (Covello et al. 2006; Iyer et al. 1998; Simon and Keith 2008). The availability of oxygen in the body can change very rapidly. Thus, the organism necessitates effective adaptation mechanisms to react to oxygen deprivation. Hypoxia induces systemic as well as cellular responses at the molecular level. These range from short-term adaptation mechanisms, such as the increase of the respiratory rate and the switch to anaerobic metabolism, to long-ranging alterations, e.g. the induction of erythropoiesis and angiogenesis (Pugh and Ratcliffe 2003; Semenza and Wang 1992; Stockmann and Fandrey 2006).

However, the imbalance between oxygen availability and demand also plays a pivotal role in the pathogenesis of numerous diseases like myocardial infarction, stroke, inflammation and tissue repair as well as cancer and tumor growth (Eltzschig and Carmeliet 2011; Harris 2002; Ratcliffe 2013; Semenza 2011). Thus, a deeper understanding of the oxygen-sensing mechanisms and hypoxia signaling pathways are highly relevant for defining novel potential therapeutic targets to treat hypoxia-associated diseases.

1.2 Oxygen sensing via the hypoxia-inducible factor pathway

The hypoxia-inducible factors (HIFs) are the master regulators of oxygen-dependent gene expression of basically all animal cells (Bishop and Ratcliffe 2014). The transcription

factors HIFs are inactive in normoxic conditions but activated upon exposure to hypoxia. In a hypoxic environment, HIF transcriptionally regulates the expression of various target genes involved in the anaerobic metabolism, oxygen transport, angiogenesis, cellular survival and proliferation in order to increase oxygen delivery and reduce oxygen consumption (Bishop and Ratcliffe 2014; Schofield and Ratcliffe 2004).

1.2.1 The structure of HIF

HIF transcription factors are heterodimers that consist of an oxygen-regulated α-subunit (HIFα) and a constitutively expressed β-subunit (HIFβ), which is also termed aryl hydrocarbon receptor nuclear translocator (ARNT) (Schofield and Ratcliffe 2004). Three isoforms of HIFα (HIF-1α, HIF-2α and HIF-3α) are known in mammalian cells. HIF-1α and HIF-2α display similarities in their structure, but demonstrate significant differences concerning their expression patterns and target genes. Whereas HIF-1α is expressed ubiquitously in all nucleated cells, HIF-2α expression is restricted to certain cell types present in tissues which contribute to the systemic delivery of O_2, e.g. the lung, the heart, and the endothelium (Patel and Simon 2008; Semenza 2011). Furthermore, HIF-1α is predominantly stabilized in the early phase of hypoxia, whereas HIF-2α seems to be involved in the adaptation to prolonged hypoxic states (Koh et al. 2011). HIF-3α exhibits various alternately spliced forms and variants with different or even opposite regulatory functions that seem to inhibit HIF-1α- and HIF-2α-induced effects (Duan 2016).

HIF-1α and HIF-1β are both composed of a basic helix-loop-helix (bHLH) protein sequence that allows binding of specific DNA motifs in hypoxia-responsive elements (HREs) and a Per-ARNT-Sim (PAS) domain that facilitates dimerization of the subunits (Wang et al. 1995) (Figure 1). The HIF-1α subunit contains an oxygen-dependent degradation domain (ODD) with two conserved prolines (Pro402 and Pro564) acting as binding sites for the von Hippel-Lindau tumor suppressor protein (pVHL) upon hydroxylation by prolyl 4-hydroxylase domain enzymes (PHD) (Huang et al. 1998; Ivan et al. 2001; Jaakkola et al. 2001). Furthermore, the subunit includes two transactivation domains (TAD) located at the *N-terminus* (N-TAD) and the *C-terminus* (C-TAD). The C-TAD domain encloses the conserved asparagine residue 803 (Asn803) that can activate transcription upon binding with coactivators like CREB-binding protein (CBP)/p300 (Jiang et al. 1996; Kallio et al. 1998; Pugh et al. 1997). Hydroxylation of the asparagine residue by factor inhibiting HIF (FIH) regulates transcriptional activity by preventing association with the aforementioned coactivators (Lando et al. 2002; Mahon et al. 2001).

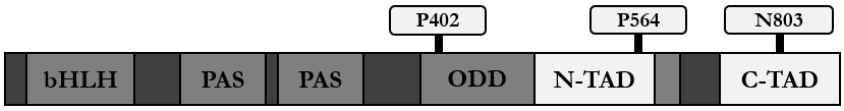

Figure 1: Protein structure of the human hypoxia-inducible factor-1α. Hypoxia-inducible factor-1α (HIF-1α) possesses a basic helix-loop-helix (bHLH) and a Per-ARNT-SIM (PAS) domain which impart DNA-binding and dimerization with HIF-1β. Two transactivation domains (TAD) are present in HIF-1α: The N-TAD is integrated in the oxygen-dependent degradation (ODD) domain, whereas the C-TAD is located at the C-terminal end. The ODD contains two conserved prolines (P402 and P564), which can be hydroxylated by prolyl 4-hydroxylase domain enzymes. The C-TAD includes an asparagine residue (N803) which can be modified by factor inhibiting HIF-1.

1.2.2 The regulation of the HIF pathway

The HIF signal transduction pathway is rigidly regulated through post-translational modification (Figure 2). In hypoxic conditions, HIF-1α translocates from the cytoplasm into the nucleus and heterodimerizes with HIF-1β (Chilov et al. 1999). The resulting complex binds at specific HREs to DNA, recruits the CBP/p300 coactivator protein and is subsequently capable to induce the expression of target genes (Arany et al. 1996; Kallio et al. 1998).

In well-oxygenated conditions, the PHDs 1, 2 and 3 hydroxylate the proline residues Pro402 and Pro564 of the ODD (Bruick and McKnight 2001; Huang et al. 1998; Ivan et al. 2001; Jaakkola et al. 2001; Yu et al. 2001). The hydroxylated proline residues function as recognition elements and binding sites for pVHL, a ubiquitin E3 ligase (Maxwell et al. 1999; Yu et al. 2001). The ubiquitin E3 ligase complex marks HIF-1α by polyubiquitination for proteasomal degradation (Salceda and Caro 1997). This degradation pathway is tightly and rapidly controlled. Reoxygenation after hypoxic incubation leads to a depletion of HIF within minutes (Jewell et al. 2001).

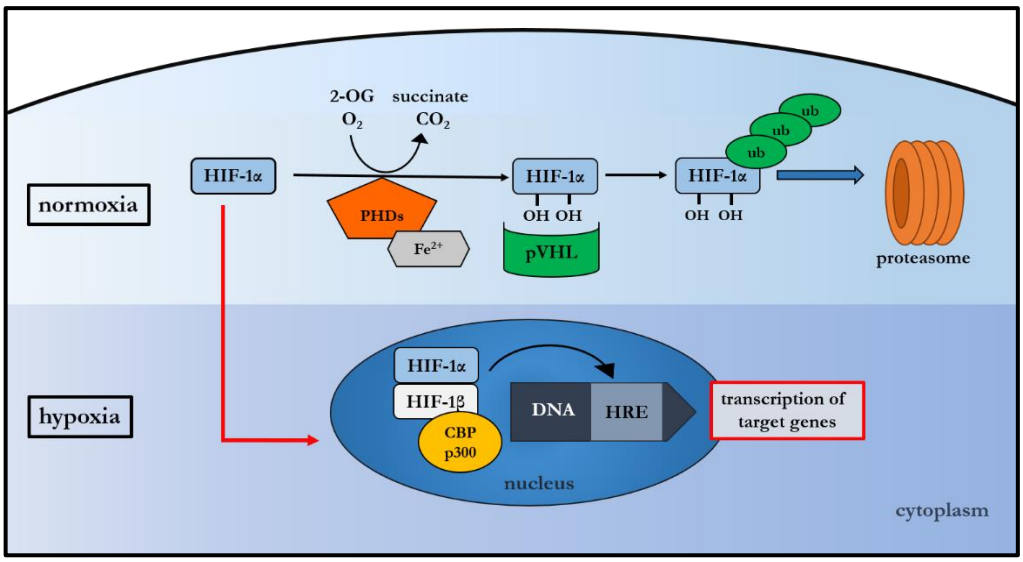

Figure 2: Overview of the regulation of the HIF-1α protein levels. In normoxia hypoxia-inducible factor 1α (HIF-1α) is located in the cytoplasm and hydroxylated by prolyl 4-hydroxylase domain enzymes (PHDs). PHDs require Fe^{2+}, oxygen and 2-oxoglutarate (2-OG) for adequate enzymatic activity. The hydroxylation causes polyubiquitination (ub) of HIF-1α by the von Hippel-Lindau tumor suppressor protein (pVHL) and subsequent proteasomal degradation. In hypoxia, HIF-1α is stabilized and translocated into the nucleus to dimerize with hypoxia-inducible factor-1β (HIF-1β). After recruitment of the coactivator protein CBP/300, the complex binds to hypoxia-responsive elements (HREs) and the transcription of target genes is induced.

Apart from being regulated via HIF-1α stability, the expression of HIF target genes is controlled by direct modulation of the transcriptional activity. In normoxic conditions, FIH-1 hydroxylates the Asn803 within the C-TAD of HIF-1α. This hydroxylation causes a conformational alteration of the protein that inhibits the recruitment of the coactivators p300 and CBP, thereby preventing the transcription of the HIF target genes (Lando et al. 2002; Mahon et al. 2001). Further fine-tuning of HIF-activation seems to be mediated by interaction with heat shock protein 90, acetylation and sumoylation (Kaelin and Ratcliffe 2008).

1.2.3 Prolyl 4-hydroxylase domain enzymes

PHDs act as cellular oxygen sensors in metazoan cells. They belong to the iron-dependent dioxygenases superfamily and require oxygen and 2-oxoglutarate as co-substrates for their enzymatic activity (Kaelin and Ratcliffe 2008). The K_m values of these enzymes are reported to be set slightly above the oxygen concentration in ambient air at sea level (Ehrismann et al. 2007; Hirsila et al. 2003). This property enables the enzymes to be modulated tightly according to the oxygen availability, thus, making them suitable oxygen sensors in the HIF pathway (Bruick and McKnight 2001; Epstein et al. 2001).

At least three different PHDs are known to be present in mammals: PHD1 (also termed egg-laying defective nine homolog (EGLN) 2), PHD2 (also called EGLN1) and PHD3 (also known as EGLN3) (Epstein et al. 2001). A fourth member of the PHD enzyme

family was discovered a few years ago, but the function of this transmembrane protein has not been completely characterized yet (Koivunen et al. 2007). All three isoforms named above are ubiquitously expressed, but their expression levels vary between different tissues (Appelhoff et al. 2004).

Whereas PHD2 is constitutively expressed at a high level in all tissues, PHD1 mRNA is mainly expressed in hormone responsive tissues and PHD3 mRNA can predominantly be found in skeletal and heart muscle cells (Lieb et al. 2002). PHD2 is the most abundant isoform and has been shown to be the critical isoform for setting low levels of HIF-1α in normoxia (Berra et al. 2003; Huang et al. 2002). The outstanding role of PHD2 in regulating HIF-1α levels was further emphasized by the finding that only PHD2 knockout murine embryos show a fatal dysregulation in their development leading to embryonic lethality, whereas PHD1 and PHD3 knockout mice are viable (Takeda et al. 2006).

In addition to the tissue specific expression pattern, the PHD isoforms also display a distinct intracellular distribution: PHD1 prevails in the nucleus, PHD2 is mainly localized in the cytoplasm and PHD3 is present both in the cytoplasm and the nucleus (Metzen et al. 2003).

1.2.3.1 The PHD hydroxylation reaction

PHD enzymes catalyze the hydroxylation of Pro564 and Pro402 within the HIF-1α subunit by metabolizing molecular oxygen. One oxygen atom is incorporated into the HIF molecule to form hydroxyproline. The second oxygen atom is utilized for the coupled oxidative decarboxylation of 2-oxoglutarate to succinate and CO_2 (Berra et al. 2006; Schofield and Ratcliffe 2004). Moreover, PHDs depend on non-heme bound Fe^{2+} for activation of O_2 and coordinated substrate binding. Ascorbate is needed as a co-factor in order to regenerate Fe^{3+} caused by uncoupled reactions (Bishop and Ratcliffe 2014). As a consequence, the activity of the PHDs can not only be regulated by the oxygen tension but also by the abundance of co-substrates and co-factors. Based on this finding, dimethyloxalylglycine (DMOG), which acts as a 2-oxoglutarate analogue, is widely used for inhibiting PHD function leading to an accumulation of stabilized HIF-1α in normoxia (Mole et al. 2003).

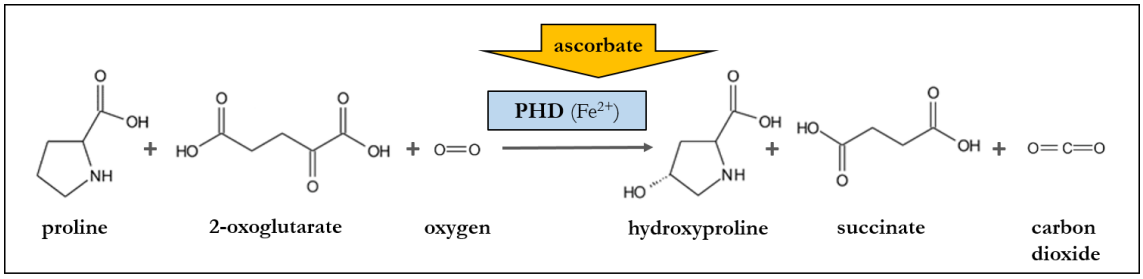

Figure 3: Hydroxylation reaction of the hypoxia-inducible factor-1α proline residues. Prolyl 4-hydroxylases (PHDs) utilize O_2 and 2-oxoglutarate as substrates to form succinate and CO_2 during the hydroxylation of HIF-1α. Fe^{2+} is required as a co-factor. Fe^{2+} is regenerated by reduction of Fe^{3+} through ascorbate.

1.3 Membrane trafficking

The term membrane trafficking comprises all processes of membrane flow between the cell surface and intracellular membrane-enclosed compartments. Thus, membrane trafficking modulates the membrane composition and mediates the distribution of cargo molecules to various destinations inside and outside the cell (Doherty and McMahon 2009). Communication with the extracellular environment occurs by the release of cargo molecules to the extracellular space, termed exocytosis, and through internalization of membrane-attached or membrane-enclosed cargo molecules by endocytosis. Given the fact, that the plasma membrane acts as an interface between the extra- and the intracellular space, membrane trafficking is essential for the general maintenance of cellular homeostasis. In addition, the exchange of plasma membrane between the cell surface and endosomal compartments facilitates specific cellular processes, e.g. the regulation of signal perception and transduction, cell adhesion and migration, thereby playing a critical role in human physiology (Lanzetti 2007; Miaczynska 2013). Notably, defects in vesicular trafficking are associated with a huge variety of malignant, neuronal and infectious diseases (Howell et al. 2006; Mosesson et al. 2008; Olkkonen and Ikonen 2006). Elucidation of the fundamental principles coordinating membrane trafficking will thus provide a greater understanding of relevant pathomechanisms.

1.3.1 Endocytosis

Endocytosis is defined as the constitutive or regulated invagination of the plasma membrane resulting in the formation of vesicles that are destined for internalization. Among others, this mechanism is utilized for, e.g. the acquisition of nutrients, antigen uptake, clearance of apoptotic cells, membrane recycling, protein trafficking and signal transduction, thereby representing an essential process in most eukaryotic cells (Di Fiore and von Zastrow 2014; Doherty and McMahon 2009; Grant and Donaldson 2009). Several modes of plasma-membrane deformation give rise to transport vesicles which subsequently undergo progressive changes in their vesicular identity through maturation of the vesicle

itself or through fusion with defined pre-existing membrane-enclosed organelles (Huotari and Helenius 2011; Scott et al. 2014).

1.3.1.1 Modes of endocytosis

Different modes of endocytosis are classified according to the components of the protein coat that is involved in the budding process of the nascent vesicle from the plasma membrane and the regulatory proteins that facilitate the endocytic events (Doherty and McMahon 2009). The most extensively studied endocytic mechanism is clathrin-mediated endocytosis (CME).

CME has been shown to be important for the selective internalization of receptor-bound ligands (e.g., epidermal growth factor (EGF) and transferrin (trf)), hence regulating essential signaling and biosynthetic pathways (Robinson 2015). Clathrin is composed of three heavy chains (approximate molecular weight 190 kDa) and three light chains (approximate molecular weight 29 kDa) that polymerize to form a triskelion. Several triskelion structures assemble to build a distinctive three-dimensional hexagonal lattice which allows for membrane bending and vesicle budding (Edeling et al. 2006; Pearse 1975; Robinson 2015; Ungewickell and Branton 1981). The adaptor protein 2 (AP2) acts as a cargo-recognition molecule and initiates coat assembly by linking clathrin to the membrane bilayer. Besides AP2, various other accessory adaptor, scaffolding and sorting proteins contribute to the specificity of the cargo uptake. Fission of the vesicle is accomplished by the catalytic guanosine triphosphatase (GTPase) dynamin. Once the vesicle is detached from the membrane, the clathrin coat can be released and the vesicle undergoes endosomal trafficking (Doherty and McMahon 2009).

Besides Clathrin-dependent endocytosis, Clathrin-independent mechanisms contribute to the overall cellular endocytic uptake (Doherty and McMahon 2009). Nevertheless, non-clathrin mechanisms were found to be less elucidated due to a lack of specific marker molecules. One well-investigated clathrin-independent mode of endocytosis is the uptake via caveolae.

Caveolae are specialized flask- or omega-shaped invaginations of the plasma membrane with a diameter of 50 – 80 nm (Palade 1953; Yamada 1955). The occurrence of caveolae is associated with sphingolipid-cholesterol microdomains, which display distinct areas of tightly packed and highly ordered lipids within the plasma membrane. Their morphology, as well as their function, is modulated by cavins (Parton and Simons 2007; Rothberg et al. 1992). The lipid rafts are stabilized by clusters of caveolin proteins. Caveolins are integral membrane proteins that can be classified into three different subtypes. Caveolin-1 and caveolin-3 mediate the invagination of the membrane bilayer and are indispensable for caveolae formation, whereas caveolin-2 is not required for this process (Thomas and Smart 2008). Although there is initial evidence that caveolin-2 may be involved in the regulation of endocytosis and cell differentiation, the function of this protein is still poorly

characterized (Liu et al. 2014; Shmuel et al. 2007). After caveolae invagination the fission process is mediated by dynamin recruitment and substantial rearrangement of the actin cytoskeleton is induced (Pelkmans et al. 2002). The extent to which the uptake via caveolae contributes to the total cellular endocytic capacity varies between different cell types and conditions (Chaudhary et al. 2014; Thomsen et al. 2002). Caveolae have been reported to be involved in the sequestration of multimerized glycosyl-phosphatidylinositol (GPI)-anchored proteins (Mayor et al. 1994). Interestingly, overexpression of caveolin-1 increases the abundance of caveolae and simultaneously inhibits clathrin-independent endocytosis suggesting a negative regulatory role for caveolins irrespective of their structural function in caveolae (Chaudhary et al. 2014).

Apart from the pathways described above, several other mechanistically distinct modes of clathrin- and caveolin-independent endocytosis have been unraveled. Ruffling of the membrane can lead to the formation of large, uncoated compartments for gross, non-selective fluid uptake called macropinocytosis. Macropinocytosis is an actin-mediated process, which is especially important for macrophages and dendritic cells (Lim and Gleeson 2011). Phagocytosis is another actin-dependent mechanism which is also mainly utilized by immune leukocytes including macrophages, monocytes, neutrophils and dendritic cells for the internalization of large solid particles (> 300 nm in diameter), such as cell debris and pathogens (Aderem and Underhill 1999). Fluid phase markers are additionally incorporated via an actin-dependent mechanism involving dorsal ruffles that also seem to play a role in the sequestration of receptor tyrosine kinases after ligand engagement (Buccione et al. 2004). Alternate modes of endocytosis include the protein Flotillin, which forms microdomains similar to caveolae and is involved in the uptake of GPI-anchored proteins, cholera toxin B subunit and several proteoglycan bound ligands to give just a few examples (Meister and Tikkanen 2014). GPI-linked proteins and fluid-phase markers are furthermore endocytosed via a pathway utilizing uncoated actin-dependent vesicles called CLIC (clathrin-independent carriers) and travel into a specialized early endosomal compartment named GEEC (GPI-anchored proteins enriched early endosomal compartments). This route is termed the CLIC/GEEC pathway (Mayor et al. 2014). Moreover, there are reports on regulating factors like RhoA controlling interleukin-2 receptor endocytosis and Arf6-dependent pathways being involved in major histocompatibility complex (MHC) internalization (Doherty and McMahon 2009). However, the concrete contributions of the aforementioned pathways to the overall endocytic capacity of the cell require further investigation. Furthermore, it is noteworthy that many cargos can be internalized through multiple mechanisms that may overlap, a fact that contributes to the complexity of endocytic concepts.

1.3.2 Endosomal sorting and trafficking

Upon endocytosis, transport vesicles merge into a common dynamic network of membrane-enclosed compartments and become subject to highly orchestrated sorting

events coordinating the intracellular distribution of the cargo molecules (Figure 4) (Mellman 1996). These compartments are termed endosomes and their identity can be classified according to their morphological characteristics, intraluminal pH, marker proteins such as Rab family GTPases, and specific membrane composition (Deneka and van der Sluijs 2002; Di Paolo and De Camilli 2006; Maxfield and McGraw 2004; Pfeffer 2001). Rab GTPases are essential for the regulation of membrane trafficking since they control vesicle formation and correct fusion through the recruitment of distinct effector proteins to specific compartments (Pfeffer 2013; Wandinger-Ness and Zerial 2014).

The endosomal sorting machinery of eukaryotic cells comprises a set of three functionally different but dynamic vesicular compartments: early endosomes, recycling endosomes and late endosomes. Regardless of the route of endocytosis, all material internalized by the cell is sent to the early endosome compartment that functions as the first sorting site for proteins and lipids (Scott et al. 2014). Fusion of the newly pinched off vesicles from the plasma membrane with the early endosomes is mediated by Rab5 and early endosome antigen 1 (EEA1) (Simonsen et al. 1998). Due to the acidic intraluminal milieu (pH approximately 6.0) of the early endosomes, most ligands are released from their receptors at this point (Maxfield and McGraw 2004; Scott et al. 2014). Early endosomes can be morphologically subdivided into two different portions: A tubular part processes the cargo destined for recycling to the plasma membrane and for retrograde transport to the *trans*-Golgi network, whereas a vesicular portion collects ligands and solutes that will undergo lysosomal degradation (Maxfield and McGraw 2004; Scott et al. 2014).

From the tubular portion of the early endosomes, cargo molecules can I) be directly transported back to the plasma membrane with a $t_{1/2}$ for lipids of approximately 2 minutes which is mediated by Rab4, II) undergo recycling via the recycling endosomes which is regulated by Rab11 ($t_{1/2}$ of trf receptors approximately 10 minutes) or III) may be passed on to the Golgi apparatus (Maxfield and McGraw 2004; van der Sluijs et al. 1992). This delivery of molecules to the *trans*-Golgi network is termed retrograde transport. Membrane recycling from the endocytic recycling compartments and the *trans*-Golgi network to the plasma membrane is also coordinated by Rab11 (Chen et al. 1998; Ren et al. 1998). In contrast, the vesicular portion of the early endosomes matures into late endosomes. This maturation includes the acquisition of acid hydrolases, changes in the membrane composition, alteration in effector proteins and movement from the peripheral cytoplasm to the perinuclear space along microtubules within approximately 8 - 15 minutes (Huotari and Helenius 2011; Maxfield and McGraw 2004).

The recycling endosomal compartment is a tubular network with a pH of 6.5 (Yamashiro et al. 1984). Cargo molecules can either passage through the recycling endosomes to be taken back to the membrane or transit to the *trans*-Golgi network for retrograde transport (Bonifacino and Rojas 2006).

The majority of the endocytosed cargo is recycled back to the cell surface with the result that the degradation route via late endosomes represents just a side pathway limited to highly selected cargo and membrane components (Huotari and Helenius 2011). Late endosomes are characterized by Rab7 and function as transport intermediates in the degradation pathway delivering cargo molecules to the lysosomes (Feng et al. 1995). For lysosomal degradation, proteins get tagged by a ubiquitin ligase and are sorted into the late endosome to form intraluminal vesicles within the late endosomes yielding multivesicular bodies (Piper and Katzmann 2007). The multivesicular bodies undergo a maturation process including a drop in luminal pH and acquisition of lysosomal components till they finally fuse with lysosomes (Huotari and Helenius 2011). Lysosomes are acidic (ph 4.0 – 5.0) and hydrolase-rich membrane-enclosed compartments responsible for protein degradation (Mindell 2012). In conclusion, this degradation pathway displays a regulatory mechanism to terminate signaling (Huotari and Helenius 2011).

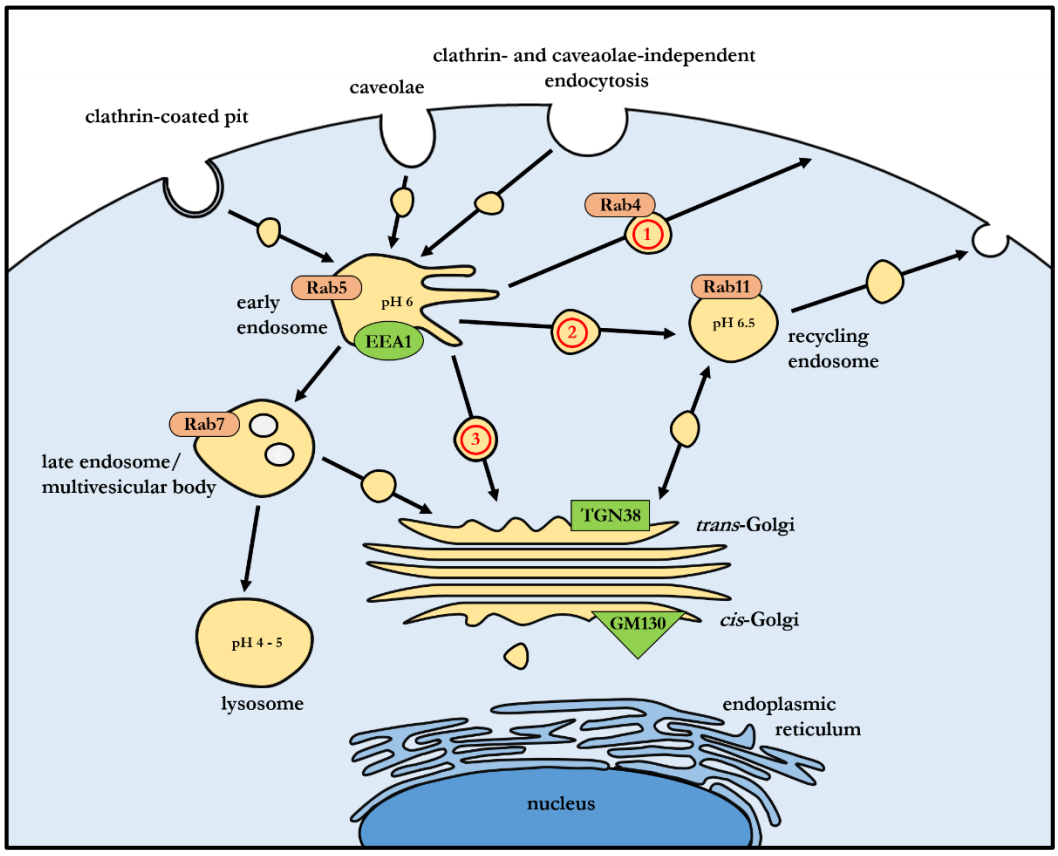

Figure 4: Endosomal sorting and trafficking. Internalized vesicles fuse irrespective of the underlying endocytic pathway with the early endosome compartment. From the tubular sorting part of the early endosomes cargo can be directly recycled back to the plasma membrane (1), transit to the recycling endosome (2) or undergo retrograde transport to the *trans*-Golgi network (3). The vesicular segment of the early endosome maturates into late endosomes. This portion contains cargo that is ultimately delivered to the lysosomes for degradation. Maturation of endosomes is associated with an increase in acidification. The identity of endosomal compartments is determined by specific marker proteins and Rab-GTPases.

1.3.2.1 Methods to analyze intracellular trafficking pathways

Marker proteins are utilized to study different pathways in the endosomal system: The endocytic route of the EGF receptor is the most common model to investigate the influence of endocytosis on signaling. Engagement of EGF to the receptor results in accelerated clathrin-dependent internalization of the complex und subsequent delivery via the degradative pathway to lysosomes resulting in an inactivation of the receptor (Sorkin and Goh 2009). Whereas the uptake of the EGF receptor is strictly regulated and exclusively occurs after ligand engagement, trf receptor internalization is ligand-independent and thus happens constitutively (Hopkins et al. 1985). Upon clathrin-mediated internalization of a ligand bound trf receptor, the complex is transported to the early endosomes where the iron dissociates from trf (Hopkins and Trowbridge 1983; van Renswoude et al. 1982). Unlike most other ligands, trf is not released from the receptor at this stage and the complete trf receptor-apotransferrin complex is recycled back directly and indirectly via recycling endosomes to the cell surface (Dautry-Varsat et al. 1983).

Not only protein cargos experience a highly regulated transport via the endosomal compartments, but also lipids follow a coordinated sorting and delivering system (Mukherjee et al. 1999). However, just a fractional part of the extensive network of interacting proteins and the complex series of membrane trafficking subprocesses has been unveiled so far (Scott et al. 2014).

1.3.3 Retrograde transport and the Golgi apparatus

Newly synthesized proteins destined for the secretory pathway are routed from the endoplasmic reticulum (ER) to the Golgi cisternae, afterwards to the *trans*-Golgi network (TGN) and subsequently undergo transport via secretory vesicles to the plasma membrane. This forward/anterograde pathway is counterbalanced by membrane retrieval via the backward/retrograde pathway to the TGN (Bonifacino and Rojas 2006). Both pathways meet at several points of which the Golgi apparatus is of particular interest (Griffiths and Simons 1986; Rodriguez-Boulan and Musch 2005; Rohn et al. 2000).

The Golgi apparatus consists of stapled cisternae, termed Golgi stack, in which newly synthesized lipids and proteins are modified. The complex receives proteins from the endoplasmic reticulum via the *cis*-Golgi. The TGN constitutes the exit site of the complex for anterograde transport as well as the entering site for retrograde transport and functions as the key station for sorting proteins for particular destinations (Bonifacino and Rojas 2006; Griffiths and Simons 1986; Klumperman 2011). The structure of the Golgi complex can be investigated by applying marker proteins such as TGN38, which is an integral membrane protein located in the TGN, and Golgi matrix protein of 130 kDa (GM130), a peripheral cytoplasmic protein that is found in the *cis*-Golgi network (Luzio et al. 1990; Nakamura et al. 1995). Although TGN38 is predominantly located in the TGN, about 10%

of TGN38 is steadily cycling between the cell surface and the TGN via the early endosome compartment (Ghosh et al. 1998).

The retrograde transport, which is important in the intracellular sorting of receptors and transmembrane enzymes, can be exploited by toxins (Bonifacino and Rojas 2006). One example of a toxin travelling from the plasma membrane via the retrograde pathway to the Golgi network is cholera toxin. Cholera toxin consists of two moieties. The A-moiety displays enzymatic activity in the cytosol, the B-moiety attaches to cell surface receptors (De Haan and Hirst 2004). After binding of the B subunit to GM1-gangliosides, cholera toxin internalization is cholesterol-dependent but is not confined to a specific uptake mechanism. The toxin can enter the cell via clathrin- or caveolin-dependent mechanisms as well as caveolin-1- and clathrin-independent routes as, e.g. the CLIC-GEEC pathway and Arf6-dependent endocytic events (Lajoie et al. 2009). Inside the cell cholera toxin is delivered to the early endosomes in order to undergo retrograde transport to the TGN and the ER, where the enzymatic moiety is released from the ligand subunit (Bonifacino and Rojas 2006; Sandvig and van Deurs 2005). Finally, the A subunit is translocated to the cytosol to inhibit GTPase activity by ribosylation and thereby causes pathological changes in the water and electrolyte balance culminating in diarrhoeal disease. Hence, cholera toxin (B subunit) is an adequate tool to study intracellular endosomal retrograde trafficking.

1.4 The impact of hypoxia on membrane trafficking

Endocytosis controls a huge array of cellular activities such as signal transduction and intercellular communication. These events also play a pivotal role in the cellular adaptation to hypoxic conditions. Studies on how hypoxic adaptation mechanisms and the endocytic machinery are intertwined have provided growing evidence for hypoxia functioning as a regulatory factor for specific membrane uptake and protein internalization.

In alveolar epithelial cells (AEC) it was found that hypoxia modulates the endocytosis of Na^+,K^+-ATPase α 1 subunits at the basolateral membrane. Upon hypoxic exposure, AEC showed a decrease in the abundance of membrane Na^+,K^+-ATPase α 1 subunits attributable to an increased clathrin-dependent endocytic uptake (Dada et al. 2003; Dada and Sznajder 2007). This phenomenon seems to be mediated by reactive oxygen species, RhoA and protein kinase C zeta (Dada et al. 2007; Gusarova et al. 2009).

A hypoxia-induced increase in endocytosis was also established by Yu et al. (Yu et al. 2016). The research group demonstrated that hypoxia downregulates matrixmetalloproteinase-2 via intensified caveolin-1-dependent endocytosis, a process that eventually may contribute to fibrosis in hypoxic tissue.

Defective and unbalanced endocytosis influencing cellular properties, such as signaling or adhesion is regarded to be a 'hallmark of malignant cells' (Mosesson et al. 2008). Furthermore, it is known that hypoxia deteriorates the outcome of cancerous diseases

(Semenza 2011). Studies examining the impact of hypoxia on the endocytic machinery of cancer cells have elucidated critical interrelations (Wang and Ohh 2010).

Yoon et al. demonstrated that hypoxia promotes carcinoma aggressiveness by influencing the endosomal recycling machinery. Oxygen deprivation stimulated Rab11-mediated recycling of integrin α6β4 resulting in an increased surface expression and hence a more invasive phenotype (Yoon et al. 2005). Tumor aggressiveness is also increased by intensified und deregulated activation of receptor tyrosine kinases. Wang et al. described a HIF-dependent downregulation of the Rab5 effector rabaptin-5 in hypoxic tumor cells leading to a delayed early endosome fusion and subsequent retention of stimulated EGF receptors in the endocytic pathway. This deceleration in endocytosis causes a delay in the deactivation of the EGF receptor through lysosomal degradation and promotes prolonged and deregulated signaling of the receptor tyrosine kinase, consequently contributing to disease progression (Wang et al. 2009). Apart from these mechanisms, HIF-dependent upregulation of caveolin-1 has been reported to modulate EGF signaling in hypoxic tumor cells. HIF induces the expression of caveolin-1, thereby favoring the formation of an augmented number of caveolae. These microdomains enable EGFR dimerization and activation in the absence of a ligand, consequently enhancing the oncogenic potential of the tumor (Wang et al. 2012).

According to the aforementioned studies, hypoxia has been shown to impact endocytosis via HIF-1α. Notably, recent reports suggest that hypoxia regulates trafficking of membrane receptors directly via PHDs and independent of HIF function. Garvalov et al. found PHD3 to interact with endocytic adaptor proteins that promote EGF receptor internalization (Garvalov et al. 2014). PHD3 exerts a scaffolding property irrespective of HIF-1α and HIF-2α stabilization. A further study describing a direct interaction between a prolyl hydroxylase and a regulator for receptor trafficking has been performed by Park et al.. This research group discovered that trafficking of the glutamate receptor in hypoxia is dependent on the influence of EGL-9 on LIN-10, a protein that mediates membrane recycling (Park et al. 2012).

For a considerable time, only the endocytic transport of a few selected proteins in hypoxic conditions and, thus, just distinct endocytic routes had been investigated. Bourseau-Guilmain et al. therefore examined 2016 the influence of oxygen deprivation on the global protein turnover (Bourseau-Guilmain et al. 2016). They delineated a HIF-independent downregulation of the global surface proteome and impaired membrane protein internalization in hypoxia. The downregulation of the global membrane protein endocytosis was reported to be governed through caveolin-1-dependent inhibition of dynamin-dependent membrane raft endocytosis. However, several proteins were highlighted to be subject to increased internalization and to escape the hypoxia-induced downregulation. In a further publication the same research group demonstrated that

hypoxia promotes the internalization of all major classes of lipoproteins (Menard et al. 2016).

In addition to endocytic processes, also exocytosis has been exemplified to be influenced by hypoxia (Carini et al. 2004). Carini et al. demonstrated that hypoxic preconditioning of cells causes movement of endosomes and lysosomes towards the plasma membrane, which finally results in the fusion of the membrane-enclosed compartments with the cell surface. This mechanism was hypothesized to be responsible for the preservation of the intracellular pH in hypoxia and thus to improve cellular survival. Notably, this mechanism requires integrity of the cytoskeleton.

In conclusion, several studies assign a pivotal regulating role to endocytosis in the framework of cellular adaptation to hypoxic environments since the availability of oxygen influences the abundance of cell surface proteins and their internalization process. Despite these initial evidences for altered overall membrane trafficking in hypoxia, the global exchange of the plasma membrane with endosomal compartments has not been investigated in detail up to now.

1.5 The role of actin in membrane trafficking

Physiological membrane trafficking requires accurate coordination of numerous interacting proteins to ensure efficient and correct delivery of cargoes to distinct intracellular compartments. As a complex meshwork of interlinking protein structures that extend throughout the whole cytoplasm, the cytoskeleton performs a crucial function within this coordination process. The cytoskeleton of eukaryotic cells is predominantly composed of three different kinds of filaments: microfilaments, also referred to as actin filaments, intermediate filaments and microtubules. All of these polymers exhibit a fast turnover within seconds to minutes in order to respond rapidly to changing cellular demands (Pollard and Cooper 2009).

Actin represents the most abundant protein in eukaryotic cells (Dominguez and Holmes 2011). Among the aforementioned cytoskeleton polymers, actin predominately influences the maintenance of the cellular shape, cell motility and polarity and the regulation of transcription (Dominguez and Holmes 2011; Olson and Nordheim 2010; Pollard and Borisy 2003).

Notably, actin plays a direct role in endocytic processes. In yeast actin polymerization has been reported to be necessary for coat internalization (Kaksonen et al. 2003). In mammalian cells phagocytosis, micropinocytosis and circular dorsal ruffles require actin (Mooren et al. 2012). Findings concerning a possible role of actin in CME remain controversial, but there is evidence that in certain settings actin could provide forces needed for vesicle invagination, scission and endosome maturation (Derivery et al. 2009; Mooren et al. 2012; Smythe and Ayscough 2006). Furthermore, actin dynamics are

involved in endosomal sorting and trafficking. This includes vesicle dynamics at the Golgi complex where actin supplies transport structures for organelle movement (Duleh and Welch 2010; Lanzetti 2007; Morel et al. 2009). In summary, the actin cytoskeleton is essential for the overall membrane trafficking and remodeling (Granger et al. 2014).

1.5.1 The regulation of the actin architecture by actin-binding proteins

Actin microfilaments (F-actin) are polar structures with an approximate diameter of 8 nm consisting of assembled globular actin monomers (G-actin). These actin filaments are further organized in different kinds of scaffolds such as branched actin networks or actin bundles. Actin-bundles are present in, e.g. microvilli (parallel bundles) or stress fibers (antiparallel bundles). The modulation of the overall actin architecture is mediated by actin-binding proteins (Blanchoin et al. 2014).

Actin-binding proteins assist in actin assembly, stabilizing and crosslinking as well as disassembly and severing of actin filaments (Blanchoin et al. 2014). Actin bundling proteins that have the unique ability to create tight actin filament bundles constitute a subclass of actin-binding proteins. Prominent representatives of this family are plastins (Delanote et al. 2005). The structure of plastins is evolutionary highly conserved from yeast to humans implying a fundamental role in cellular activities. Plastins possess two tandem actin-binding domains to cross-link actin filaments and two aminoterminal EF-hands for Ca^{2+}-binding (Delanote et al. 2005).

In vertebrates, plastins occur in three different isoforms: T-plastin (also known as plastin 3) is expressed in all cells derived from solid tissue (Lin et al. 1988). L-plastin (also known as plastin 2) is present in hematopoetic cells and I-plastin (also known as plastin 1 or fimbrin) expression is restricted to the small intestine, the colon, the kidney and hair cell stereocilia (Lin et al. 1988; Revenu et al. 2012; Shin et al. 2013). Dysregulated expression of plastins has been reported to be associated with cancerous and neurodegenerative diseases (Shinomiya 2012). In this context, it has been shown that L-plastin is expressed in neoplastic cells of non-hematopoetic origin and T-plastin shows increased abundance in chemo- and radio-resistant cancer cells (Delanote et al. 2005; Samstag and Klemke 2007; Stevenson et al. 2012).

Regulation in a Ca^{2+}-dependent manner has been described for L- and I-plastin whereas T-plastin appears to be Ca^{2+}-insensitive (Shinomiya 2012). Other possible regulation mechanisms include phosphorylation of plastin which has been found for L-plastin (Delanote et al. 2005). Although the mechanistic links between the membrane and the cytoskeleton are not completely understood, emerging evidence imply that actin-binding proteins are also modulated by phosphoinositides and membrane-associated GTPases like Rho GTPases acting as an interface between the membrane and the cytoskeleton (Bezanilla et al. 2015; de Curtis and Meldolesi 2012). This link allows integration of extracellular

signals detected at the plasma membrane by causing dynamic remodeling of the actin meshwork leading to alterations in the cellular compartmentalization (Bezanilla et al. 2015).

1.5.2 The role of plastins in endocytosis and membrane trafficking

The function of the plastin homologue Sac6 was further analyzed in yeast in order to investigate, which cellular processes are affected by actin-bundling (Adams et al. 1991). Studies on how Sac6 is involved in the actin-mediated internalization processes delineated a functional connection between the actin-filament-crosslinking protein Sac6 and coat internalization at endocytic sites (Kaksonen et al. 2005). The important role of actin-bundling proteins for endocytosis in yeast has been confirmed by Skau et al. by showing that fimbrin1 is essential for the regulation of endocytic actin patches and polarized actin cables (Skau et al. 2011).

Moreover, T-plastin has been reported to be associated with the internalization process of Shigella toxin and Salmonella protein in mammalian cells indicating an important role of plastins for membrane trafficking processes also in animal cells (Adam et al. 1995; Zhou et al. 1999). Further evidence confirming T-plastin to act as a regulator for membrane dynamics was provided by Giganti et al. who demonstrated that T-plastin modulates the wholesale intracellular actin turnover and actin-based movement in mammalian cells independently of its actin bundling capacity (Giganti et al. 2005). In line with these results L- and T-plastin overexpressing Cos-1 cells were shown to exhibit intensified endocytosis (Hagiwara et al. 2011). Moreover, Hosseinibarkooie et al. found that overexpression of T-plastin restored impaired endocytosis that occurs in spinal muscular atrophy (Hosseinibarkooie et al. 2016).

1.5.3 The impact of hypoxia on actin architecture and plastin function

Hypoxia-related diseases comprising brain edema and pulmonary hypertension display dysregulation of the cytoskeleton (Zieseniss 2014). In this context, hypoxia has been shown to affect the actin architecture by initiating actin rearrangement which is, at least partially, mediated by alterations in the activation level of the actin-binding protein cofilin (Vogler et al. 2013). Modulation of the activity of plastin-bundling proteins due to hypoxia has also been established by Chang et al., who unveiled an effect of hypoxia on Sac6 in yeast (Chang et al. 2012).

However, despite these primary findings regarding the influence of hypoxia on the actin cytoskeleton via modulation of plastins, the impact of oxygen deprivation on actin- and plastin-regulated membrane trafficking requires further study.

1.6 Methods for analyzing membrane trafficking

Membrane trafficking is a complex cellular process that is orchestrated in a tightly controlled manner. Analysis of the internalization of plasma membrane and subsequent intracellular vesicle trafficking requires visualization of the membrane-enclosed vesicles. This visualization can be accomplished by using confocal microscopy and applying fluorescent dyes that stain the lipid bilayer. A well suited membrane probe is the styryl dye FM (N-(3-triethylammoniumpropyl)-4-(4-(dibutylamino) styryl) pyridinium dibromide). FM dyes were developed to examine synaptic vesicle dynamics and were first described in 1992 (Betz et al. 1992). These probes specifically mark membrane-enclosed compartments and have evolved to an extensively used method to investigate endo- and exocytosis in synaptic but also non-neuronal preparations (Cochilla et al. 1999; Gaffield and Betz 2006; Hoopmann et al. 2012).

The FM molecule consists of a hydrophobic tail, a middle region containing two aromatic rings that are linked by a double bond bridge, and a hydrophilic head (Betz et al. 1992) (Figure 5). The tail is anchored in the plasma membrane whereas the hydrophilic moiety prevents the penetration of the dye through the membrane (Gaffield and Betz 2006). The fluorescent properties are determined by the quantity of double bonds linking the two rings (Gaffield and Betz 2006).

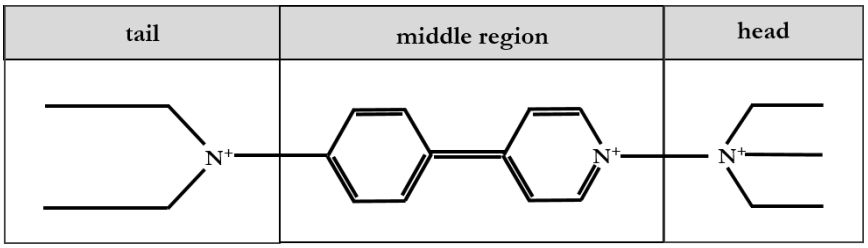

Figure 5: The membrane dye FM 1-43 comprises three functional regions. The length of the lipophilic tail determines the dye's membrane affinity and washout kinetics. The charged head ensures that the dye does not pervade the membrane. The chemical structure of the middle region defines the fluorescence properties.

When the cell surface is exposed to a solution containing dissolved FM, the FM dye partitions into the outer leaflet of the membrane. During endocytosis, FM becomes trapped in the vesicles (Figure 6). This process is independent from specific uptake mechanisms or distinct endosomal routes and, thus, allows for the investigation of all organelles involved in the endocytic process (Gaffield and Betz 2006).

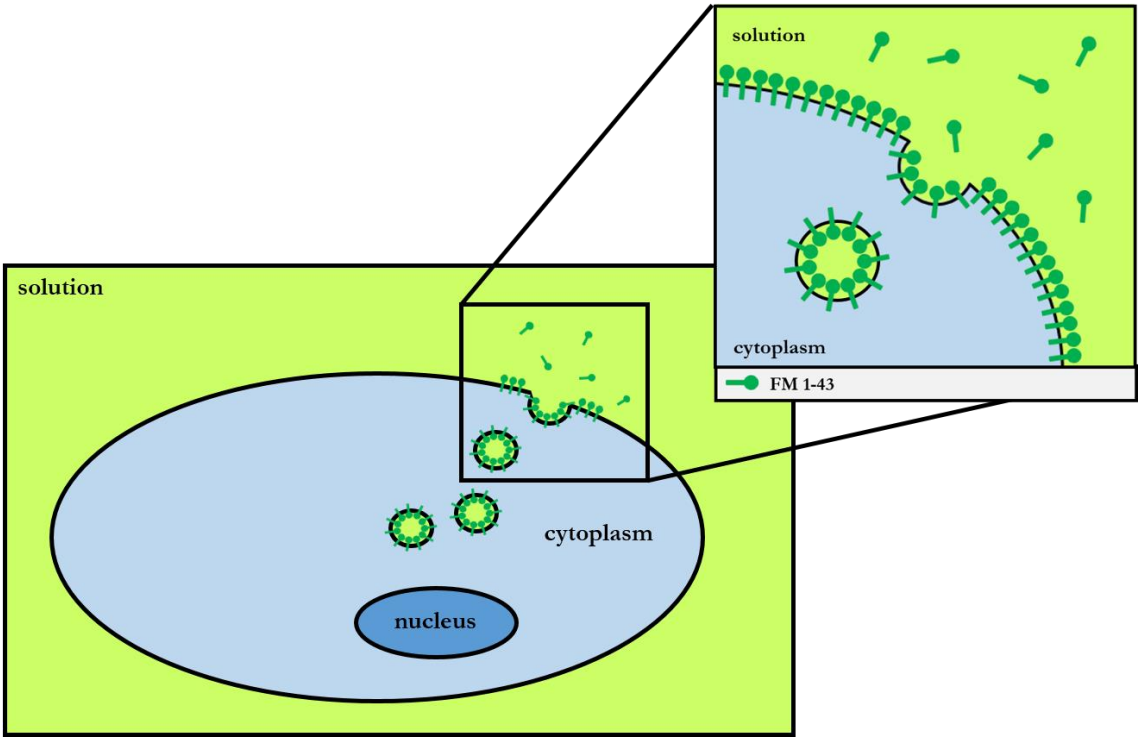

Figure 6: FM 1-43 is internalized via membrane uptake. FM specifically labels the plasma membrane that is exposed to the extracellular environment. The dye becomes trapped in vesicles during endocytosis and hence visualizes intracellular membrane trafficking.

Since FM explicitly marks the vesicle membrane and can be found in solution just at a minimal extent, the fluorescence intensity is directly proportional to the amount of internalized membrane, hence, providing a method to quantify membrane trafficking processes (Gaffield and Betz 2006; Henkel et al. 1996) (Figure 6). Accordingly, destaining reflects vesicle exocytosis because this mechanism represents the only escape for FM from the cell (Henkel et al. 1996).

In order to determine the identity of the membrane-enclosed compartments involved in the membrane trafficking process, the organelle membrane and the specific marker proteins for the respective compartment have to be detected simultaneously. Unfortunately, FM dyes are not optimally fixable and largely lost upon permeabilization. Consequently, subsequent immunostaining with fluorescently labelled antibodies for establishing the molecular identity of the labelled organelle is not possible. Revelo et al. circumvent this problem by developing a novel membrane probe termed membrane-binding fluorophore-cysteine-lysine-palmitoyl group (mCLING) that labels the plasma membrane and remains attached to membranes even after following immunostaining procedures (Revelo et al. 2014).

mCLING is composed of an octapeptide that is coupled to a palmitoyl tail acting as a membrane anchor and a fluorophore (Revelo et al. 2014). The probe has been established to reliably report endocytosis and to not impair membrane trafficking processes (Revelo et al. 2014). Thus, mCLING facilitates the discrimination of different membrane-bound

organelles by enabling membrane and fluorescent antibody staining of marker proteins at the same time.

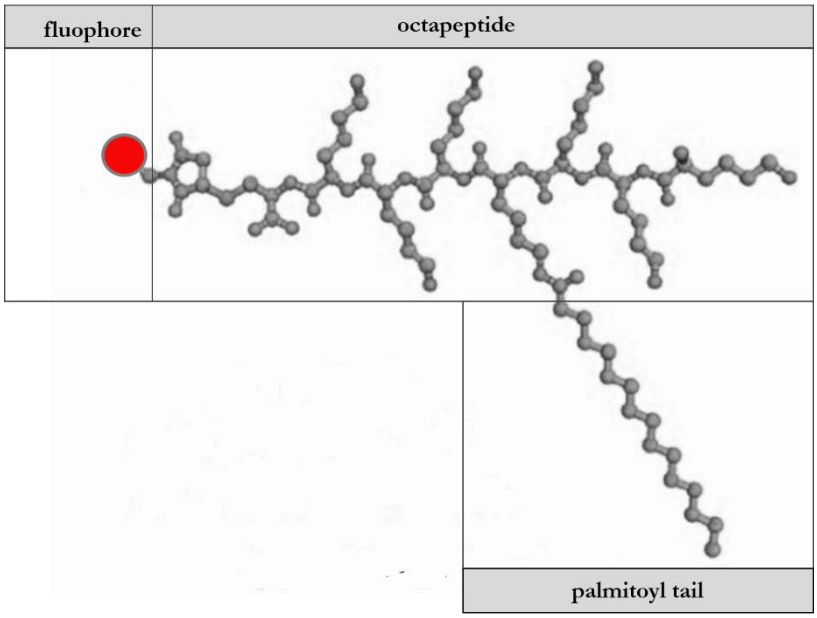

Figure 7: The mCLING molecule contains three distinct modules. The central octapeptide is linked to a palmitoyl tail that integrates into the membrane. Furthermore, the peptide is connected to a fluorophore. [Figure modified after Revelo et al. 2014.]

1.7 Aim of this thesis

Membrane trafficking is an essential feature of eukaryotic cells. By sorting, activating or degrading internalized cargo and receptors, the endosomal network plays a key role in the adaptation of cells to their environment. The availability of oxygen is not only a crucial factor in normal physiological development, but also in the genesis of pathophysiological conditions. To this end, quantitative studies on the impact of low oxygen levels on endosomal trafficking might offer new routes to modulate the cellular hypoxic response for therapeutic benefits. There is increasing evidence for an interplay between hypoxia and membrane trafficking. As outlined above, the following findings were generated in the literature so far: (1) Hypoxia causes downregulation of global proteome internalization but (2) upregulates distinct endocytic and sorting pathways in a specific manner. (3) Oxygen deprivation causes alterations in the actin cytoskeleton that is involved in membrane trafficking processes. (4) Actin-binding proteins that modulate the actin meshwork can be influenced by low levels of oxygen. (5) Hypoxia-induced changes in the endocytic uptake can be mediated by HIF or be HIF-independent.

However, despite these initial evidence for altered membrane trafficking in hypoxia, the general effect of low oxygen levels on wholesale membrane turnover, including the exchange of the plasma membrane with endosomal compartments in eukaryotic cells, remains unexplored. In this research project, new concepts of hypoxia-induced effects on

the entire endosomal system shall be integrated with previously established views of hypoxia-influenced endocytosis to present a more coherent picture.

Thus, the aim of this research project was to investigate the effect of hypoxia on membrane trafficking. To this end, the following questions and sub-goals were defined:

1. Does hypoxia influence the wholesale cellular membrane turnover? First studies should aim to quantify the membrane trafficking activity in cells grown in normoxic conditions in comparison to cells cultured in hypoxic conditions. In a second step, the effect should be further characterized by studying the time-dependence and reversibility.
2. If success is met to point 1, a further purpose of this project would be to investigate the membrane trafficking route that is affected by hypoxic induction. Therefore, the identity of the involved compartments should be determined and structural changes of organelles involved in the endocytic pathways should be examined.
3. Does the transcription factor HIF-1α influence membrane trafficking? The functional role of the master regulator HIF-1α in hypoxia-influenced membrane trafficking should be analyzed.
4. Which underlying mechanism mediates hypoxia-dependent membrane trafficking? In this regard, the role of the actin cytoskeleton and the actin-bundling proteins I-plastin, L-plastin and T-plastin should be elucidated.

2 Material and Methods

2.1 Material

All chemicals, if not otherwise indicated, were purchased from Sigma-Aldrich Corporation, Munich, Germany or Carl Roth GmbH & Co. KG, Karlsruhe, Germany.

Table 1: Reagents

Reagent	**Company**
Amersham Hyperfilm™ ECL (enhanced chemiluminescence)	GE Healthcare, Little Chalfont Buckinghamshire, UK
Bovine serum albumin (BSA)	AppliChem, Darmstadt, Germany
4',6-diamidino-2-phenylindole (DAPI)	Thermo Fisher Scientific, Darmstadt, Germany
DC™ Protein Assay	Bio-Rad, Munich, Germany
Digitonin	Sigma-Aldrich Corporation, Munich, Germany
DMOG	Enzo Life Sciences GmbH, Lörrach, Germany
Dulbecco's Modified Eagle Medium (DMEM)	PAN-Biotech, Aidenbach, Germany
Fetal calf serum (FCS)	PAN-Biotech, Aidenbach, Germany
Immobilon Western Chemiluminescent Horseradish Peroxidase (HRP) Substrate	Merck, Darmstadt, Germany
PageRuler Prestained Protein Ladder	Thermo Fisher Scientific, Darmstadt, Germany
Penicillin/Streptomycin (Pen/Strep)	PAN-Biotech, Aidenbach, Germany
Protease Inhibitor Cocktail Tablets, cOmplete Tablets, Mini, EASYpack	Roche Diagnostics, Mannheim, Germany
Puromycin	Thermo Fisher Scientific, Darmstadt, Germany
Trypsin/ Ethylenediaminetetraacetic acid (EDTA) Solution	PAN-Biotech, Aidenbach, Germany

Table 2: Buffers and solutions

Buffer name	Ingredients
Lysis buffer	400 mM NaCl, 1 mM EDTA, 10 mM Tris/HCl pH 8, 0.1% TritonX100
Mowiol/1,4-diazabicyclo-[2.2.2]-octane (DABCO)	0,1% DABCO in Mowiol
Phosphate-buffered Saline (PBS)	137 mM NaCl, 2.7 mM KCL, 4.3 mM $Na_2HPO_47H_2O$, 1.4 mM KH_2PO_4, pH 7.4
Ringer's buffer	130 mM NaCl, 4 mM KCl, 5 mM $CaCl_2$, 1 mM $MgCl_2$, 40 mM Glucose, 10 mM HEPES, pH 7.4
Ripa buffer	150 mM NaCl, 1% NP40, 0.5% sodiumdeoxycholate, 0.1% SDS, 50 mM Tris/HCl pH 8
5x sodium dodecyl sulfate (SDS) electrophoresis buffer	125 mM Tris, 1.25 M glycine, 0.5% SDS, pH 8.3
2 x SDS sample buffer	100 mM Tris/HCl, pH 6.8, 4% SDS, 0.2% bromphenol blue, 20% glycerol, 5% mercaptoethanol
Western blot blocking solution	5% milk in PBS
Western blot transfer buffer	25 mM Tris, 192 mM glycine, ad 800 ml with H_2O, 200 ml methanol

Table 3: Membrane and endocytosis dyes

Reagent	Fluorescence dye	Company	Cat Number
Cholera toxin B subunit	Alexa 555	Thermo Fisher Scientific, Darmstadt, Germany	C-34776
EGF	Tetramethylrhodamine	Thermo Fisher Scientific, Darmstadt, Germany	E3481
FM® 1-43 Dye	(*N*-(3-triethylammoniumpropyl)-4-(4-(dibutylamino) styryl) pyridinium dibromide)	Thermo Fisher Scientific, Darmstadt, Germany	T3163
mCLING	ATTO647N	Synaptic Systems, Göttingen, Germany	710 006AT1
Transferrin	Alexa Fluor 546	Thermo Fisher Scientific, Darmstadt, Germany	T23364

Table 4: Kits

Kit	Company	Cat Number
First strand cDNA Synthesis Kit	Thermo Fisher Scientific, Darmstadt, Germany	#K1612
Plasma Membrane Protein Extraction Kit	Abcam, Cambridge, UK	ab65400
SensiFAST™ Probe Lo-ROX Kit	Bioline GmbH, Luckenwalde, Germany	QT625-05
TRIzol®Reagent	Thermo Fisher Scientific, Darmstadt, Germany	15596018

Table 5: Antibodies used for immunostaining

Antibody	Origin	Company	Cat Number	Dilution
anti-EEA1	mouse	BD Biosciences, Heidelberg, Germany	#610457	1:100
anti-GM130	mouse	BD Biosciences, Heidelberg, Germany	#610822	1:100
anti-TGN38	mouse	BD Biosciences, Heidelberg, Germany	#610899	1:100
anti-mouse IgG-antibodies FITC	goat	Santa Cruz Biotechnology, Heidelberg, Germany	sc-2010	1:50
anti-mouse IgG-antibodies TR labelled	goat	Santa Cruz Biotechnology, Heidelberg, Germany	sc-2781	1:50

Table 6: Antibodies used for western blot analysis

Antibody	Origin	Company	Cat Number
anti-β-actin	mouse	Sigma-Aldrich Corporation, Munich, Germany	A5441
anti-HIF-1α	mouse	BD, Heidelberg, Germany	#610959
anti-Na^+/K^+-ATPase	rabbit	Cell Signaling, Frankfurt, Germany	#3010
anti-hPHD2	rabbit	Novus, Abingdon, UK	NB100-137
anti-mPHD2	rabbit	Novus, Abingdon, UK	NB100-2219
anti-T-plastin	rabbit	Thermo Fisher Scientific, Darmstadt, Germany	PA5-27883
horseradish peroxidase-conjugated secondary goat anti-rabbit	goat	Santa Cruz Biotechnology, Heidelberg, Germany	sc-2004
horseradish peroxidase-conjugated secondary goat anti-mouse	goat	Santa Cruz Biotechnology, Heidelberg, Germany	sc-2005

2.2 Cell lines

MDA-MB 231 is a human breast carcinoma cell line (Cailleau et al. 1974). The cells were obtained from the Deutsche Sammlung von Mikroorganismen und Zellkultur (DSMZ). The cell identity was authenticated by using a short tandem repeat analysis.

Mouse embryonal fibroblasts (MEF) were established in the group of Prof. R. S. Johnson, Department of Physiology, University of Cambridge (Ryan et al. 2000). The MEF +/+ cells were isolated from wild type mice at day E9.5 and the MEF-/- cells were isolated from HIF-1α-knockout mice also at day E9.5. The cells were immortalized by transfection with a SV40 large T antigen- and H-ras containing plasmid.

Dr. rer. nat. A. Zieseniss (Institute for Cardiovascular Physiology, University Medical Centre Göttingen) utilized MEF cells to establish PHD2 knockdown clones. Dr. rer. nat. M. Wottawa (Institute for Cardiovascular Physiology, University Medical Centre Göttingen) generated MDA-MB 231 shI-plastin, MDA-MB 231 shL-plastin and MDA-MB 213 shT-plastin cells. MDA-MB 231 shHIF-1α knockdown cells were kindly provided by the group of Prof. Dr. R. Wenger (Institute of Physiology, University of Zurich, Switzerland).

2.3 Cell culture

MDA-MB 231 and MEF-derived cell lines were cultured in high glucose DMEM supplemented with 10% heat inactivated FCS and 1% Pen/Strep. In order to subcultivate the cells a solution containing 0.05% trypsin and 0.02% EDTA was used to detach the adherent cells. The Puromycin-resistant cell knockdown clones were selected in a cell culture medium supplemented with 2 µg/ml Puromycin. All experiments were performed in a regular humidified incubator in normoxic conditions (37 °C, 5% CO_2, 20% O_2) (Binder GmbH, Tuttlingen, Germany) or in hypoxic conditions (37 °C, 5% CO_2, 1% O_2) using an adjustable hypoxic humidified workstation (INVIVO$_2$ 400; Ruskinn Technology, Bridgend, UK). To exclude contamination, the cells were regularly tested for mycoplasma by using DAPI staining and polymerase chain reaction (PCR) analysis. In all cell culture experiments the cell density was less than 50%.

2.4 RNA extraction

RNA extraction was performed by acid guanidinium thiocyanate-phenol-chloroform extraction using the commercially available mixture TRIzol®Reagent (Chomczynski and Sacchi 1987; Rio et al. 2010). This method allows separation of nucleic acids upon extraction due to phenol phase separation.

MDA-MB 231 cells were plated in 6-well dishes and cultivated in standard cell culture conditions overnight. The following day the cells were either incubated for 6 or 48 hours (hrs) in normoxic (20% O_2) or hypoxic conditions (1% O_2). One set of cells grown in normoxic conditions was treated with the oxoglutarate analogue DMOG in a concentration of 1 mM. The cells were washed twice with PBS and lysed by adding 500 µl TRIzol® Reagent. After incubation for 5 min at room temperature (RT) to allow complete dissociation of the nucleoprotein complexes, 100 µl chloroform was added and the samples were vortexed for 15 sec and subsequently incubated at RT for 5 min. The samples were centrifuged at 12000 x *g* for 15 min at 4 °C (Eppendorf centrifuge 5415R, Eppendorf AG, Hamburg, Germany) to separate the aqueous RNA-containing phase from the protein-containing organic phase. The upper aqueous phase was transferred to a fresh cup and 25 µl isopropyl alcohol was added to precipitate RNA. After incubation at RT for 10 min, the samples were centrifuged at 12000 x *g* for 15 min at 4 °C. The supernatant was discarded and the RNA containing pellet was washed with 500 µl 75% ethanol by vortexing and subsequent centrifuging at 7500 x *g* for 5 min at 4 °C. Afterwards the pellet was dried for 10 min and then resuspended in 20 µl RNase-free water by incubation for 10 min at 55 °C. The isolated RNA was stored at -80 °C.

The RNA purity was assessed by measuring the optical absorption of the sample at 260 nm and 280 nm wavelength by utilizing the SmartSpec™ Plus Spectrophotometer (Bio-Rad, Munich, Germany). RNA absorb at 260 nm while contaminants like protein exhibit strong

absorption at 280 nm. A 260 nm/280 nm ratio of 1.8 is generally regarded as an indication of high RNA purity whereas contamination lowers the ratio.

2.5 cDNA synthesis

The complementary DNA (cDNA) synthesis was performed by reverse transcription which utilizes RNA-dependent DNA polymerase (Coffin and Fan 2016; Kacian et al. 1972; Verma et al. 1972).

The First Strand cDNA Synthesis Kit was used to generate cDNA. 2 µg RNA were mixed with 1 µl oligo(dT)18 primer. Oligo(dT)18 primers attach to the poly A tail at the 3'-end of the mRNA and thereby lead to the transcription of all mRNA templates. Afterwards nuclease-free water was added up to a total volume of 11 µl. The solution was mixed and incubated for 5 min at 65 °C to allow for primer annealing. Then the sample was shortly stored on ice and 4 µl 5x reaction buffer, 1 µl RiboLockTM ribonuclease inhibitor (20 U/µl), 2 µl 10 mM dNTP and 2 µl M-MuLV reverse transcriptase mix (20 U/µl) were added. The sample was gently mixed and incubated for 1 hour at 37 °C for the synthesis of cDNA. For termination of the reaction, the M-MuLV Reverse Transcriptase was inactivated by heating the sample to 70 °C for 5 min. The product of the first strand cDNA synthesis was used for analysis by real-time quantitative polymerase chain reaction (qRT PCR).

2.6 Quantitative real-time polymerase chain reaction

qRT PCR is an amplification method for nucleic acids which allows for the quantification of the product via a fluorescent reporter molecule (Higuchi et al. 1992; Kubista et al. 2006; Mullis and Faloona 1987). One cycle of the PCR includes the denaturation of the double-stranded DNA, the annealing and hybridization of the primers complementary to the DNA template, and the synthesis of a new strand by a thermostable Taq polymerase. The DNA-intercalating dye SYBR Green I, which turns fluorescent when bound to double-stranded DNA, is added for the quantification of DNA copies. Thus, the increase in DNA product results in an enhanced fluorescence signal which is measured by a photodetector in real-time after each cycle.

qRT PCRs were performed using the SensiFAST™ Probe Lo-ROX Kit according to the manufacturer's instructions. 1 µl cDNA, 12.5 µl SensiMix SYBER Low-Rox (2x), 0.5 µl forward primer (Biomers, Ulm, Germany) with a concentration of 20 pmol and 0.5 µl reverse primer (Biomers, Ulm, Germany) with a concentration of 20 pmol were mixed. The primer sequences are listed in Table 8. H_2O was added to a total volume of 25 µl. The fluorescent signal was measured by the MX3000P light cycler (Agilent Technologies, Waldbronn, Germany). For annealing temperatures of the primers please also refer to Table 8. Analysis was performed by using the MxPro software. The fold change of the

mRNA expression was calculated using the ΔΔCT method. The cycle number at which the amplification curve of the respective gene traverses the threshold represents the CT-value. The ribosomal *L28* mRNA was used as housekeeping gene and normalization to the *L28* value was done to adjust differences in the amount of cDNA. The relative expression value of the gene of interest (ΔCT) was determined by subtraction of the CT-value of the housekeeping gene *L28* from the CT-value of the gene of interest.

$$\Delta CT = CT_{\text{gene of interest}} - CT_{\text{housekeeping gene}}$$

A comparison between the control and modified samples is possible by calculation of the ΔΔCT-value. The ΔΔCT-value was obtained by applying the following formula:

$$\Delta\Delta CT = \Delta CT_{\text{gene of interest (test condition)}} - \Delta CT_{\text{gene of interest (control condition)}}$$

$$\text{ratio} = 2^{-\Delta\Delta CT}$$

The ratio displays the fold change of the expression level of the gene of interest in the modified samples in comparison to the mean of the control condition.

Table 7: Thermal profile of qRT PCR

	Step	**Temperature**	**Duration**	**Number of cycles**
	initial denaturation	95 °C	2 min	1
PCR	denaturation	95 °C	5 sec	30 - 40
	annealing	primer specific (Table 8)	10 sec	
	extension	72 °C	20 sec	

Table 8: Primer sequences

Target gene	**Oligonucleotide sequence**	**Annealing temperature**
L28	5'-GCAATTCCTTCCGCTACAAC-3' 5'-TGTTCTTGCGGATCATGTGT-3'	60 °C
PHD3	5'-AGATCGTAGGAACCCACACG-3' 5'-CAGATTTCAGAGCACGGTCA-3'	60 °C
PLS1	5'-GGTACTTGGATCTCCAGTGGG-3' 5'- TTGCATTAGTGACACAAACTCTTCA-3'	62 °C
PLS2	5'-CTTGTGACCACACACCCAGG-3' 5'-TCCATTGCCATCAGTATCAACTTT-3'	60 °C
PLS3	5'-TAAGGACAAGACGATCAGCTCC-3' 5'-TATGAGCACATTTCAGGCGTGC-3'	60 °C

2.7 Protein extraction and quantification

MDA-MB 231 cells and MEF cells were plated on 5 cm dishes and cultivated in standard cell culture conditions overnight. For the experiment the cells were either incubated in normoxia (20% O_2) or hypoxia (1% O_2) for 6 or 48 hrs. Subsequently, cells were washed with 4 °C cold PBS, lysis buffer was added, and cells were scraped off the dish. To investigate plastin abundance in whole cell extracts, the cells were lysed in 250 µl Ripa buffer. For HIF-1α and PHD2 detection, the cells were lysed with 250 µl lysis buffer. Both lysis buffers were supplemented with protease inhibitors to prevent protein degradation. The cell lysates were transferred into an Eppendorf cup and centrifuged at maximum speed (12000 x *g*) for 5 min. The pellet was discarded and the supernatant was stored in a fresh tube.

Membrane proteins were isolated from MDA-MB 231 cells using the Plasma Membrane Protein Extraction Kit. After discarding the medium, the cells were detached by scraping in PBS and centrifuged at 600 x *g* for 5 min at 4 °C. Hereafter, the pellet was resuspended in 1 ml icecold Homogenize Buffer in a Dounce homogenizer. The resulting homogenate was transferred to a 1.5 ml Eppendorf cup and centrifuged at 700 x *g* for 10 min at 4 °C. The pellet was discarded and the supernatant was collected in a fresh 1.5 ml tube to be centrifuged at 10000 x g for 30 min at 4 °C. After this step the supernatant contained the cytosol fraction, whereas the total cellular membrane protein comprising proteins from both the plasma membrane and intracellular organelle membranes was concentrated in the pellet. To specifically isolate and purify the proteins located in the cell surface membrane, the pellet was resuspended in 200 µl of the Upper Phase Solution and 200 µl Lower Phase Solution was added. Afterwards, the solution was well mixed and incubated in a tube labelled "A" on ice for 5 min. Meanwhile, a fresh tube marked as "B" was prepared. It contained 200 µl of the Upper Phase Solution mixed with 200 µl Lower Phase Solution. Both tubes were centrifuged at 1000 x *g* for 5 min at 4 °C. The upper phase from tube A was transferred to a new tube labelled with "C" and kept on ice. In order to increase the protein yield, the tube A lower phase was extracted once more by adding 100 µl of the Upper Phase Solution from tube B, mixed well and then centrifuged at 1000 x *g* for 5 min at 4 °C. Again, the upper phase was transferred to tube C. For further purification 100 µl of the Lower Phase Solution from B was added to the combined upper phase in tube C. Tube C was centrifuged at 1000 x *g* for 5 min at 4 °C. The upper phase was transferred to a new tube and diluted in 5 volumes H_2O, kept on ice for 5 min and spun at top speed for 10 min at 4 °C. The supernatant was removed. Finally, the pellet contained the plasma membrane protein fraction and was stored at -80 °C. In order to determine the protein concentration, a Bradford protein assay was performed.

2.8 Bradford protein assay

A Bradford protein assay is a colorimetric method to estimate protein concentrations (Bradford 1976). It is based in the absorbance shift of Coomassie brilliant blue G-250 after binding to proteins (465 nm to 595 nm). The increase of absorbance at 595 nm is proportional to the amount of protein in the solution. A sample of 2 µl cell suspension was dissolved in 200 µl Protein-Assay-Reagent containing Coomassie brilliant blue G-250. Standard concentrations of protein (BSA 0 – 5 µg/µl) were prepared and the absorbance of the protein solutions at 595 nm was measured by the Microplate Reader Model 680 (Bio-Rad, München, Germany). The protein amount was determined by means of the regression curve derived from the standard series.

2.9 SDS polyacrylamide gel electrophoresis

Sodium dodecylsulfate polyacrylamide gel electrophoresis (SDS-PAGE) was used to separate the protein sample by size of the polypeptide (Laemmli 1970). Sodium dodecyl sulfate is an anionic detergent applying negative charge to the proteins and thereby allows a fractionation according to their molecular weight during gel electrophoresis. To denature the proteins, the cell lysate was boiled for 5 min at 95 °C. Equal amounts of proteins were diluted in 2 x SDS sample buffer and loaded into the SDS-PAGE gel. The composition of the stacking and resolving gel is given in Table 9. To determine the protein size the PageRuler Prestained Protein Ladder was filled in a separate line. 5 x SDS electrophoresis buffer was added and electrophoresis was performed at a constant current of 80 mA/cm^2 for 3 to 4 hrs.

Table 9: Composition of the resolving and stacking gel for SDS-PAGE

	Resolving gel (10%) (50 ml)	**Stacking gel (5%)** (10 ml)
H_2O	19.8 ml	6.8 ml
30% acrylamide mix	16.7 ml	1.7 ml
1.5 M Tris pH 8.8	12.5 ml	-
1.5 M Tris pH 6.8	-	1.25 ml
10% SDS	0.5 ml	0.1 ml
1% ammonium persulfate	0.5 ml	0.1 ml
Tetramethylethylenediamine	0.02 ml	0.01 ml

2.10 Western blot

Western blotting allows the identification of specific proteins from a mixture of extracted proteins, their analysis by immunostaining and comparison of protein amounts between samples cultured in different conditions (Burnette 1981; Towbin et al. 1979).

After gel electrophoresis, the proteins were transferred onto nitrocellulose membranes (GE Healthcare, Amersham, UK) by semi-dry blotting. The gel, the nitrocellulose membrane and the filter paper were soaked with western blot transfer buffer and stacked in the PerfectBlue Semi-Dry Electroblotter (PeqLab, Erlangen, Germany) with a constant current setting of 2 mA/cm^2 for 1 hour. Negatively charged proteins travelled towards the positive anode and were transferred onto the membrane. The transfer was assessed by Ponceau S staining. To prevent non-specific binding of the antibodies, the membrane was blocked utilizing 5% milk in PBS (blocking solution) for 1 hour. For specific protein staining the membrane was incubated overnight at 4 °C with primary antibodies (please refer to Table 6) in blocking solution. The next day, the membrane was washed (3 x 10 min) with PBS. Horseradish peroxidase-conjugated secondary antibodies that recognized the respective primary antibody were applied for 1 hour to detect the immunocomplexes. The membrane was washed three times with PBS. For signal development chemiluminescent HRP substrate was applied to the membrane and incubated for 1 min. The peroxidase catalyzes the oxidation of luminol dissolved in the HRP substrate solution generating a chemiluminescence signal that is used for the specific detection of a protein band. The blot was imaged by utilizing the LAS3000 Imager (Fujifilm, Düsseldorf, Germany) or by using chemiluminescence sensitive films (GE Healthcare, Little Chalfont Buckinghamshire, UK).

2.11 FM 1-43 staining

FM dyes are used to label endocytic vesicles and visualize endosomal trafficking (Gaffield and Betz 2006).

2.11.1 FM-staining: short- and long-term hypoxia experiments

MDA-MB 231 and MEF-derived cell lines were seeded on glass cover slips one day prior to the experiment and incubated overnight at 20% O_2. The next day, the cells were incubated in normoxia (20% O_2) or hypoxia (1% O_2) for 6 (short-term hypoxia) or 48 hrs (long-term hypoxia) as indicated. A set of cells grown under normoxic conditions was treated with DMOG in a concentration of 1 mM. During the last 30 min of incubation 5 µM FM 1-43 was added to the cells to allow dye uptake. To investigate the FM 1-43 uptake capacity by confocal microscopy, cells were washed three times with DMEM and fixed with 4% paraformaldehyde (PFA) in PBS for 30 min. The release of FM 1-43 via exocytosis was studied to control for cell integrity. Therefore cells were incubated with 5 µM FM 1-43 for 30 min, washed, incubated for additional 30 min at 37 °C in dye-free cell

culture medium for dye release and fixed with 4% PFA in PBS for 30 min at 37 °C. Afterwards, the cells were washed again twice with PBS. PFA autofluorescence was quenched by incubating the cells with 50 mM NH_4Cl in PBS for 15 min. The cells were directly imaged after the staining procedure utilizing the confocal microscope TCS SP5 (Leica) with a HCX Plan Apochromat 63x, 1.4 NA oil immersion objective, which is operated with the LAS AF imaging software (version 2.7.9723; Leica). FM 1-43 was excited with an Argon laser at the 488 nm line.

2.11.2 FM-staining: FM reoxygenation experiments

MDA-MB 231 cells were seeded on glass cover slips one day prior to the experiment and incubated overnight at 20% O_2. The next day, the cells were incubated in normoxia or hypoxia for 6 hrs. Afterwards, cells were reoxygenated (1% O_2 to 20% O_2) for 30 min or 2 hrs. Subsequent staining followed the protocol as described above.

2.12 mCLING staining

mCLING is a membrane dye which is applied to track vesicle endocytosis. As a special feature, it allows identification of the stained compartments by subsequent immunofluorescent staining because it remains attached to the membranes after fixation and permeabilization (Revelo et al. 2014).

MDA-MB 231 cells were seeded on glass cover slips one day prior to the experiment and incubated overnight at 20% O_2. The cells were incubated in normoxic (20% O_2) or hypoxic (1% O_2) conditions for 6 hrs. Afterwards, the cells were washed three times with Ringer's buffer and incubated in prewarmed Ringer's buffer supplemented with 0.4 µM ATTO647N-labelled mCLING for 15 min at 37 °C. In the next step, the cells were washed with Ringer's buffer and fixed with 4% PFA dissolved in PBS and supplemented with 0.2% glutaraldehyde for 20 min on ice and additional 20 min at RT. The cells were washed briefly with PBS and PFA autofluorescence was quenched by adding 100 mM NH_4Cl and 100 mM glycine in PBS for 30 min at RT. The mCLING-stained cells were used for subsequent immunostaining.

Imaging was performed by using a Leica TCS SP5 confocal microscope (Leica Microsystems GmbH, Wetzlar, Germany) with a HCX Plan Apochromat 100×, 1.4 NA oil immersion objective, which is operated with the LAS AF imaging software (version 2.7.3.9723; Leica). Atto647N (mCLING) was excited with a Helium-Neon Laser at 633 nm.

2.13 Immunofluorescence staining

Immunofluorescence staining is a technique to visualize the localisation and distribution of molecules within the cell, which thereby allows for the identification of cellular

compartments. It is based on the specific binding of the fluorescently labelled antibodies to their target antigens (Coons et al. 1942).

The cells were seeded on glass cover slips and cultivated in standard cell culture conditions for 24 hrs. After incubation in 20% or 1% O_2 for 6 hrs, the cells were washed twice in PBS and fixed with 4% PFA for 20 min. Subsequently, cells were washed with PBS and treated with 100 µM digitonin in PBS for 5 min to permeabilize the cell membrane. Non-specific binding was blocked with 2% BSA in PBS for 20 min. The cells were incubated with the primary antibodies (please refer to Table 5) for 6 hrs followed by a washing step. For the detection of the antigen-antibody complex, a FITC-labelled secondary antibody, which was raised against the Fc region of the primary antibody, was added for 1 hour. By incubation in a DAPI containing solution for 5 min, the cell nuclei were visualized. Finally, the samples were mounted with Mowiol supplemented with the antifade reagent DABCO. The fluorescence was analyzed by using the confocal microscope TCS SP5 (Leica) with a HCX Plan Apochromat 63x, 1.4 NA oil immersion objective, which is operated with the LAS AF imaging software (version 2.7.9723; Leica).

2.14 Functional endocytosis assays

Specific marker proteins are incorporated by different means and follow particular intracellular pathways. Thus, the analysis of the cargo-specific uptake elucidates the influence of the testing condition on endocytic trafficking.

2.14.1 Protocol for the marker proteins EGF and transferrin

MDA-MB 231 cells were plated on glass coverslips and cultivated in standard cell culture conditions overnight. The following day, the cells were incubated in hypoxia or normoxia for 6 hrs. The cells were incubated with 0.4 ng/ml tetramethylrhodamine-EGF or 25 µg/ml Alexa Fluor546-Transferrin in Ringer's buffer at 37 °C for 10 min to allow uptake of the fluorescently labelled cargos. Afterwards the cells were washed in PBS and fixed with 4% PFA for 10 min on ice followed by 20 min incubation at 37 °C. After a further washing step in PBS, the background signal was attenuated by quenching with 50 mM NH_4Cl for 15 min and embedded with Mowiol/DABCO.

2.14.2 Protocol for the marker protein cholera toxin

When using the endocytosis marker Alexa 555-Cholera toxin, the cells were incubated with 10 µg/ml cargo in DMEM on ice for 30 min to permit binding to the cell membrane. After that, the cells were washed and incubated in DMEM for 40 min at 37 °C to allow incorporation of the marker. The cells were fixed with 4% PFA for 10 min on ice followed by 20 min incubation at 37 °C. After a further washing step in PBS, the samples were quenched with 50 mM NH_4Cl for 15 min and mounted with Mowiol/DABCO.

Imaging of the endocytosis reporter proteins was done using the Axio Observer D1 fluorescence microscope (Carl Zeiss, Oberkochen, Germany).

2.15 Data processing

The analysis of the microscopy data presented in this study was performed by applying custom-made MATLAB routines (The Mathworks Inc., Natick, MA, USA) designed by Prof. Silvio O. Rizzoli (Department of Neuro- and Sensory Physiology, University Medical Centre Göttingen).

For quantifying membrane trafficking, the fluorescence intensities of FM 1-43-labelled organelles were analyzed. FM 1-43-labelled organelles were defined as groups of pixels displaying fluorescence intensities above the mean FM 1-43 background value. The routine was applied on tif files generated by the Leica LAS AF software and the intracellular area under analysis was determined by user input.

Endocytosis levels and organelle abundance that were obtained from functional endocytosis assays and immunofluorescence staining were determined by using a similar custom-written MATLAB macro. The fluorescence intensities of the cellular regions stained by the different fluorescently labelled dyes were calculated. Labelled organelles were defined as groups of pixels displaying fluorescence intensities above the background value. The routine was applied on tif files generated by the Leica LAS AF software and AxioVision imaging software and the area under analysis was determined by user input.

To examine the presence of various proteins on mCLING-labelled organelles, two-color confocal images of mCLING-labelled and immunostained cells were analyzed. Pearson's correlation coefficients were determined by applying a custom-written MATLAB routine. This MATLAB routine was designed based on a macro to calculate Pearson's correlation coefficients described by Revelo et al. and adapted according to specific requirements caused by the experimental settings (Revelo et al. 2014). The macro was applied on tif files generated by the Leica LAS AF software and the area supposed to be analyzed was captured in boxes (30 pixels long and 30 pixels wide, 20.2-nm pixels) drawn on organelles in both channels. As a positive control for 100% co-localization, cells were stained with anti-TGN38 and subsequently incubated with TR-labelled and FITC-labelled secondary antibodies. The correlation of the marker proteins and mCLING-stained structures was calculated as percent of maximum expected correlation determined by the positive control (% of control).

2.16 Statistical analysis

All graphs shown in this study correspond to means ± standard error of the mean (SEM). The statistical significance was calculated with GraphPad Prism v4.0 (GraphPad Software Inc.). For the analysis of FM 1-43 and immunofluorescence stainings the paired Student's *t*-

test was conducted. The correlation analysis of mCLING and immunofluorescence co-stained samples and comparison of mRNA levels was done by unpaired Student's *t*-test. The p-values are indicated in the respective figure legends. Results that were derived from erroneous experimentation (e.g. due to contaminated cells) were excluded from the analysis. Blinding was not undertaken since each dataset could be easily assigned to the respective condition by the experimenters.

Corel Draw X3 (Corel Corporation) was used for creating the figures and Microsoft Office Word 2013 (Microsoft Corporation) was applied to author the text. Endnote (Thomson Reuters) was used for the management of bibliographic references.

3 Results

Cells rely on membrane trafficking to maintain their cellular integrity. In particular, membrane trafficking enables cells to control the homeostasis of their membrane-enclosed compartments by sending membranes from the inner compartments to the plasma membrane. The properties of the plasma membrane are simultaneously influenced by the retrieval of plasma membrane components via the retrograde transport pathway. These mechanisms qualify cells to adapt rapidly to changes in the cellular environment. Given the absence of precise knowledge about the impact of hypoxia on membrane trafficking, this study was designed to examine the effect of decreased oxygen concentrations on overall membrane transport.

3.1 Hypoxia induces increased membrane trafficking in MDA-MB 231 cells

3.1.1 Hypoxia stimulates endocytic membrane uptake

In order to investigate the effect of hypoxia on membrane trafficking, the total endocytic capacity of MDA-MB 231 cells in normoxia (20% O_2) compared to hypoxia (1% O_2) was determined by performing FM 1-43 stainings. The fluorescent styryl dye FM 1-43 inserts into the outer leaflet of the cell membrane. Since the dye uptake by the cell is independent of specific endocytic mechanisms or pathways, the staining visualizes the entirety of all organelles involved in the endocytic process.

The exposure of the breast carcinoma cell line MDA-MB 231 to 6 hrs of hypoxia (1% O_2) resulted in an enhanced uptake of the FM 1-43 dye compared to normoxia (20% O_2) as shown in Figure 8 pointing to an increase in membrane trafficking. To exclude non-specific incorporation of the dye and ensure viability of the cells, in parallel one set of MDA-MB 231 cells was incubated in a dye-free buffer subsequent to staining with FM 1-43 dye. The organelles containing FM 1-43 released a large portion of the dye by exocytosis in normoxic and hypoxic conditions. This proved the integrity of the membrane trafficking process in the treated cells and the specific incorporation of the dye in the cell membrane.

In hypoxia not only the FM 1-43 fluorescence intensity was altered, but also the morphology of the FM 1-43 stained organelles changed to discernible tubular structures, whereas in normoxia mainly vesicular structures were visible.

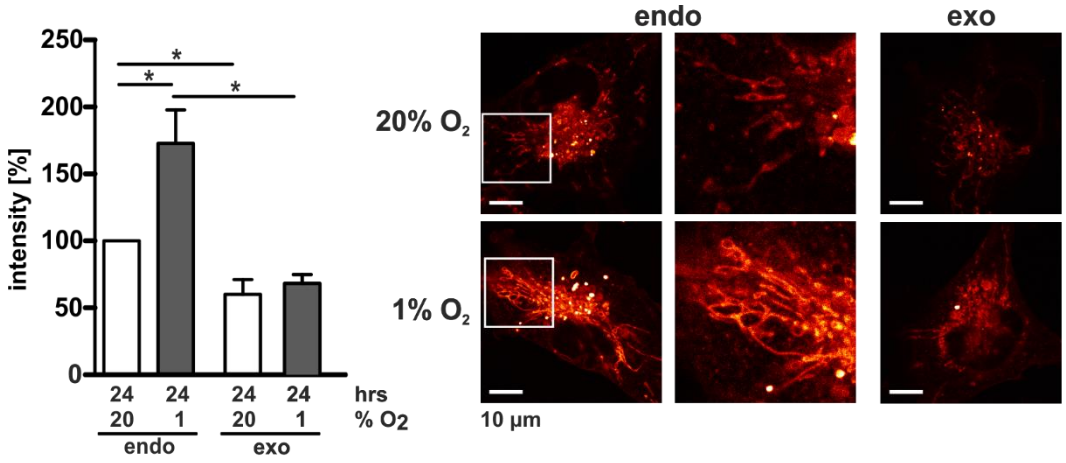

Figure 8: Short-term hypoxia increases endocytic membrane trafficking. The membrane uptake in MDA-MB 231 cells was analyzed regarding their endocytosis (endo) and exocytosis (exo) activities by applying the dye FM 1-43 after exposure to normoxia (20% O_2) or hypoxia (1% O_2) for 6 hrs. The cells were imaged using confocal microscopy and the fluorescence intensity was measured by applying a custom-written MATLAB routine. Data are shown as mean ± SEM as percentage of the 20% O_2 endo sample, * $p<0.05$ (paired *t*-test). Representative stainings of the endo or exo samples and zooms of the stained structures are shown on the right. Scale bars: 10 µm. Seven independent experiments were analyzed.

To investigate if the increase in membrane trafficking was just a response to short-term hypoxia (6 hrs 1% O_2) or if it could be also observed after exposure to long-term hypoxia, FM-studies in MDA-MB 231 cells preincubated in hypoxia for 48 hrs were performed.

MDA-MB 231 cells incubated for 48 hrs in hypoxic conditions also showed an increased membrane trafficking activity comparable to the 6 hrs hypoxia experiments (Figure 9).

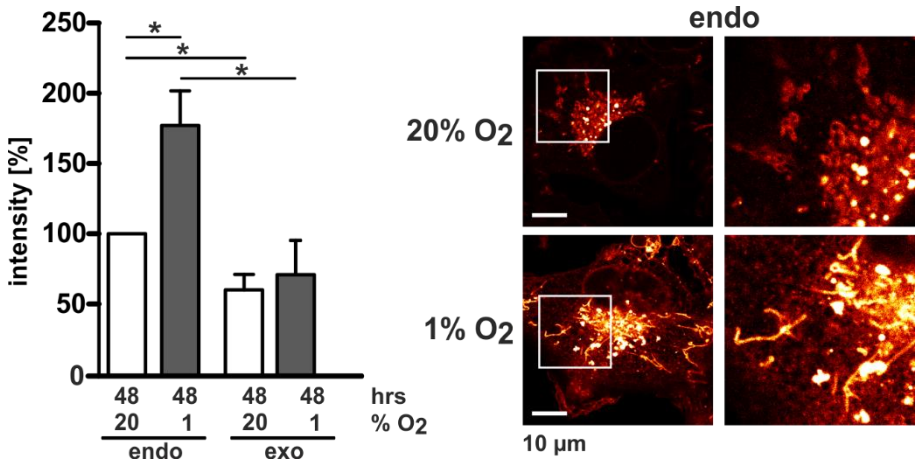

Figure 9: Long-term hypoxia increases membrane trafficking. MDA-MB 231 cells were analyzed regarding endocytosis (endo) and exocytosis (exo) activities applying the dye FM 1-43 after exposure of the cells to normoxia (20% O_2) or hypoxia (1% O_2) for 48 hrs. Data are shown as mean ± SEM as percentage of the 20% O_2 sample, * $p<0.05$ (paired *t*-test). Representative stainings of the endo or exo samples and a zoom of the stained structures are shown on the right. Scale bars: 10 µm. Four independent experiments were analyzed.

3.1.2 The hypoxia-induced membrane trafficking is quickly reversed upon reoxygenation

In this set of experiments, the impact of reoxygenation on hypoxia-accelerated membrane-trafficking was investigated. Additionally, the time course of the phenotype reversal was determined.

After reoxygenation of the cells for 2 hrs or just 30 min subsequent to the hypoxic induction of 6 hrs, the hypoxic phenotype in MDA-MB 231 cells was reversed (Figure 10). This observation suggests a fast oxygen sensing and adaptation mechanism.

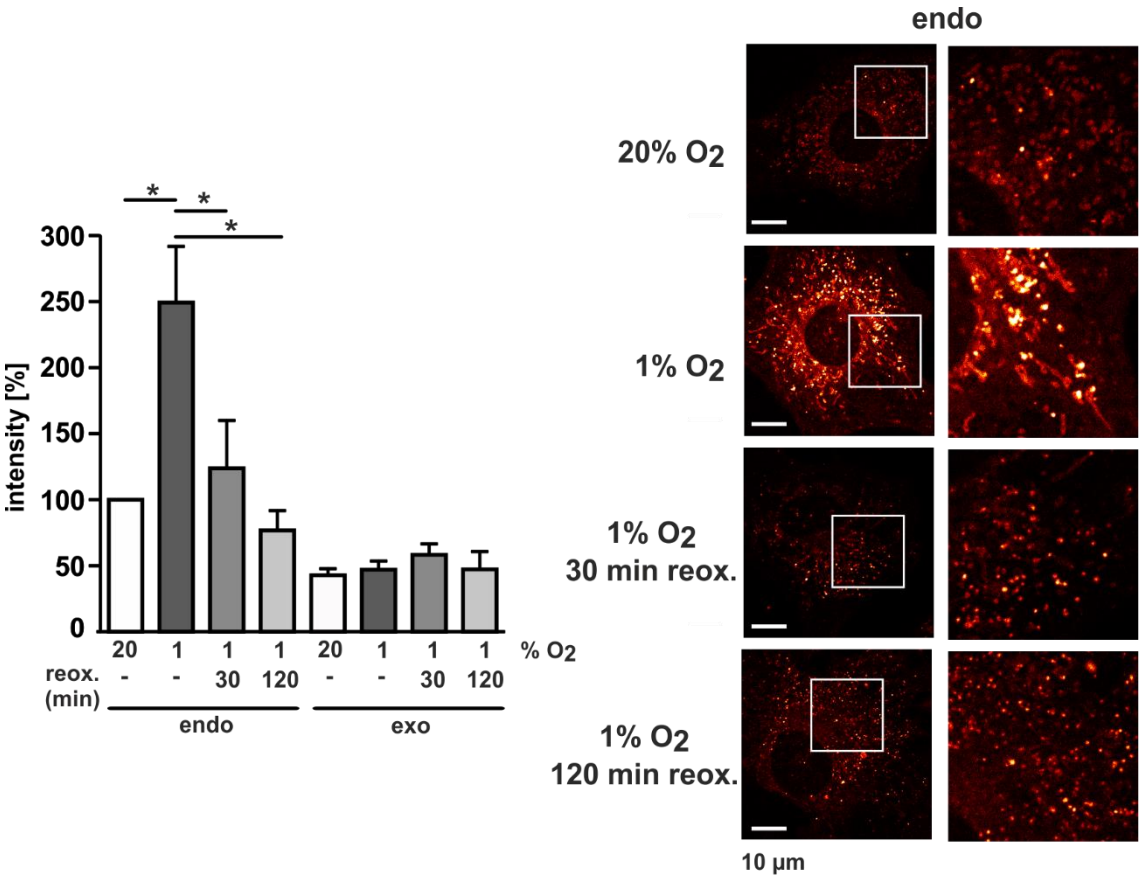

Figure 10: Hypoxia-induced endocytic activity is quickly reversed upon reoxygenation. MDA-MB 231 cells were incubated in normoxia (20% O_2) or hypoxia (1% O_2) for 6 hrs with or without subsequent reoxygenation (reox) (for 30 min or 120 min) at 20% O_2 as indicated. Data are shown as mean ± SEM as percentage of the 20% O_2 sample, * $p<0.05$ (paired *t*-test). Representative stainings of the endo or exo samples and a zoom of the stained structures are shown on the right. Scale bars: 10 µm. Five independent experiments were analyzed.

3.2 Hypoxia causes structural alterations in the composition of the Golgi apparatus

As demonstrated by FM 1-43 stainings, the morphology of the endocytosed vesicles in hypoxia was clearly distinct from the normoxic samples. Noticeable tubular structures that were stained by the FM 1-43 dye resembled the morphology of the TGN. Since other

compartments involved in the membrane trafficking process like early endosomes, recycling endosomes, and late endosomes also contain tubular structures, similarities in the morphology alone were not sufficient for the identification of the dye-loaded cellular structures. By performing immunofluorescence stainings with specific antibodies, the morphology of the different compartments, which are active in the communication between plasma membrane and Golgi apparatus, was analyzed.

Early endosomes function as the first sorting compartments for incorporated molecules in the endocytic pathway. Proceeding from these endosomes, the molecules are distributed to their target sites within the cell. One specific marker for the early endosomes is the peripheral membrane protein EEA1. EEA1 stainings of MDA-MB 231 cells incubated in normoxia (20% O_2) and hypoxia (1% O_2) did not show any significant differences in the intensity of the early endosome staining proving a constant amount of labelled proteins (Figure 11a).

The Golgi apparatus is involved in the secretory/anterograde and the endocytic/retrograde pathway. It consists of flattened membrane-enclosed cisternae and associated vesicles. A striking feature of the Golgi network is the distinct polarity in its function: Proteins which are synthesized in the endoplasmic reticulum enter at the *cis*-Golgi site and are transported to the *trans*-Golgi site. The TGN also receives proteins from the endosomes (retrograde pathway). TGN38 is an integral protein predominantly localized in the *trans*-Golgi network whereas the Golgi matrix protein GM130 is peripherally associated with the *cis*-compartment.

In contrast to the early endosome compartment, the structure of the Golgi apparatus was significantly changed after the incubation of the cells in hypoxia. The intensity of the TGN38 staining was increased (Figure 11b) suggesting an increase in the tagged protein abundance and, thus, a morphological change of the TGN. In contrast, a significant decrease in the intensity of the marker GM130 was observed (Figure 11c).

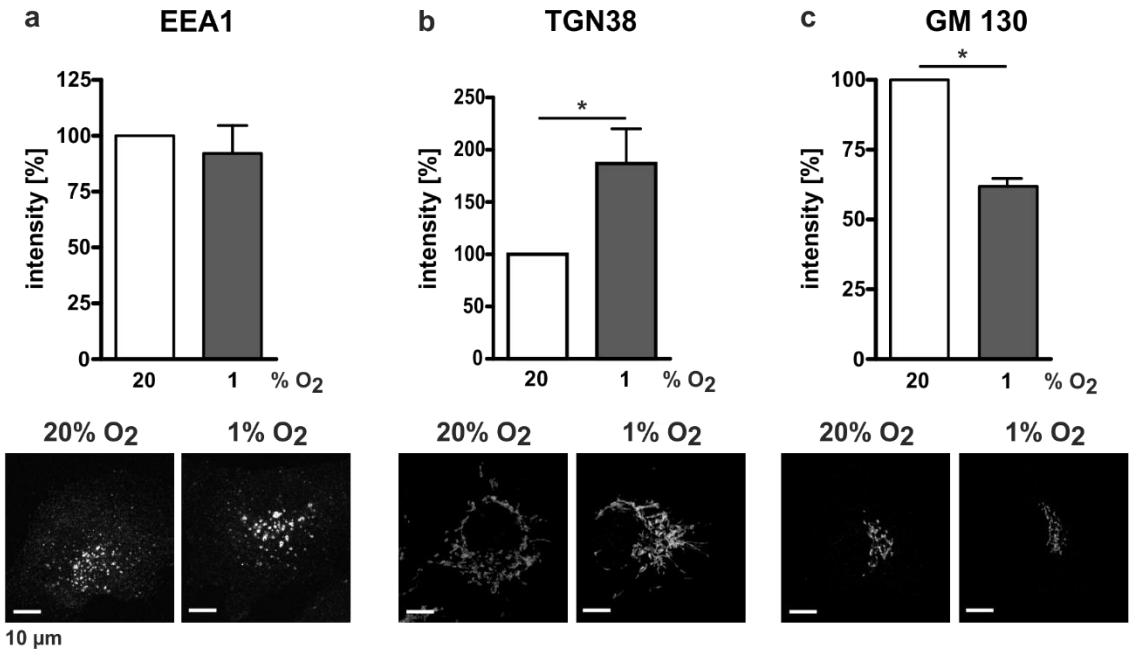

Figure 11: Hypoxia causes changes in the protein composition of the Golgi apparatus. MDA-MB 231 cells grown in normoxia (20% O_2) or hypoxia (1% O_2) for 6 hrs were analyzed for morphological changes in the early endosomes and the *trans*- or *cis*-Golgi apparatus by immunofluorescence stainings of EEA1 (a), TGN38 (b), or GM130 (c). Stained cells were analyzed by confocal microscopy. Data are shown as mean ± SEM as percentage of the 20% O_2 sample, * $p<0.05$ (paired *t*-test). Representative stainings are shown below the graphs. Scale bars: 10 µm. Four (EEA1), eight (TGN38) and four (GM130) independent experiments were analyzed.

Taken together, these results and the enhanced membrane uptake provided initial evidence for a hypoxia-induced enlargement of the *trans*-Golgi network due to an intensification of the retrograde membrane transport.

3.3 Hypoxia promotes retrograde membrane trafficking to the *trans*-Golgi network

3.3.1 The retrograde membrane transport of cholera toxin B subunit is intensified in hypoxia

Based on the hypothesis that hypoxia causes an increase in the retrograde membrane trafficking, the endocytic uptake of several fluorescently labelled cargoes (EGF, trf and cholera toxin) was compared in normoxia and hypoxia in MDA-MB 231 cells to differentiate which incorporation mechanism might be involved in the manifestation of the phenotype.

To analyze the endocytic uptake of cargoes mediated by clathrin-dependent endocytosis in normoxia and hypoxia, EGF and trf were used. Whereas EGF is incorporated directly after interaction with the receptor, the trf receptor is endocytosed constitutively and independently of binding to trf. Upon endocytosis, the molecules are delivered to the early endosomes. EGF is then transported via the late endosomes to the lysosomes, where it is

rapidly degraded. In contrast to this, trf recycles back to the cell surface directly or takes a circuit via the recycling endosome compartment.

The uptake of EGF was unchanged in hypoxia (1% O_2) (Figure 12a), but the incorporation of trf was significantly decreased (Figure 12b).

Furthermore, the cholera toxin B subunit, which is pre-eminently internalized by clathrin-independent means, was tested as a marker molecule. Within the cell, this protein complex is sorted to the TGN and the ER via the retrograde pathway. In contrast to trf and EGF, the cholera toxin B uptake was significantly enhanced after hypoxic induction (Figure 12c).

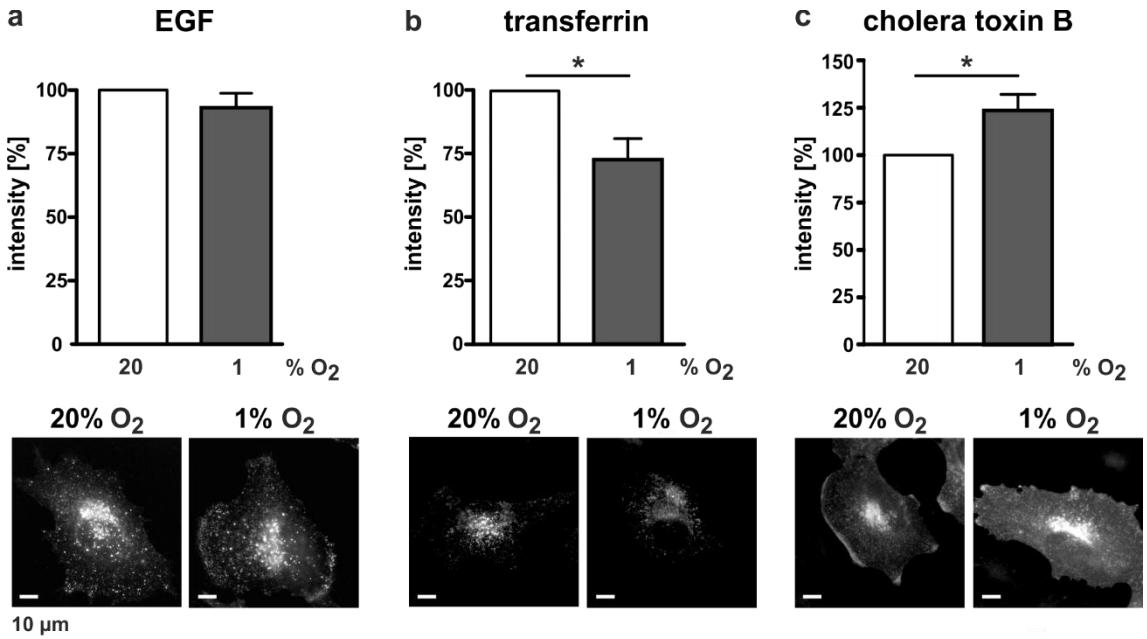

Figure 12: Hypoxia increases the retrograde transport of cholera toxin B. MDA-MB 231 cells grown in normoxia (20% O_2) or hypoxia (1% O_2) for 6 hrs were incubated with fluorescently labelled EGF (a), transferrin (b), or cholera toxin B subunit (c). PFA-fixed cells were analyzed by epifluorescence microscopy. The amount of the transported cargoes was analyzed by determining the fluorescence intensities within the cells. Data are mean ± SEM as percentage of the 20% O_2 sample, * $p<0.05$ (paired *t*-test). Representative stainings are shown below the graphs. Scale bars: 10 µm. Four (EGF and transferrin) or six (cholera toxin B) independent experiments were analyzed in each setup.

To sum up, these experiments unraveled that hypoxia affects specific endocytic pathways: Receptor-mediated and clathrin-dependent endocytosis of trf and its intracellular recycling pathways was significantly impaired. In contrast, retrograde transport of cholera toxin B subunit, which is internalized via various, mainly clathrin- and caveolin-independent routes, to the *trans*-Golgi network was intensified.

3.3.2 Hypoxia induces membrane transport to the *trans*-Golgi network

Ensuing from the hints for altered vesicle transport to and morphological alterations of the TGN, the next set of experiments was planned to further elucidate the identity of the

compartments that are involved in the hypoxia-induced membrane trafficking. For membrane staining the newly developed membrane probe mCLING was applied. mCLING is taken up during endocytosis like the styryl dye FM 1-43, but additionally allows fixation of the samples and co-staining with specific marker proteins.

By determining the Pearson's correlation coefficients of mCLING stained organelles with FITC-labelled marker proteins, a significant colocalization of TGN38 with mCLING stained membranes in hypoxia was detected (Figure 13a). This finding substantiated the changes in the Golgi compartment described above. The alteration in the Golgi composition due to an increased retrograde membrane transport to the TGN was counterbalanced by a decrease in colocalization of the labelled membranes with GM130 and EEA1 (Figure 13b and c).

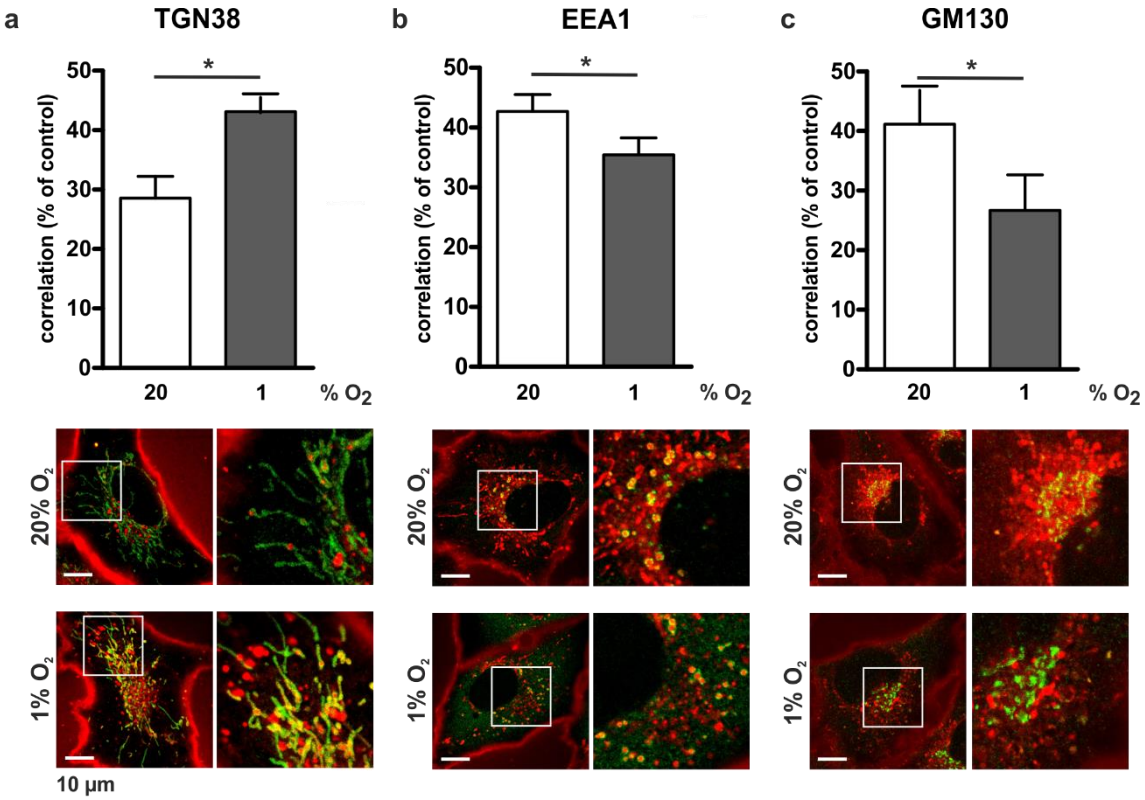

Figure 13: Hypoxia enhances retrograde membrane trafficking to the *trans*-Golgi network. MDA-MB 231 cells exposed to normoxia (20% O_2) or hypoxia (1% O_2) for 6 hrs were incubated for 15 min with mCLING (red), co-stained with antibodies (green) against TGN38 (a), EEA1 (b), or GM130 (c) and imaged by confocal microscopy. Co-localizations of mCLING stained membranes and the indicated marker proteins were analyzed by determining the correlation coefficients using a custom-written MATLAB macro. Data are presented as mean ± SEM as percentage of a positive control showing 100% colocalization. * $p<0.05$ (unpaired *t*-test). Representative co-stainings and a zoom of the stained structures are shown below the graphs. Scale bars: 10 µm. Five independent experiments were analyzed in each setup.

These results verified the aforementioned results and revealed that hypoxia causes an increased membrane transport to the TGN, whereas the trafficking to other organelles like the early endosomes and the *cis*-Golgi is reduced.

3.4 Membrane trafficking in hypoxia is independent of HIF-1α and the HIF-1α regulating PHDs

Many cellular adaptation processes to hypoxia are governed by the transcription factor HIF, which is the key regulator of oxygen-dependent gene expression. HIF is a heterodimer that is composed of an oxygen-regulated α-subunit (HIFα) and a constitutively expressed β-subunit (HIFβ). In normoxic conditions, HIFα is hydroxylated by PHDs and subsequently undergoes proteasomal degradation. As a consequence of oxygen deprivation, HIFα is stabilized, heterodimerizes with HIFβ and the resulting complex induces the expression of hypoxia-related target genes. HIF-1α is the only isoform that is expressed ubiquitously in all nucleated cells. Hence, the role of HIF-1α as a potential regulatory factor of the hypoxia-inducible membrane trafficking was further assessed.

Protein analysis by western blotting demonstrated a significant stabilization of HIF-1α in MDA-MB 231 cells after incubation for 6 and 48 hrs in hypoxia (Figure 14).

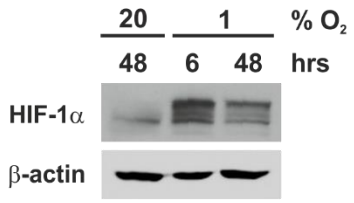

Figure 14: HIF-1α is stabilized in MDA-MB 231 cells incubated in hypoxic conditions. Protein lysates of MDA-MB 231 cells were analyzed by western blotting regarding HIF-1α protein levels in normoxia or after incubation in hypoxia for 6 and 48 hrs. β-actin was used as a loading control.

The amount of stabilized HIF-1α is controlled by the oxygen- and oxoglutarate-dependent PHDs which function as cellular oxygen sensors. Among the three known isoforms, PHD2 is the most abundant and relevant isoform to equilibrate the HIF-1α level in normoxia. To mimic hypoxic conditions, MDA-MB 231 cells incubated in normoxia were treated with the oxoglutarate analogue DMOG, which causes an inhibition of the PHD function.

Treatment of MDA-MB 231 cells with 1 mM DMOG led to a strong stabilization of HIF-1α in normoxia (Figure 15).

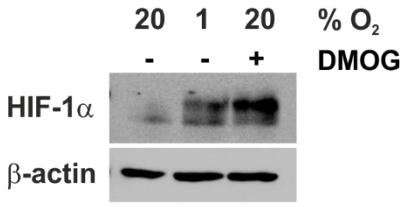

Figure 15: Inhibition of PHD activity with DMOG causes a high HIF-1α protein level in normoxia. MDA-MB 231 cells were exposed for 6 hrs to 20% O_2, 1% O_2 or 1 mM DMOG at 20% O_2. Cells were subsequently lysed and HIF-1α and β-actin protein levels were determined by western blot analysis.

In order to evaluate, if the hypoxia-induced alteration in membrane trafficking is influenced by the activity of the PHDs and the subsequent stabilization of HIF-1α, FM 1-43 stainings were performed in cells treated with DMOG.

As demonstrated above, hypoxia significantly increased membrane trafficking in the control cells. However, the treatment of MDA-MB 231 cells with DMOG did not affect the FM 1-43 uptake pointing to an oxygen sensing and regulation mechanism that is independent of the PHD function (Figure 16).

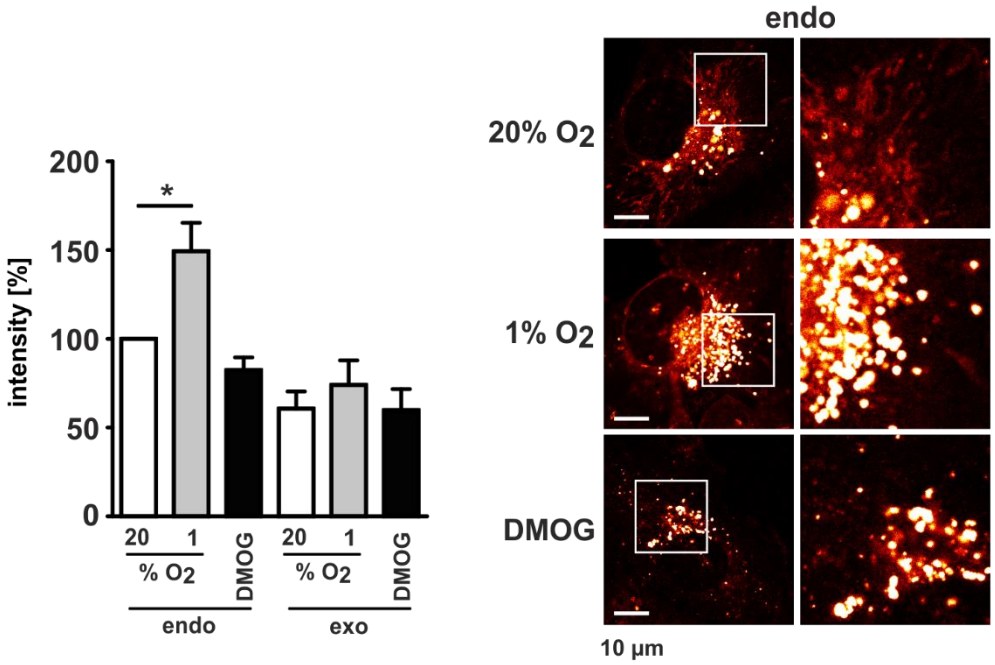

Figure 16: Inhibition of PHDs has no effect on endocytosis. MDA-MB 231 cells were analyzed regarding endocytosis (endo) and exocytosis (exo) activities using the dye FM 1-43 after exposure of the cells to 1 mM DMOG or a solvent control for 6 hrs in 20% O_2 or 1% O_2. Data are shown as mean ± SEM as percentage of the 20% O_2 sample, * $p<0.05$ (paired *t*-test). Representative stainings of the endo samples analyzed by confocal microscopy and zooms of the stained structures are shown on the right. Scale bars: 10 µm. Four independent experiments were analyzed in each setup.

3.4.1 MDA-MB 231 shHIF-1α cells demonstrate a HIF-1α independent hypoxia-induced membrane trafficking

To further investigate, if the hypoxia-induced membrane trafficking is mediated via HIF-1α, studies in different HIF-1α-deficient cell types were performed. Firstly, MDA-MB 231 cells stably transduced with a shRNA targeting HIF-1α were analyzed at protein level.

The protein analysis of shHIF-1α cells, in which specifically the expression of HIF-1α was reduced, showed no HIF-1α-stabilization neither in normoxic nor in hypoxic conditions proving an effective knockdown of HIF-1α (Figure 17).

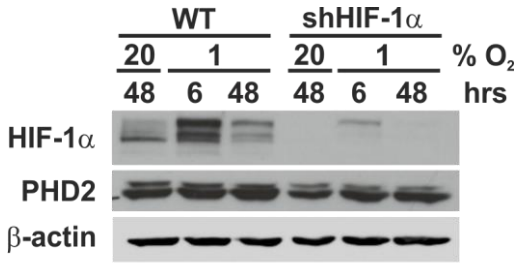

Figure 17: MDA-MB 231 shHIF-1α cells exhibit decreased levels of HIF-1α. MDA-MB 231 wt cells (WT) and MDA-MB 231 cells constitutively expressing a shRNA targeting HIF-1α (shHIF-1α) were incubated in normoxic and hypoxic conditions for 6 or 48 hrs. Protein extracts were analyzed by western blotting using HIF-1α and PHD2 antibodies. β-actin was chosen as a loading control.

To analyze, if the transcription factor HIF-1α is involved in regulating the membrane trafficking, the HIF-1α knockdown cells were stained with FM 1-43.

As described above, the exposure of MDA-MB 231 wt cells to hypoxia resulted in an increased uptake of FM 1-43. FM-studies with HIF-1α-deficient MDA-MB 231 cells also revealed this hypoxia-induced phenotype despite their inability to stabilize HIF-1α in hypoxia providing further evidence that HIF-1α does not mediate the increased membrane trafficking in hypoxic conditions (Figure 18).

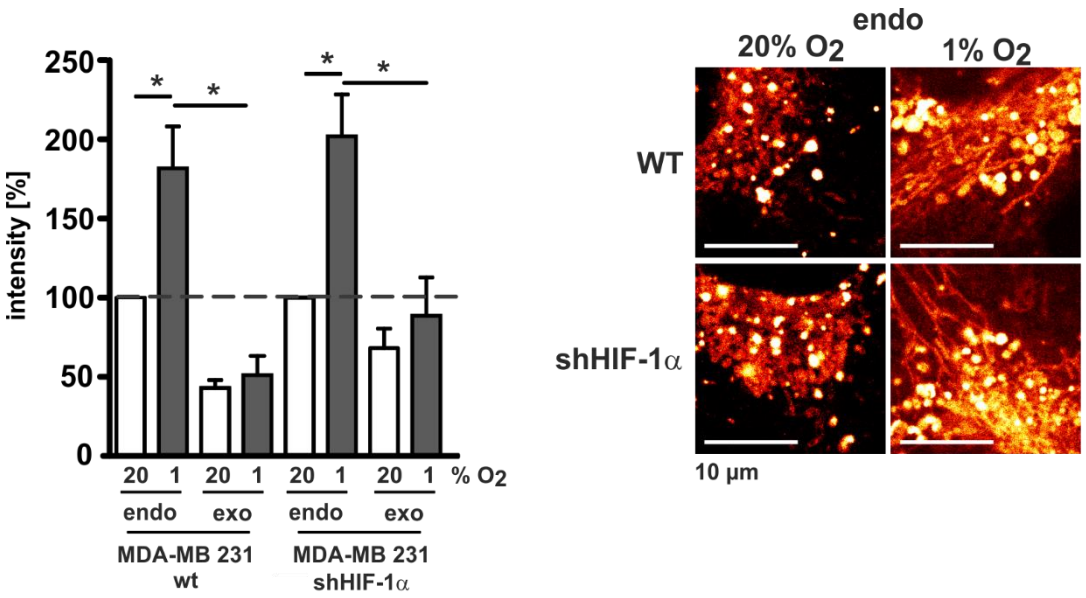

Figure 18: Hypoxia-induced membrane trafficking is independent of HIF-1α. MDA-MB 231 wt cells and MDA-MB 231 shHIF-1α cells were analyzed regarding their endocytosis (endo) and exocytosis (exo) activities applying the dye FM 1-43 after exposure to normoxic (20% O_2) or hypoxic (1% O_2) conditions for 6 hrs. Data are shown as mean ± SEM as percentage of the 20% O_2 sample, * $p<0.05$ (paired *t*-test). Representative stainings of the endo samples analyzed by confocal microscopy are shown next to the graph. Scale bars: 10 µm. Six independent experiments were analyzed in each setup.

3.4.2 Analysis of mouse embryonic fibroblasts excluded an importance of HIF-1α for the hypoxia-mediated membrane trafficking

To further validate the finding obtained with MDA-MB 231 shHIF-1α cells, additional FM 1-43 experiments with MEF cells were conducted. MEF+/+ cells were originally isolated from wild type mouse embryos. MEF-/- cells, which were obtained from HIF-1α knockout embryos, display a HIF-1α loss of function phenotype. In our study MEF wt cells were stably transfected with a shRNA targeting PHD2 to generate a HIF-1α gain of function phenotype. A western blot was performed to confirm the HIF-1α knockout and the PHD2 knockdown at the protein level.

The protein analysis of MEF-/- cells demonstrated a lack of HIF-1α expression in hypoxia. In contrast, shPHD2 cells showed an increase in the HIF-1α protein levels in normoxic conditions (20% O_2) (Figure 19).

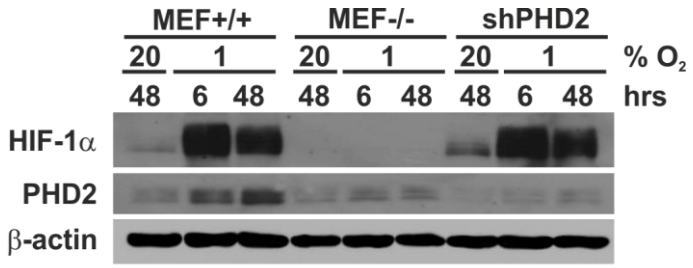

Figure 19: MEF-/- cells show no HIF-1α expression whereas MEF shPHD2 cells stabilize HIF-1α in normoxic conditions. MEF+/+, MEF-/- and MEF shPHD2 cells were incubated in normoxic and hypoxic conditions for 6 or 48 hrs. Cells were lysed and protein extracts were analyzed by western blotting applying anti-HIF-1α and anti-PHD2 antibodies. β-actin was used as a protein loading control.

In MEF+/+ cells increased membrane trafficking could be detected subsequent to hypoxic induction similar to the effect observed in human MDA-MB 231 wt cells. This observation evinces that the hypoxia-induced phenotype is not species- or cell type-specific.

FM-studies with MEF-/- cells carrying the HIF-1α knockout and MEF shPHD2 cells showing high levels of HIF-1α in normoxia and hypoxia also displayed an enhanced uptake of FM 1-43 in hypoxia. This finding excluded that the transcription factor HIF-1 affects the hypoxia-induced endocytosis phenotype (Figure 20).

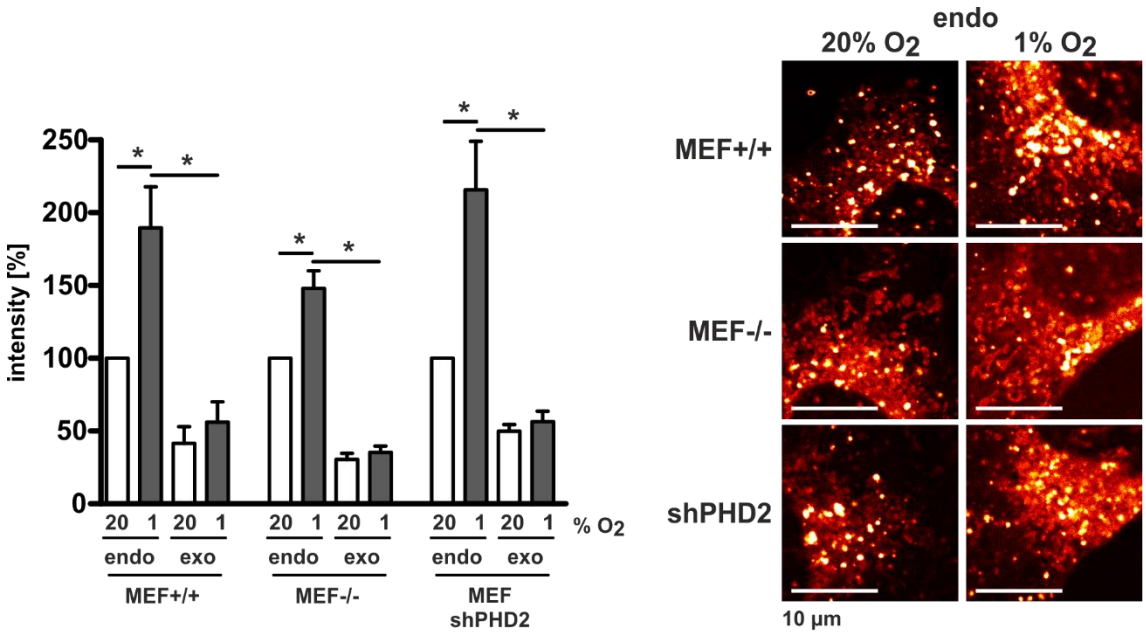

Figure 20: Membrane trafficking in hypoxia is independent of HIF-1α. MEF+/+, MEF-/- and MEF shPHD2 cells were analyzed regarding endocytosis (endo) and exocytosis (exo) activities using the dye FM 1-43 after exposure of the cells to 20% O_2 or 1% O_2 for 6 hrs. Data are shown as mean ± SEM as percentage of 20% O_2 sample, * $p<0.05$ (paired *t*-test). Representative stainings of the endo samples analyzed by confocal microscopy are shown on the right. Scale bars: 10 µm. Six independent experiments were analyzed in each setup.

In conclusion, the results so far indicate that the hypoxia-induced increase in membrane trafficking is regulated by a HIF-1α-independent oxygen sensing and adaptation machinery.

3.5 T-plastin mediates the increased retrograde transport in hypoxia

3.5.1 T-plastin is recruited to the plasma membrane in hypoxia

To approach the underlying molecular mechanism of the hypoxia-induced increased retrograde transport, the group of Prof. Katschinski analyzed the differential abundance of membrane and membrane-associated proteins in MDA-MB 231 cells after preincubation in normoxia or hypoxia by performing a SILAC screen (Wottawa et al. 2017). Interestingly, among the 81 proteins, which were identified to be above twofold more abundant in the membranes in hypoxia (1% O_2), all known members of the plastin family, i.e. I-plastin, L-plastin and T-plastin were found. Plastins are actin-bundling proteins, which have been reported to be involved in actin-mediated endocytosis. Furthermore, studies provided initial evidence that the function of plastin proteins is influenced by hypoxia. Therefore, their role in the hypoxia-inducible membrane trafficking mechanisms was further analyzed.

First, the increased abundance of T-plastin in the plasma membrane in hypoxia was validated by western blot analysis of cytoplasmic and membrane protein extracts (Figure 21). Whereas the cytosolic protein fraction did not demonstrate any alterations in the protein amount of T-plastin in hypoxic conditions compared to normoxic conditions, the T-plastin protein abundance in the plasma membrane fraction was significantly enhanced in hypoxia. Thus, the western blot analysis confirmed the findings previously obtained in the SILAC screen.

Exclusively T-plastin could be detected at protein level by western blotting using commercially available antibodies. A reason for this finding could be the low protein abundance of I- and L-plastin in MDA-MB 231 cells due a cell type-specific expression of the isoforms. This assumption was substantiated by mass spectrometry that revealed a significantly lower abundance of I- and L-plastin in comparison to T-plastin in MDA-MB 231 cells (Wottawa et al. 2017).

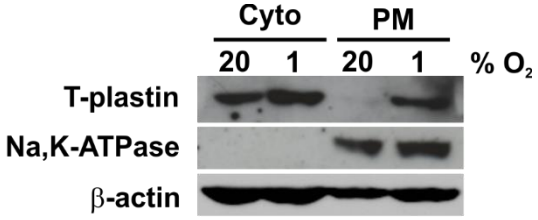

Figure 21: T-plastin is recruited to the plasma membrane in hypoxia. MDA-MB 231 cells were incubated in normoxia (20% O_2) or hypoxia (1% O_2) for 6 hrs. Subsequently, cytosolic (Cyto) and membrane (PM) proteins were isolated and analyzed for the abundance of T-plastin by western blotting. β-actin was used as a protein loading control. The plasma membrane protein Na,K-ATPase was used as a control for the efficiency and purity of the membrane protein extraction.

To address the question, if the increased abundance of I-plastin, L-plastin and T-plastin in the membrane fraction was due to enhanced transcription, their RNA levels were determined by qRT PCR.

The mRNA expression of all analyzed plastin isoforms was not altered in hypoxia compared to normoxia excluding the hypothesis that the expression of plastins is regulated at the mRNA level (Figure 22). As a positive control for the successful cultivation of the cells in hypoxia, the well described hypoxia-inducible expression of *PHD3* was utilized. PHD3 mRNA levels were found to be increased by more than tenfold in hypoxia.

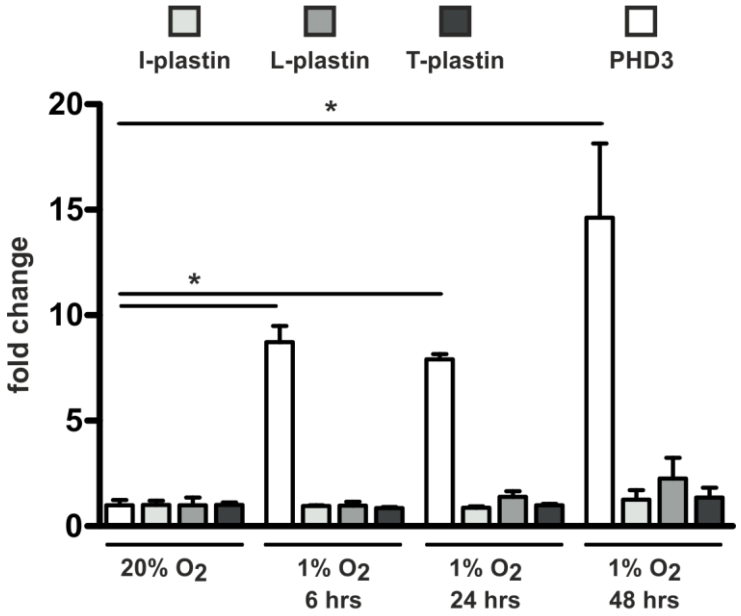

Figure 22: I-, L- or T-plastin mRNA levels are not altered in hypoxic conditions. PHD3, I-, L- and T-plastin mRNA levels were quantified by qRT PCR in MDA-MB 231 cells grown in normoxia (20% O_2) or hypoxia (1% O_2) for 6 or 48 hrs. The mRNA levels acquired at 20% O_2 were set to 1. * $p<0.05$ (unpaired *t*-test).

In conclusion, the increase of the protein amount of T-plastin in the plasma membrane in hypoxic conditions was not caused by enhanced transcription. These findings imply that the elevated T-plastin protein abundance in the plasma membrane in hypoxia originates from a spatial redistribution of the protein within the cell.

3.5.2 Plastin knockdown cells were established for further analysis

To gain further insight into the role of the plastins in the hypoxia-induced membrane trafficking, stably transduced cells expressing a shRNA targeting either I-, L- or T-plastin (shI-plastin, shL-plastin and shT-plastin) were established in the group of Prof. Katschinski.

The knockdown efficiency of all three plastin shRNA cell lines was analyzed by quantification of I-, L- or T-plastin mRNA levels using qRT PCR. The knockdown efficiency of I-, L- or T-plastin at the RNA level was > 90% in all three cell clones (Figure 23).

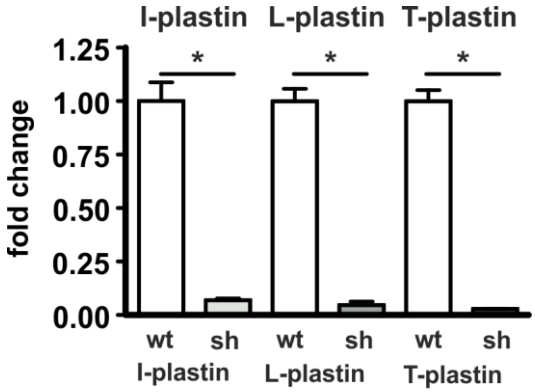

Figure 23: Determination of knockdown efficiency demonstrates successful downregulation of I-, L- or T-plastin in the respective knockdown cells. I-, L- or T-plastin mRNA expression was assessed in MDA-MB 231 wt cells or cells, which were stably transduced with a shRNA targeting either I-, L-, or T-plastin. All cell lines were incubated in normoxic conditions. mRNA levels obtained in wt cells were set to 1. * $p<0.05$ (unpaired *t*-test).

The specific knockdown of T-plastin in MDA-MB 231 cells was corroborated at protein level in a western blot (Figure 24). In shT-plastin cells T-plastin expression was neither detected in normoxic nor under hypoxic conditions.

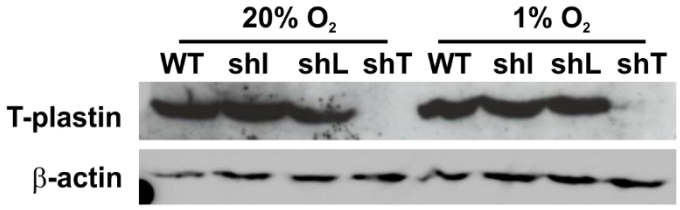

Figure 24: T-plastin knockdown cells show a reduction of T-plastin protein. The T-plastin protein amount was determined by western blot analysis of whole cells extracts isolated from MDA-MB 231 wt cells (WT) or stably transduced cells expressing a shRNA targeting I-, L-, or T-plastin (shI, shL, shT). Cells were either incubated in normoxia (20% O_2) or in hypoxia (1% O_2) for 6 hrs. β-actin was used as protein loading control.

Western blots are not shown for shI- and shL-plastin cells since the respective proteins could not be detected by western blotting with commercially available antibodies.

3.5.3 Knockdown of T-plastin impairs hypoxia-induced membrane trafficking

FM 1-43 studies in MDA-MB 231 wt cells and plastin knockdown clones preincubated in normoxia and hypoxia were conducted to further investigate the influence of I-, L- or T-plastin on the hypoxia-induced membrane trafficking.

As described above, in MDA-MB 231 wt cells the fluorescence intensity was greatly enhanced after incubation in hypoxia for 6 hrs compared to normoxia. The hypoxic induction of membrane uptake was also detectable in the I-plastin and L-plastin knockdown cells. Notably, the membrane trafficking activity in hypoxic T-plastin knockdown cells was significantly blunted revealing a mediating role for T-plastin in the hypoxia-induced membrane trafficking (Figure 25).

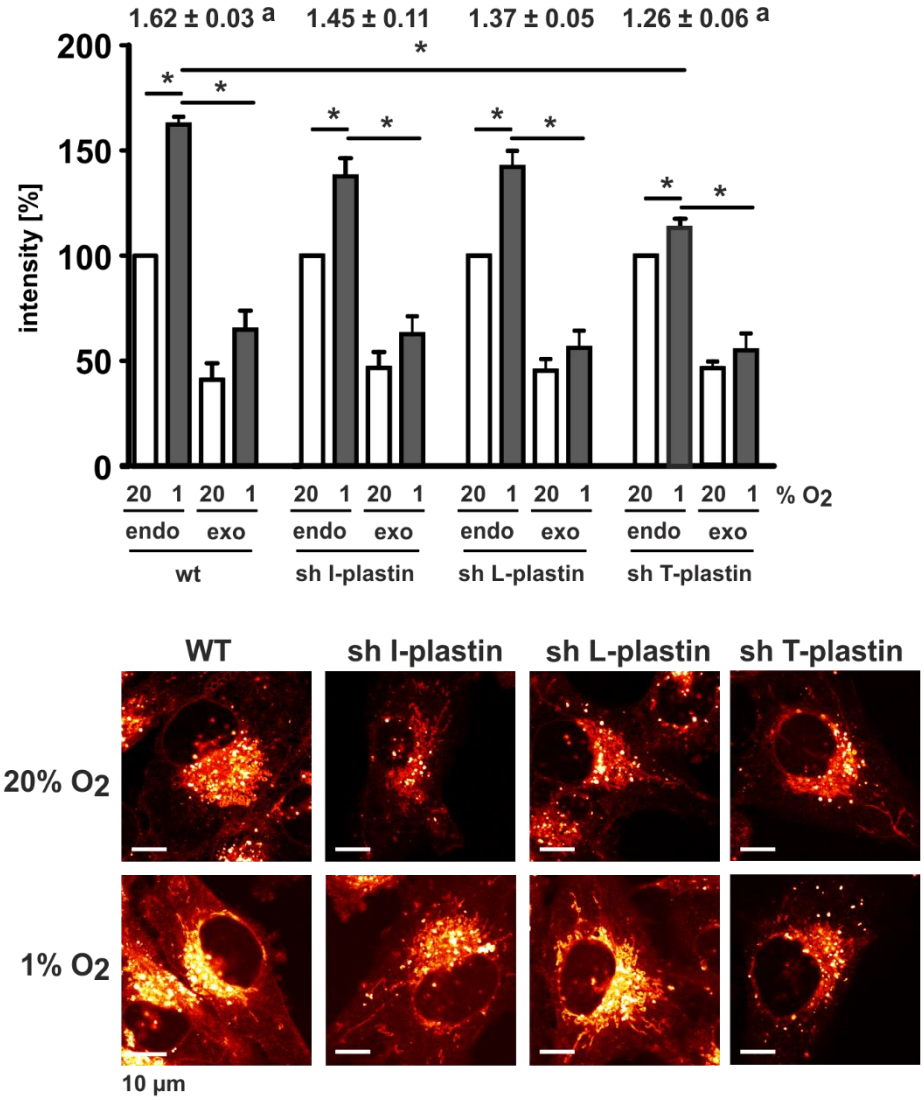

Figure 25: Knockdown of T-plastin impairs hypoxia-induced membrane trafficking. Endocytosis (endo) and exocytosis (exo) activities were analyzed in MDA-MB 231 wt cells (WT) or MDA-MB 231 cells, which were stably transduced with the indicated shRNAs, by applying the dye FM 1-43 after exposure of the cells to 20% O_2 or 1% O_2 for 6 hrs. Numbers above the bars indicate the induction factor in hypoxia compared to normoxia for each cell line (mean ± SEM). Data are mean ± SEM as percentage of 20% O_2, * $p<0.05$ (paired *t*-test), a $p<0.05$ (unpaired t-test). Representative stainings of the endo samples analyzed by confocal microscopy are shown below the graph. Scale bars: 10 µm. Seven independent experiments were analyzed in each setup.

To conclude, this observation suggests that the recruitment of T-plastin to the plasma membrane in hypoxia is involved in the intensified membrane trafficking induced by hypoxia.

4 Discussion

Endosomal traffic between the plasma membrane and membrane-enclosed compartments is a crucial mechanism of eukaryotic cells to interact with their environment. It enables cells to preserve their homeostasis by accomplishing a huge variety of specific tasks such as the control of receptor signaling and the regulation of the plasma lipid and protein composition (Doherty and McMahon 2009). Defects in vesicle trafficking are associated with cancerous and neurodegenerative diseases, some of which are also linked to hypoxic conditions that can influence the progression and outcome of diseases (Howell et al. 2006; Mosesson et al. 2008; Olkkonen and Ikonen 2006; Semenza 2011).

Several studies have revealed that hypoxia modifies vesicle internalization and processing resulting in dysregulated signaling and changed protein expression at the cell surface (Bourseau-Guilmain et al. 2016; Dada et al. 2003; Menard et al. 2016; Wang et al. 2009; Yoon et al. 2005). Adaptation to hypoxia leads to profound changes of the metabolism. Oxygen deprivation also entails a reorganization of the actin meshwork through actin-binding proteins (Chang et al. 2012; Vogler et al. 2013; Zieseniss 2014). Actin-binding proteins coordinate the actin architecture, can associate to the plasma membrane and are thereby involved in vesicle formation and transport (Bezanilla et al. 2015).

Many hypoxia-induced alterations are governed at the transcriptional level by the master regulator HIF. HIF-1α stabilization is dependent on oxygen sensitive regulation of this subunit via PHDs (Bruick and McKnight 2001; Epstein et al. 2001). In normoxic conditions, PHD2 is the main isoform to adjust the degree of HIF-1α stabilization. In previous studies, changes in the endocytic machinery have been shown to be directly regulated by PHDs or due to HIF-1α stabilization (Garvalov et al. 2014; Wang et al. 2012).

Despite the emerging evidence for hypoxia influencing membrane trafficking, the overall membrane turnover in scarce oxygen conditions has not been elucidated yet. The aim of this thesis was therefore to examine the effect of hypoxia on endosomal membrane dynamics.

4.1 Hypoxia induces increased membrane trafficking

The wholesale membrane trafficking activity of MDA-MB 231 and MEF cells was determined by making use of the styryl membrane dye FM 1-43. The membrane probe FM 1-43 is a suitable and well established dye to track vesicle internalization and trafficking because of its property to specifically stain the membrane bilayer and not the vesicle content (Henkel et al. 1996). Notably, FM uptake is independent of specific endocytic mechanisms and consequently allows to evaluate the global membrane turnover irrespective of the underlying pathway (Betz et al. 1992; Gaffield and Betz 2006).

We report that scarce oxygen availability causes changes in the endomembrane system by intensifying membrane uptake. This phenotype can be provoked owing to short- (6 hrs) and long-term (48 hrs) hypoxia. The endocytic capacity was determined by measurement of the staining intensity. The fluorescence intensity in FM stained samples is proportional to the amount of membrane internalized via endocytosis, hence displaying a possibility to quantify membrane trafficking (Gaffield and Betz 2006; Henkel et al. 1996). Accordingly, destaining reflects exocytosis since vesicle fusion with the plasma membrane is the only way for FM to leave the cell (Henkel et al. 1996). Thus, the observed drop in fluorescence intensity in cells that were allowed to undergo exocytosis provides a reliable proof for the integrity of the endosomal traffic and the viability of the cells as exocytosis is an active process that only can be accomplished by viable cells.

To our knowledge, this is the first study analyzing total membrane turnover in hypoxic conditions. So far, exclusively alterations of protein internalization owing to oxygen deprivation have been investigated. Bourseau-Guilmain et al. demonstrated a general downregulation of protein internalization due to hypoxia by using reversible membrane protein labelling and fluorescence-activated cell sorting (FACS) combined with confocal microscopy imaging and quantitative proteomics analysis (Bourseau-Guilmain et al. 2016). Based on the techniques applied, Bourseau-Guilmain et al. examined a hypoxia-dependent mechanism affecting protein turnover, which cannot be equated with membrane trafficking.

Increased membrane uptake in hypoxia was verified by an additional staining method with the non-lipophilic membrane marker wheat germ agglutinin (WGA) conducted in the Institute for Cardiovascular Physiology (Wottawa et al. 2017). WGA is a lectin that marks membranes by binding N-acetyl-D-glucosamyl and sialic acid residues present on the cell surface (Ranftler et al. 2013). Hence, this staining method is based on a completely different kind of interaction with the membrane than FM and consequently displays an appropriate approach to validate the results obtained by application of the styryl dye.

The hypoxia-induced increase in membrane trafficking activity was not restricted to the human malignant epithelial cell line MDA-MB 231 as comparable results were obtained in benign mouse embryonal fibroblasts. Similar findings were acquired in further experiments performed in primary neonatal rat cardiac fibroblasts and primary neonatal tail cardiac fibroblasts by the Dr. med. candidate J. Böttger in the Institute of Cardiovascular Physiology (Wottawa et al. 2017). In conclusion, the hypoxia-inducible membrane-trafficking phenotype was shown not to be cell type- or species-specific and thus represents a fundamental biological mechanism.

4.2 Hypoxia affects endocytosis and retrograde transport to the Golgi apparatus

4.2.1 Hypoxia controls distinct endocytic pathways in a specific manner

Hypoxia causes a decrease in the wholesale proteome internalization, but notably, rather affects distinct uptake mechanisms in a specific manner than provoking a general downregulation of all endocytic pathways (Bourseau-Guilmain et al. 2016). So far, clathrin- and caveolae-mediated, but also dynamin-dependent membrane raft endocytosis have been demonstrated to be influenced by the availability of oxygen (Bourseau-Guilmain et al. 2016; Dada and Sznajder 2007; Wang et al. 2012; Wang et al. 2009; Yu et al. 2016).

Membrane uptake as one component of membrane trafficking is accomplished by the entirety of endocytic mechanisms. To correlate our results with preexisting knowledge on hypoxia-influenced pathways and acquire hints, which endosomal pathways may participate in the hypoxia-induced membrane trafficking process, we performed endocytosis assays with pathway-specific marker proteins. By tracking fluorescently labelled EGF, the receptor-dependent CME was tested. Our experimental setting did not reveal any impact of hypoxia on EGF internalization and intracellular trafficking which is contradictory to previous reports. Wang et. al reported a delay in intracellular EGF trafficking causing a more intense staining signal (Wang et al. 2009). This discrepancy in the results could be explained by the choice of different time points as we performed the EGF endocytosis assays after 6 hrs of hypoxic incubation vs. 24 hrs exposure to hypoxia set by Wang et al..

We further assessed constitutive CME of the trf receptor and detected a decrease in trf internalization in acute hypoxia (6 hrs) after incubation with the marker for 10 min. This is in line with results obtained by Wang et al. looking at trf internalization in VHL knock out cells 30 min after exposition to the marker (Wang et al. 2009). In contrast, these findings are however not in keeping with data provided by Bourseau-Guilman et al. who analyzed trf uptake by FACS after 20 hrs of hypoxic incubation (Bourseau-Guilmain et al. 2016). The decrease in trf uptake was verified by additional experiments probing trf aptamer internalization conducted in the Institute of Cardiovascular Physiology (Wottawa et al. 2017). The trf aptamer has been shown to reliably report endocytosis since medium-accessible molecules are removed in the sample workup, thereby excluding the quantification of non-internalized fluorescence (Wilner et al. 2012).

In order to consider clathrin-independent pathways, the uptake of cholera toxin B subunit, which is endocytosed via membrane-rafts, was investigated. Cholera toxin uptake was increased upon hypoxic incubation. Bourseau-Guilman et al. also found this molecule to be a member of the selective group of proteins that override the general downregulation of protein uptake upon hypoxic induction and display increased internalization (Bourseau-Guilmain et al. 2016).

To sum up, our results corroborated a pathway-specific impact of hypoxia on the endocytic uptake of proteins. For in-depth elucidation of the affected endocytic mechanisms, the application of specific inhibitors blocking selective modes of endocytosis might be useful. However, it has to be considered that the balance between the endocytic uptake mechanisms can be impaired by these inhibitors causing incorrect results.

4.2.2 Hypoxia favors retrograde transport and causes morphological changes of the *trans*-Golgi network

Membrane trafficking encompasses the secretory pathway of eukaryotic cells sending vesicles from the endoplasmic reticulum (ER) via the Golgi apparatus to the plasma membrane, but also the retrograde transport system delivering cargo back to the Golgi apparatus (Bonifacino and Rojas 2006). Cholera toxin is an appropriate marker to visualize the retrograde pathway (Sandvig and van Deurs 2005). Thus, the increase of cholera toxin uptake provided first evidence that hypoxia might affect retrograde endosomal trafficking to the TGN.

So far, reports on hypoxia-influenced vesicle trafficking have focused on the recycling pathway which is controlled by Rab4 and Rab11 and the degradation pathway regulated by Rab7 (Wang et al. 2009; Yoon et al. 2005; Yu et al. 2016). Particular attention was directed to the early endosomes. Wang et al. described a delay in EGF receptor endocytosis due to HIF-dependent repression of rabaptin 5, a Rab5 effector, causing disturbed vesicle fusion (Wang et al. 2009).

We utilized fluorescently labelled antibodies and the membrane probe mCLING to identify the compartments involved in hypoxia-induced membrane trafficking. In contrast to FM, mCLING is a novel membrane probe which does not detach from the membrane due to fixation and allows for co-staining with fluorescently labelled antibodies, thus permitting the characterization of membrane-bound organelles (Revelo et al. 2014).

The colocalization of differentially labelled protein and membrane markers detected by fluorescence microscopy can be determined visually by evaluating the distribution of intermediate color (e.g. yellow) resulting from superposition of the respective two channels (e.g. channel one: red and channel two: green). In addition, the quantification of colocalization is a necessary prerequisite to compare different testing conditions. The calculation of the Pearson's correlation coefficient is a standard protocol in biomedical research to determine a value for the extent of colocalization in fluorescence microscopy (Dunn et al. 2011).

Simultaneous staining of the vesicles with mCLING and a fluorescently labelled antibody that was directed against TGN38 revealed an increment in the colocalization of the *trans*-Golgi marker with the membrane dye upon hypoxic exposure. This finding confirms firstly that the membrane-enclosed vesicles are indeed sent to the TGN and secondly that the retrograde membrane transport to the TGN compartment is stimulated in hypoxia.

Colocalization studies with early endosome and *cis*-Golgi markers displayed a reduced membrane transport to these compartments upon hypoxic incubation and imply, that in hypoxia membrane is sent from the early endosomes and the *cis*-Golgi to the TGN.

Further analysis of the Golgi apparatus using solely fluorescently labelled antibody stainings revealed a hypoxia-induced change in the protein composition of the Golgi network pointing to an altered morphology of the TGN, which is consistent with an intensified retrograde transport in virtue of hypoxia.

The Golgi apparatus is an important sorting and modification station for proteins, thus, competent to regulate the protein abundance and activity of surface proteins according to the cellular requirements. A prior study in AEC has revealed altered vesicle trafficking and an enlargement of the Golgi apparatus in hypoxia. These changes were associated with a loss of endothelial nitric oxide synthase (eNOS) from the cell surface and its internal sequestration (Mukhopadhyay et al. 2007). Taking this finding into consideration, one might speculate, that the functional consequence of the hypoxia-induced membrane trafficking is the regulation of membrane protein abundance and activity as one component of the cellular answer to compromising oxygen levels.

Apart from the Golgi network, the morphology of the early endosomes was examined. EEA1 stainings did not display any morphological differences in hypoxic conditions which stands in contrast to studies performed by Wang et al. who described a hypoxia-associated reduction of the early endosome size due to an impairment of Rab5-mediated vesicle fusion (Wang et al. 2009). Future experiments involving different Rab-loss of function or gain of function cells could help to determine the exact endosomal compartments affected by hypoxia since Rab GTPases specifically determine organelle identities and their function (Pfeffer 2013; Wandinger-Ness and Zerial 2014). An additional approach to visualize the trafficking pathways affected by hypoxia might include tagged Rab proteins. Protocols that detail the use of, e.g. GFP-fusion proteins and time-lapse imaging to track membrane-bound organelles in living cells can be found in the literature (Snapp and Lajoie 2011). However, fusion of a protein with a fluorescent tag might compromise the native function of the molecule and perturb physiological membrane transport, thereby evoking wrong findings.

Taken together, we report that hypoxia causes wholesale changes to the endomembrane system by promoting retrograde transport to the TGN.

4.3 T-plastin mediates the hypoxia-induced increase in retrograde membrane transport

4.3.1 T-plastin is involved in hypoxia-induced membrane trafficking

Actin-binding proteins orchestrate actin organization and act as an interface between the membrane and the actin network, thereby facilitating essential cellular functions such as endocytosis (Bezanilla et al. 2015). It has been demonstrated that the actin cytoskeleton is modulated owing to hypoxic exposure possibly, albeit partially, via hypoxia-regulated activity of actin-binding proteins, e.g. cofilin (Vogler et al. 2013; Zieseniss 2014).

A proteome screen, which was conducted to determine the membrane- and membrane-bound proteins that were more abundant on the cell surface in hypoxia led to the identification of many actin-bundling proteins such as transgelin, fascin, and all members of the plastin family (Wottawa et al. 2017). Interestingly, previous studies in yeast have highlighted a major role for the plastin homolog Sac6 in the cellular adaptation to hypoxic conditions. Chang et al. showed that an accurate actin architecture administered by Sac6 is critical for cell growth in hypoxia (Chang et al. 2012). Furthermore, this study described endocytosis to be impaired in the Sac6 deletion mutant.

Actin-bundling proteins have been reported to participate in actin-mediated endocytosis by providing an actin network that generates the forces required for vesicle inward movement at endocytic sites (Kaksonen et al. 2005; Skau et al. 2011). In mammalian cells, T-plastin has been shown to not only structure the actin cytoskeleton but also to fine-tune actin dynamics beyond its cross-linking feature (Giganti et al. 2005). Concrete evidence for an involvement of plastins in endocytic events of mammalian cells was provided by a study investigating cargo internalization in L- and T-plastin overexpressing Cos-1 cells. L- and T-plastin were shown to interact with the early endosome marker Rab5 and overexpression of the actin-bundling proteins resulted in intensified fluid-phase endocytosis (Hagiwara et al. 2011).

A regulatory role for T-plastin in the endocytosis of mammalian cells was confirmed by Hosseinibarkooie et al. (Hosseinibarkooie et al. 2016). The research group defined reduced endocytosis due to a survival motor neuron protein deficit as a pathomechanism underlying spinal muscular atrophy. Overexpression of T-plastin successfully restored endocytosis, in particular fluid-phase uptake, to normal levels and hence protected against the manifestation of the phenotype (Hosseinibarkooie et al. 2016).

Consequently, we were interested in the role of plastins in the hypoxia-induced membrane trafficking. Analysis of membrane trafficking in T-, I- and L-plastin knockdown cells exhibited T-plastin to be involved in mediating the hypoxia-induced phenotype. With regard to the aforementioned results that describe a role for plastins in fluid-phase uptake, additional experiments to clarify the role of fluid-phase endocytosis in the T-plastin-

mediated hypoxia-induced membrane trafficking were conducted in the Institute for Cardiovascular Physiology. By using the fluorescent marker calcein it was found that fluid-phase uptake was not altered in the T-plastin controlled hypoxic phenotype (Wottawa et al. 2017). This finding contrasts with the results obtained by Hagiwara et al. and Hosseinibarkooie et al. who showed fluid-phase endocytosis to be influenced by the expression level of T-plastin (Hagiwara et al. 2011; Hosseinibarkooie et al. 2016). Since every study applied different marker molecules to test for alterations in fluid-phase uptake, supplementary experiments should include Lucifer yellow stainings previously chosen by Hagiwara et al. and FITC-dextran analysis used by Hosseinibarkooie et al. to enhance comparability of the results (Hagiwara et al. 2011; Hosseinibarkooie et al. 2016).

Notably, exclusively T-plastin was found to be involved in controlling the hypoxia-induced phenotype. The plastin isoforms are expressed in a cell- and tissue-specific manner: I-plastin is predominantely expressed in intestinal cells, whereas L-plastin expression prevails in hematopoetic cells and non-hematopoetic malignant cells (Lin et al. 1988; Lin et al. 1994; Revenu et al. 2012; Samstag and Klemke 2007; Shin et al. 2013). In contrast, the expression of T-plastin was established for many different cells types (Lin et al. 1988). Hence, the isoform-dependent effect could be explained by the more general expression and function of T-plastin.

4.3.2 Hypoxia influences the spatiotemporal distribution of T-plastin

Based on the aforementioned findings, the question, how the regulation of T-plastin activity in hypoxia is mechanistically arranged, emerged. First of all, the increased abundance of T-plastin in the plasma membrane due to hypoxia detected in the proteome screen was verified by western blot analysis of the membrane protein fraction. Increased T-plastin abundance was not caused by enhanced T-plastin transcription as substantiated by measurement of mRNA using RT qPCR and T-plastin protein amount using western blot analysis. From this finding, we inferred that the increased abundance of T-plastin in the membrane fraction could be explained by a redistribution of the actin-bundling protein to the plasma membrane owing to hypoxia.

In order to investigate the spatiotemporal regulation of the isoforms L- and I-plastin, mRNA and protein analysis were performed in an analogous manner. L- and I-plastin transcription was not altered due to oxygen deprivation similarly to T-plastin. Assessment of protein levels for L- and I-plastin by western blot analysis was not possible when applying commercially available antibodies. This finding could be attributed to the low abundance of I- and L-plastin proteins in MDA-MB 231 cells which had already been discovered in the mass spectrometry analysis that displayed a 1 - 2 log difference in the intensity values obtained for T-plastin compared to I- and L-plastin (intensities: T-plastin: 4.79×10^{11}, L-plastin: 2.61×10^{9}, and I-plastin: 5.33×10^{10}) (Wottawa et al. 2017).

F-actin network organization had already been known to be controlled by spatiotemporal regulation of actin-binding proteins (Bezanilla et al. 2015). Thus, hypoxia-induced recruitment of T-plastin to the plasma membrane leading to a modification of the actin-meshwork appears to be a plausible concept for explaining the underlying mechanism that mediates the hypoxia-induced membrane trafficking. To further support this assumption, Dr. rer. nat. G. J. C. van Belle from the Institute of Cardiovascular Physiology assessed the actin filament density in hypoxia compared to normoxia by utilizing electron microscopy. After exposure of MDA-MB 231 wt cells to hypoxia, the cytoskeleton was reorganized and presented an increased density (Wottawa et al. 2017). This effect could not be reproduced in T-plastin knockdown cells demonstrating that actin bundling by T-plastin is indeed involved in the characterized cellular response to hypoxia. However, the regulatory mechanism linking oxygen availability to changes in the plastin activity remains elusive.

Rho GTPases are the master regulators of the actin architecture. These GTPases have been shown to mediate the interaction between the plasma membrane and the organization of the cytoskeleton especially affecting the cortical actin meshwork (de Curtis and Meldolesi 2012; Hall 1998). The cortical actin network directly lies underneath the cell surface and is predominantly composed of actin filaments. Hence, Rho GTPases have the capacity to regulate plasma membrane dynamics and vesicle trafficking. Membrane trafficking is influenced both by tightly coordinated interaction of different Rho GTPase families as, e.g. RhoA and Rab and through modification of actin-binding proteins by GTPases (de Curtis and Meldolesi 2012).

Emerging evidence accumulates that hypoxia regulates the actin cytoskeleton via changes in the activity of Rho GTPases (Zieseniss 2014). Dada et al. indeed demonstrated that hypoxia causes Na^+,K^+-ATPase endocytosis by ROS-induced activation of the GTPase RhoA (Dada et al. 2007). Consequently, future studies should assess the role of RhoA for hypoxia-induced membrane trafficking.

4.4 Hypoxia-mediated membrane trafficking is independent of HIF-1α stabilization and PHD function

The transcription factor HIF is the central regulator of adaptive changes in hypoxia causing a better survival by orchestrating over 100 target genes (Semenza 2012). Thus, it is of special interest, if HIF is likewise involved in mediating the hypoxia-induced membrane trafficking. In order to address this key question, analysis of membrane turnover in various HIF-1α gain and loss of function models were performed.

First of all, HIF-1α stabilization upon hypoxic incubation in MDA-MB 231 wt cells was confirmed by protein analysis. MDA-MB 231 shHIF-1α cells showed an effective knockdown of the target protein. FM-studies performed with HIF-1α knockdown cells did not reveal any influence of HIF-1α on membrane trafficking. In keeping with this, further

experiments in MEF+/+, MEF-/- and shPHD2 MEFs cells stabilizing HIF-1α validated the assumption that hypoxia-induced uptake of the membrane dye is indeed independent of HIF-1α abundance.

Although we excluded an impact of HIF-1α on the described hypoxic phenotype, we did not explicitly investigate the influence of the isoform HIF-2α. HIF-2α especially contributes to the transcriptional feedback to chronic hypoxia that is defined as persisting for more than 24 hrs (Koh and Powis 2012).

We demonstrated that long-term hypoxia (48 hrs) causes increased membrane trafficking in a comparable extent as short-term hypoxia (6 hrs). Hence, a HIF isoform-specific regulation appears unlikely. Furthermore, the MEF cells utilized in this study principally do not express HIF-2α that is functional in the cellular hypoxic response (Park et al. 2003; Ryan et al. 2000). Despite this prerequisite, the hypoxic phenotype in MEF cells was identical to cells whose adaptation to hypoxia involves HIF-2α. This result precluded a significant impact of HIF-2α on the described phenotype.

Moreover, the time course implied that hypoxia-mediated membrane trafficking is independent of the entire HIF oxygen sensing and signal transduction system: Reoxygenation experiments showed the phenotype to be extremely quickly reversible within a timeframe of just 30 min. HIFα protein levels decrease approximately 5 min after reoxygenation but their gene products display longer half-lives that contrast strongly with the rapid regulation of the membrane trafficking phenotype (Jewell et al. 2001).

Based on the assumption that PHDs do not only hydroxylate HIFs but also other proteins in an oxygen-dependent manner, the role of these oxygen sensors in the identified membrane turnover in hypoxia was analyzed (Myllyharju 2013). In addition, recent reports suggest a HIF-independent effect of PHDs on endocytic mechanisms. Garvalov et al. delineated a central regulatory role for PHD3 in EGF receptor internalization by acting as a scaffolding protein interacting directly with endocytic adaptor proteins (Garvalov et al. 2014). A further study demonstrated that hypoxia impacts trafficking of the glutamate receptor in C. elegans neurons via the spatiotemporal control of the hypoxia-inducible factor prolyl hydroxylase EGL-9 and its association with a mediator of membrane recycling (Park et al. 2012).

To this end, the function of PHDs in the described phenotype was evaluated by conducting FM-experiments in cells treated with DMOG that inhibits 2-oxoglutarate-dependent enzymes (Mole 2003). We found that the hypoxia-induced membrane trafficking was not impaired by DMOG treatment. This lack of any changes in membrane trafficking upon DMOG treatment indicated that the phenotype is highly unlikely to be mediated by PHD-regulated pathways.

Nevertheless, we performed additional experiments in shPHD2 MEF cells to selectively confirm the results for PHD2 function, which is the crucial isoform for many aspects of

oxygen homeostasis (Berra et al. 2003). In line with the aforementioned findings, the PHD2 knockdown did not influence the characterized hypoxic phenotype. However, also Garvalov et al. stated that PHD2, in contrast to PHD3, does not significantly influence receptor internalization and trafficking in hypoxic conditions (Garvalov et al. 2014).

To sum up, hypoxic membrane trafficking is independent of oxygen sensing by PHDs and HIFα stabilization. From this finding and the rapid regulation velocity, one might infer an alternative oxygen-sensing mechanism that has not been characterized yet. Future experiments could aim for correlating the magnitude of membrane trafficking to the severity of hypoxia in order to identify a possible dependence between different degrees of oxygen availability and the extent of membrane turnover suggesting a complementary oxygen sensing mechanism.

Although it is beyond the scope of this work to define the physiological function of the hypoxia-induced membrane-trafficking, one could speculate that T-plastin-associated trafficking of endosomes might be an important component for the cellular adaptation to low oxygen levels, complementing the response to hypoxia at the transcriptional level via HIF. This hypothesis is supported by a prior study that analyzed the underlying mechanisms by which hypoxic preconditioning confers protection against hypoxic stress. Carini et al. delineated that a short exposure of cells to hypoxia induces actin-dependent travelling of endosomes and lysosomes towards the plasma membrane (Carini et al. 2004). Fusion of the membrane-enclosed organelles helped to preserve the intracellular pH and hence improved cell survival.

4.5 Conclusion and outlook

Taken together, this study presents novel findings regarding the role of hypoxia as a stimulus for the membrane trafficking activity of cells.

Confocal analysis of membrane turnover applying the membrane dye FM revealed increased membrane trafficking and wholesale changes of the endomembrane system in different cell types upon hypoxic induction. This phenotype seems to constitute an elementary biological response mechanism to low oxygen levels, as the effect was not restricted to a specific cell type or species. A previous study investigated alterations of the surface proteome resulting from oxygen deprivation and depicted the overall protein internalization to be diminished in hypoxia (Bourseau-Guilmain et al. 2016). Although the process of protein internalization is clearly distinct from the process of membrane uptake, the opposed up- respectively downregulation in hypoxia appears to be difficult to reconcile. The underlying mechanisms explaining these seemingly contradictory findings remain to be elucidated.

The hypoxia-induced increase in membrane uptake involved an intensified retrograde transport of membrane-enclosed vesicles to the TGN as demonstrated by endocytosis

assays using the marker protein cholera toxin B subunit. Co-staining experiments applying the membrane dye mCLING and fluorescently labelled antibodies, which were directed against the *trans*-Golgi protein TGN38 confirmed this finding. Further microscopic analysis of the intracellular compartments revealed changes in the morphology of the TGN caused by low oxygen availability. An additional investigation of the involved endocytic mechanisms and transport pathways would be desirable. Furthermore, the kinetics of the hypoxia-induced modifications in the vesicle dynamics merit further study, e.g. by looking at more time points or by utilizing extensive life cell imaging.

Proteome analysis using SILAC technology led to the identification of actin-bundling proteins as potential mediators of the described phenotype. The recruitment of plastins to the cell membrane upon hypoxic exposure was verified by western blot analysis suggesting that the hypoxia-induced modulation of membrane trafficking is controlled by the spatiotemporal distribution of T-plastin. Direct involvement of the T-plastin isoform in the described phenotype was established by performing FM-studies in T-plastin knockdown cells. Further experiments are needed to unveil the mechanism that adjusts the activity of T-plastin according to the availability of oxygen.

The increase in membrane trafficking due to hypoxia was quickly reversed upon reoxygenation demonstrating that membrane transport is dynamically modulated owing to changing oxygen levels. The manifestation of this phenotype did not involve the HIF system and did not rely on the PHD function, implying that this link between hypoxia and membrane trafficking might be an element of an alternative, HIF-independent oxygen adaptation machinery. Further proof for this putative machinery complementing the well-established HIF-mediated response to hypoxia remain to be acquired.

The functional consequence of the hypoxia-induced membrane trafficking could not be defined within the scope of this work. T-plastin-mediated alterations in membrane turnover due to hypoxia might display a cellular mechanism that participates in the adaptation to scarce oxygen conditions. As a working hypothesis for subsequent studies, the implication of hypoxia-induced membrane trafficking on protein distribution and activity should be considered. A potential corollary of the hypoxia-induced phenotype could be the regulation of the enzymatic activity of the proprotein convertase Furin that has been described to cycle between the cell curface and the TGN (Bonifacino and Rojas 2006; Thomas 2002). One could also speculate that the described change in membrane trafficking due to hypoxia may be involved in the control of iron uptake by influencing the intracellular localization of hemojuvelin (Zhang 2010). Hemojuvelin is a critical player in the signal transduction pathway that ensures the maintenance of iron homeostasis in the organism und undergoes retrograde trafficking to the TGN in order to be processed (Maxson et al. 2009). Vesicular trafficking can also impact the metalloproteinase function (Sbai et al. 2008; Yu et al. 2016). Since metalloproteinases participate in a huge array of pathophysiological developments as, e.g. in myocardial infarction, cancer, inflammation

and fibrosis, targeting this protein family in relation to the hypoxia-inducible membrane trafficking might present interesting insights (Creemers et al. 2001; Egeblad and Werb 2002; Peng et al. 2012). In order to clarify the physiological function of the hypoxia-induced phenotype *in vivo*, experiments in cellular tissues are required.

In conclusion, our data present new insights in T-plastin-mediated intracellular communication signals. Understanding and influencing the pathogenesis of hypoxia-associated diseases is of importance for practical medicine. A better comprehension of cellular and subcellular hypoxia-induced mechanisms like membrane trafficking might help to gain new knowledge on hypoxia-associated pathologies.

5 Abstract

Hypoxia is essential for many physiological functions but also plays a pivotal role in the pathogenesis of a variety of epidemiologically highly relevant diseases. Adequate adaptation mechanisms to oxygen deprivation are a crucial prerequisite for cellular survival. Membrane trafficking is a fundamental feature of cells to adapt to their environment. Traffic of membrane-enclosed vesicles comprises the anterograde transport route of cargo from biosynthetic compartments to the plasma membrane but also cargo internalization and the retrieval of plasma membrane components via the retrograde pathway. The modulation of endosomal transport resulting in altered processing of cargo, signaling and membrane composition as a reaction to extracellular stimuli contributes to the preservation of cellular homeostasis. The aim of this study was therefore to analyze the impact of hypoxia on membrane trafficking.

To this end, we determined total membrane turnover by using the membrane marker FM 1-43 and confocal microscopy. Hypoxia caused an increase in membrane uptake upon hypoxic incubation in MDA-MB 231 and MEF cells. Reoxygenation quickly reconstituted the normoxic phenotype. The influence of oxygen deprivation on different endocytic pathways was investigated by analyzing the uptake of specific marker proteins. The intensified uptake of cholera toxin B subunit suggested an intensified retrograde transport to the *trans*-Golgi network. This finding was confirmed by performing co-staining experiments with the novel membrane probe mCLING and fluorescently labelled antibodies that were directed against compartment-specific proteins. Analysis of different HIF-1α gain and loss of function cell lines demonstrated that the manifestation of the described phenotype was independent of the HIF pathway and the PHD function. In order to elucidate the mechanism mediating this effect, proteome analysis taking advantage of the SILAC technology and western blotting were used to detect alterations in the abundance and spatiotemporal distribution of proteins owing to restricted oxygen availability. The actin-bundling protein T-plastin was found to be recruited to the plasma membrane due to low oxygen levels. T-plastin knockdown cells demonstrated blunted membrane uptake in hypoxia showing that this plastin isoform facilitates the hypoxia-induced membrane trafficking.

In summary, hypoxia causes profound changes in the membrane trafficking activity and the endomembrane system of cells by favoring retrograde transport to the *trans*-Golgi network. To our knowledge, this study was the first to investigate overall membrane trafficking in hypoxia and, thus, complements the preexisting knowledge on hypoxia-induced changes of protein internalization. Nevertheless, the characterization of the involved pathways and endosomal structures merits further study. Moreover, it is not known how the alterations of membrane and protein uptake in hypoxia are intertwined.

The manifestation of the membrane trafficking phenotype in hypoxia is very dynamically mediated by T-plastin. This finding is in line with previous reports that provided evidence for a regulatory role of this actin-bundling protein in endocytic events. The precise mechanism administering the spatiotemporal regulation of T-plastin activity in hypoxia remains yet unclear. Furthermore, in regards to future experiments, the investigation of the underlying HIF- and PHD-independent oxygen sensing machinery would be worthwhile.

The hypoxia-induced membrane trafficking is a fundamental biological function since the effect is not cell type- or species-specific. Within the scope of this work it was not possible to identify the physiological consequence of the effect and its function *in vivo*. The quick time course suggests that the T-plastin-mediated effect may be a component of a HIF-independent adaptation mechanism to oxygen deprivation influencing cellular survival, but this hypothesis requires further support through additional experiments.

The results obtained in this research project contribute to the understanding of hypoxia-induced changes at the subcellular level that occur in physiological and pathophysiological conditions. Augmenting the knowledge on cellular adaptation strategies to low oxygen levels is the foundation for the development of diagnostic and therapeutic tools to treat hypoxia-associated diseases.

6 References

Adam T, Arpin M, Prevost MC, Gounon P, Sansonetti PJ (1995): Cytoskeletal rearrangements and the functional role of T-plastin during entry of Shigella flexneri into HeLa cells. J Cell Biol 129, 367-381

Adams AE, Botstein D, Drubin DG (1991): Requirement of yeast fimbrin for actin organization and morphogenesis in vivo. Nature 354, 404-408

Aderem A, Underhill DM (1999): Mechanisms of phagocytosis in macrophages. Annu Rev Immunol 17, 593-623

Appelhoff RJ, Tian YM, Raval RR, Turley H, Harris AL, Pugh CW, Ratcliffe PJ, Gleadle JM (2004): Differential function of the prolyl hydroxylases PHD1, PHD2, and PHD3 in the regulation of hypoxia-inducible factor. J Biol Chem 279, 38458-38465

Arany Z, Huang LE, Eckner R, Bhattacharya S, Jiang C, Goldberg MA, Bunn HF, Livingston DM (1996): An essential role for p300/CBP in the cellular response to hypoxia. Proc Natl Acad Sci U S A 93, 12969-12973

Berra E, Benizri E, Ginouves A, Volmat V, Roux D, Pouyssegur J (2003): HIF prolyl-hydroxylase 2 is the key oxygen sensor setting low steady-state levels of HIF-1alpha in normoxia. EMBO J 22, 4082-4090

Berra E, Ginouves A, Pouyssegur J (2006): The hypoxia-inducible-factor hydroxylases bring fresh air into hypoxia signalling. EMBO Rep 7, 41-45

Betz WJ, Mao F, Bewick GS (1992): Activity-dependent fluorescent staining and destaining of living vertebrate motor nerve terminals. J Neurosci 12, 363-375

Bezanilla M, Gladfelter AS, Kovar DR, Lee WL (2015): Cytoskeletal dynamics: a view from the membrane. J Cell Biol 209, 329-337

Bishop T, Ratcliffe PJ (2014): Signaling hypoxia by hypoxia-inducible factor protein hydroxylases: a historical overview and future perspectives. Hypoxia (Auckl) 2, 197-213

Blanchoin L, Boujemaa-Paterski R, Sykes C, Plastino J (2014): Actin dynamics, architecture, and mechanics in cell motility. Physiol Rev 94, 235-263

Bonifacino JS, Rojas R (2006): Retrograde transport from endosomes to the trans-Golgi network. Nat Rev Mol Cell Biol 7, 568-579

Bourseau-Guilmain E, Menard JA, Lindqvist E, Indira Chandran V, Christianson HC, Cerezo Magana M, Lidfeldt J, Marko-Varga G, Welinder C, Belting M (2016): Hypoxia regulates global membrane protein endocytosis through caveolin-1 in cancer cells. Nat Commun 7, 11371

Bradford MM (1976): A rapid and sensitive method for the quantitation of microgram quantities of protein utilizing the principle of protein-dye binding. Anal Biochem 72, 248-254

Bruick RK, McKnight SL (2001): A conserved family of prolyl-4-hydroxylases that modify HIF. Science 294, 1337-1340

Buccione R, Orth JD, McNiven MA (2004): Foot and mouth: podosomes, invadopodia and circular dorsal ruffles. Nat Rev Mol Cell Biol 5, 647-657

Burnette WN (1981): "Western blotting": electrophoretic transfer of proteins from sodium dodecyl sulfate-polyacrylamide gels to unmodified nitrocellulose and radiographic detection with antibody and radioiodinated protein A. Anal Biochem 112, 195-203

Cailleau R, Young R, Olive M, Reeves WJ (1974): Breast Tumor-Cell Lines from Pleural Effusions. J Natl Cancer Inst 53, 661-674

Carini R, Castino R, De Cesaris MG, Splendore R, Demoz M, Albano E, Isidoro C (2004): Preconditioning-induced cytoprotection in hepatocytes requires Ca(2+)-dependent exocytosis of lysosomes. J Cell Sci 117, 1065-1077

Carreau A, El Hafny-Rahbi B, Matejuk A, Grillon C, Kieda C (2011): Why is the partial oxygen pressure of human tissues a crucial parameter? Small molecules and hypoxia. J Cell Mol Med 15, 1239-1253

Chang YC, Lamichhane AK, Kwon-Chung KJ (2012): Role of actin-bundling protein Sac6 in growth of Cryptococcus neoformans at low oxygen concentration. Eukaryot Cell 11, 943-951

Chaudhary N, Gomez GA, Howes MT, Lo HP, McMahon KA, Rae JA, Schieber NL, Hill MM, Gaus K, Yap AS, et al. (2014): Endocytic crosstalk: cavins, caveolins, and caveolae regulate clathrin-independent endocytosis. PLoS Biol 12, e1001832

Chen W, Feng Y, Chen D, Wandinger-Ness A (1998): Rab11 is required for trans-golgi network-to-plasma membrane transport and a preferential target for GDP dissociation inhibitor. Mol Biol Cell 9, 3241-3257

Chilov D, Camenisch G, Kvietikova I, Ziegler U, Gassmann M, Wenger RH (1999): Induction and nuclear translocation of hypoxia-inducible factor-1 (HIF-1): heterodimerization with ARNT is not necessary for nuclear accumulation of HIF-1alpha. J Cell Sci 112 (Pt 8), 1203-1212

Chomczynski P, Sacchi N (1987): Single-step method of RNA isolation by acid guanidinium thiocyanate-phenol-chloroform extraction. Anal Biochem 162, 156-159

Cochilla AJ, Angleson JK, Betz WJ (1999): Monitoring secretory membrane with FM1-43 fluorescence. Annu Rev Neurosci 22, 1-10

Coffin JM, Fan H (2016): The Discovery of Reverse Transcriptase. Annu Rev Virol 3, 29-51

Coons AH, Creech HJ, Jones RN, Berliner E (1942): The Demonstration of Pneumococcal Antigen in Tissues by the Use of Fluorescent Antibody. J Immunol 45, 159-170

Covello KL, Kehler J, Yu H, Gordan JD, Arsham AM, Hu CJ, Labosky PA, Simon MC, Keith B (2006): HIF-2alpha regulates Oct-4: effects of hypoxia on stem cell function, embryonic development, and tumor growth. Genes Dev 20, 557-570

Creemers EE, Cleutjens JP, Smits JF, Daemen MJ (2001): Matrix metalloproteinase inhibition after myocardial infarction: a new approach to prevent heart failure? Circ Res 89, 201-210

Dada LA, Sznajder JI (2007): Hypoxic inhibition of alveolar fluid reabsorption. Adv Exp Med Biol 618, 159-168

Dada LA, Chandel NS, Ridge KM, Pedemonte C, Bertorello AM, Sznajder JI (2003): Hypoxia-induced endocytosis of Na,K-ATPase in alveolar epithelial cells is mediated by mitochondrial reactive oxygen species and PKC-zeta. J Clin Invest 111, 1057-1064

Dada LA, Novoa E, Lecuona E, Sun H, Sznajder JI (2007): Role of the small GTPase RhoA in the hypoxia-induced decrease of plasma membrane Na,K-ATPase in A549 cells. J Cell Sci 120, 2214-2222

Dautry-Varsat A, Ciechanover A, Lodish HF (1983): pH and the recycling of transferrin during receptor-mediated endocytosis. Proc Natl Acad Sci U S A 80, 2258-2262

de Curtis I, Meldolesi J (2012): Cell surface dynamics - how Rho GTPases orchestrate the interplay between the plasma membrane and the cortical cytoskeleton. J Cell Sci 125, 4435-4444

De Haan L, Hirst TR (2004): Cholera toxin: a paradigm for multi-functional engagement of cellular mechanisms (Review). Mol Membr Biol 21, 77-92

Delanote V, Vandekerckhove J, Gettemans J (2005): Plastins: versatile modulators of actin organization in (patho)physiological cellular processes. Acta Pharmacol Sin 26, 769-779

Deneka M, van der Sluijs P (2002): 'Rab'ing up endosomal membrane transport. Nat Cell Biol 4, 33-35

Derivery E, Sousa C, Gautier JJ, Lombard B, Loew D, Gautreau A (2009): The Arp2/3 activator WASH controls the fission of endosomes through a large multiprotein complex. Dev Cell 17, 712-723

Di Fiore PP, von Zastrow M (2014): Endocytosis, signaling, and beyond. Cold Spring Harb Perspect Biol 6, piia016865

Di Paolo G, De Camilli P (2006): Phosphoinositides in cell regulation and membrane dynamics. Nature 443, 651-657

Doherty GJ, McMahon HT (2009): Mechanisms of endocytosis. Annu Rev Biochem 78, 857-902

Dominguez R, Holmes KC (2011): Actin structure and function. Annu Rev Biophys 40, 169-186

Duan C (2016): Hypoxia-inducible factor 3 biology: complexities and emerging themes. Am J Physiol Cell Physiol 310, 260-269

Duleh SN, Welch MD (2010): WASH and the Arp2/3 complex regulate endosome shape and trafficking. Cytoskeleton (Hoboken) 67, 193-206

Dunn KW, Kamocka MM, McDonald JH (2011): A practical guide to evaluating colocalization in biological microscopy. Am J Physiol Cell Physiol 300, 723-742

Edeling MA, Smith C, Owen D (2006): Life of a clathrin coat: insights from clathrin and AP structures. Nat Rev Mol Cell Biol 7, 32-44

Egeblad M, Werb Z (2002): New functions for the matrix metalloproteinases in cancer progression. Nat Rev Cancer 2, 161-174

Ehrismann D, Flashman E, Genn DN, Mathioudakis N, Hewitson KS, Ratcliffe PJ, Schofield CJ (2007): Studies on the activity of the hypoxia-inducible-factor hydroxylases using an oxygen consumption assay. Biochem J 401, 227-234

Eltzschig HK, Carmeliet P (2011): Hypoxia and inflammation. N Engl J Med 364, 656-665

Epstein AC, Gleadle JM, McNeill LA, Hewitson KS, O'Rourke J, Mole DR, Mukherji M, Metzen E, Wilson MI, Dhanda A, et al. (2001): C. elegans EGL-9 and mammalian homologs define a family of dioxygenases that regulate HIF by prolyl hydroxylation. Cell 107, 43-54

Feng Y, Press B, Wandinger-Ness A (1995): Rab 7: an important regulator of late endocytic membrane traffic. J Cell Biol 131, 1435-1452

Gaffield MA, Betz WJ (2006): Imaging synaptic vesicle exocytosis and endocytosis with FM dyes. Nat Protoc 1, 2916-2921

Garvalov BK, Foss F, Henze AT, Bethani I, Graf-Hochst S, Singh D, Filatova A, Dopeso H, Seidel S, Damm M, et al. (2014): PHD3 regulates EGFR internalization and signalling in tumours. Nat Commun 5, 5577

Ghosh RN, Mallet WG, Soe TT, McGraw TE, Maxfield FR (1998): An endocytosed TGN38 chimeric protein is delivered to the TGN after trafficking through the endocytic recycling compartment in CHO cells. J Cell Biol 142, 923-936

Giganti A, Plastino J, Janji B, Van Troys M, Lentz D, Ampe C, Sykes C, Friederich E (2005): Actin-filament cross-linking protein T-plastin increases Arp2/3-mediated actin-based movement. J Cell Sci 118, 1255-1265

Granger E, McNee G, Allan V, Woodman P (2014): The role of the cytoskeleton and molecular motors in endosomal dynamics. Semin Cell Dev Biol 31, 20-29

Grant BD, Donaldson JG (2009): Pathways and mechanisms of endocytic recycling. Nat Rev Mol Cell Biol 10, 597-608

Griffiths G, Simons K (1986): The trans Golgi network: sorting at the exit site of the Golgi complex. Science 234, 438-443

Gusarova GA, Dada LA, Kelly AM, Brodie C, Witters LA, Chandel NS, Sznajder JI (2009): Alpha1-AMP-activated protein kinase regulates hypoxia-induced Na,K-ATPase endocytosis via direct phosphorylation of protein kinase C zeta. Mol Cell Biol 29, 3455-3464

Hagiwara M, Shinomiya H, Kashihara M, Kobayashi K, Tadokoro T, Yamamoto Y (2011): Interaction of activated Rab5 with actin-bundling proteins, L- and T-plastin and its relevance to endocytic functions in mammalian cells. Biochem Biophys Res Commun 407, 615-619

Hall A (1998): Rho GTPases and the actin cytoskeleton. Science 279, 509-514

Harris AL (2002): Hypoxia-a key regulatory factor in tumour growth. Nat Rev Cancer 2, 38-47

Henkel AW, Lubke J, Betz WJ (1996): FM1-43 dye ultrastructural localization in and release from frog motor nerve terminals. Proc Natl Acad Sci USA 93, 1918-1923

Higuchi R, Dollinger G, Walsh PS, Griffith R (1992): Simultaneous amplification and detection of specific DNA sequences. Biotechnology (NY) 10, 413-417

Hirsila M, Koivunen P, Gunzler V, Kivirikko KI, Myllyharju J (2003): Characterization of the human prolyl 4-hydroxylases that modify the hypoxia-inducible factor. J Biol Chem 278, 30772-30780

Hoopmann P, Rizzoli SO, Betz WJ (2012): Imaging synaptic vesicle recycling by staining and destaining vesicles with FM dyes. Cold Spring Harb Protoc 2012, 77-83

Hopkins CR, Trowbridge IS (1983): Internalization and processing of transferrin and the transferrin receptor in human carcinoma A431 cells. J Cell Biol 97, 508-521

Hopkins CR, Miller K, Beardmore JM (1985): Receptor-mediated endocytosis of transferrin and epidermal growth factor receptors: a comparison of constitutive and ligand-induced uptake. J Cell Sci Suppl 3, 173-186

Hosseinibarkooie S, Peters M, Torres-Benito L, Rastetter RH, Hupperich K, Hoffmann A, Mendoza-Ferreira N, Kaczmarek A, Janzen E, Milbradt J, et al. (2016): The Power of Human Protective Modifiers: PLS3 and CORO1C Unravel Impaired Endocytosis in Spinal Muscular Atrophy and Rescue SMA Phenotype. Am J Hum Genet 99, 647-665

Howell GJ, Holloway ZG, Cobbold C, Monaco AP, Ponnambalam S (2006): Cell biology of membrane trafficking in human disease. Int Rev Cytol 252, 1-69

Huang J, Zhao Q, Mooney SM, Lee FS (2002): Sequence determinants in hypoxia-inducible factor-1alpha for hydroxylation by the prolyl hydroxylases PHD1, PHD2, and PHD3. J Biol Chem 277, 39792-39800

Huang LE, Gu J, Schau M, Bunn HF (1998): Regulation of hypoxia-inducible factor 1alpha is mediated by an O2-dependent degradation domain via the ubiquitin-proteasome pathway. Proc Natl Acad Sci USA 95, 7987-7992

Huotari J, Helenius A (2011): Endosome maturation. EMBO J 30, 3481-3500

Ivan M, Kondo K, Yang H, Kim W, Valiando J, Ohh M, Salic A, Asara JM, Lane WS, Kaelin WG, Jr. (2001): HIFalpha targeted for VHL-mediated destruction by proline hydroxylation: implications for O2 sensing. Science 292, 464-468

Iyer NV, Kotch LE, Agani F, Leung SW, Laughner E, Wenger RH, Gassmann M, Gearhart JD, Lawler AM, Yu AY, et al. (1998): Cellular and developmental control of O2 homeostasis by hypoxia-inducible factor 1 alpha. Genes Dev 12, 149-162

Jaakkola P, Mole DR, Tian YM, Wilson MI, Gielbert J, Gaskell SJ, von Kriegsheim A, Hebestreit HF, Mukherji M, Schofield CJ, et al. (2001): Targeting of HIF-alpha to the von Hippel-Lindau ubiquitylation complex by O2-regulated prolyl hydroxylation. Science 292, 468-472

Jewell UR, Kvietikova I, Scheid A, Bauer C, Wenger RH, Gassmann M (2001): Induction of HIF-1alpha in response to hypoxia is instantaneous. FASEB J 15, 1312-1314

Jiang BH, Rue E, Wang GL, Roe R, Semenza GL (1996): Dimerization, DNA binding, and transactivation properties of hypoxia-inducible factor 1. J Biol Chem 271, 17771-17778

Kacian DL, Bank A, Terada M, Spiegelman S, Marks PA, Dow L, Metafora S (1972): In-Vitro Synthesis of DNA Components of Human Genes for Globins. Nature-New Biol 235, 167-169

Kaelin WG, Jr., Ratcliffe PJ (2008): Oxygen sensing by metazoans: the central role of the HIF hydroxylase pathway. Mol Cell 30, 393-402

Kaksonen M, Sun Y, Drubin DG (2003): A pathway for association of receptors, adaptors, and actin during endocytic internalization. Cell 115, 475-487

Kaksonen M, Toret CP, Drubin DG (2005): A modular design for the clathrin- and actin-mediated endocytosis machinery. Cell 123, 305-320

Kallio PJ, Okamoto K, O'Brien S, Carrero P, Makino Y, Tanaka H, Poellinger L (1998): Signal transduction in hypoxic cells: inducible nuclear translocation and recruitment of the CBP/p300 coactivator by the hypoxia-inducible factor-1alpha. EMBO J 17, 6573-6586

Klumperman J (2011): Architecture of the mammalian Golgi. Cold Spring Harb Perspect Biol 3, pii a005181

Koh MY, Powis G (2012): Passing the baton: the HIF switch. Trends Biochem Sci 37, 364-372

Koh MY, Lemos R, Jr., Liu X, Powis G (2011): The hypoxia-associated factor switches cells from HIF-1alpha- to HIF-2alpha-dependent signaling promoting stem cell characteristics, aggressive tumor growth and invasion. Cancer Res 71, 4015-4027

Koivunen P, Tiainen P, Hyvarinen J, Williams KE, Sormunen R, Klaus SJ, Kivirikko KI, Myllyharju J (2007): An endoplasmic reticulum transmembrane prolyl 4-hydroxylase is induced by hypoxia and acts on hypoxia-inducible factor alpha. J Biol Chem 282, 30544-30552

Kubista M, Andrade JM, Bengtsson M, Forootan A, Jonak J, Lind K, Sindelka R, Sjoback R, Sjogreen B, Strombom L, et al. (2006): The real-time polymerase chain reaction. Mol Aspects Med 27, 95-125

Laemmli UK (1970): Cleavage of structural proteins during the assembly of the head of bacteriophage T4. Nature 227, 680-685

Lajoie P, Kojic LD, Nim S, Li L, Dennis JW, Nabi IR (2009): Caveolin-1 regulation of dynamin-dependent, raft-mediated endocytosis of cholera toxin-B sub-unit occurs independently of caveolae. J Cell Mol Med 13, 3218-3225

Lando D, Peet DJ, Gorman JJ, Whelan DA, Whitelaw ML, Bruick RK (2002): FIH-1 is an asparaginyl hydroxylase enzyme that regulates the transcriptional activity of hypoxia-inducible factor. Genes Dev 16, 1466-1471

Lanzetti L (2007): Actin in membrane trafficking. Curr Opin Cell Biol 19, 453-458

Lieb ME, Menzies K, Moschella MC, Ni R, Taubman MB (2002): Mammalian EGLN genes have distinct patterns of mRNA expression and regulation. Biochem Cell Biol 80, 421-426

Lim JP, Gleeson PA (2011): Macropinocytosis: an endocytic pathway for internalising large gulps. Immunol Cell Biol 89, 836-843

Lin CS, Aebersold RH, Kent SB, Varma M, Leavitt J (1988): Molecular cloning and characterization of plastin, a human leukocyte protein expressed in transformed human fibroblasts. Mol Cell Biol 8, 4659-4668

Lin CS, Shen W, Chen ZP, Tu YH, Matsudaira P (1994): Identification of I-plastin, a human fimbrin isoform expressed in intestine and kidney. Mol Cell Biol 14, 2457-2467

Liu Y, Jang S, Xie L, Sowa G (2014): Host deficiency in caveolin-2 inhibits lung carcinoma tumor growth by impairing tumor angiogenesis. Cancer Res 74, 6452-6462

Luzio JP, Brake B, Banting G, Howell KE, Braghetta P, Stanley KK (1990): Identification, sequencing and expression of an integral membrane protein of the trans-Golgi network (TGN38). Biochem J 270, 97-102

Mahon PC, Hirota K, Semenza GL (2001): FIH-1: a novel protein that interacts with HIF-1alpha and VHL to mediate repression of HIF-1 transcriptional activity. Genes Dev 15, 2675-2686

Maxfield FR, McGraw TE (2004): Endocytic recycling. Nat Rev Mol Cell Biol 5, 121-132

Maxson JE, Enns CA, Zhang AS (2009): Processing of hemojuvelin requires retrograde trafficking to the Golgi in HepG2 cells. Blood 113, 1786-1793

Maxwell PH, Wiesener MS, Chang GW, Clifford SC, Vaux EC, Cockman ME, Wykoff CC, Pugh CW, Maher ER, Ratcliffe PJ (1999): The tumour suppressor protein VHL targets hypoxia-inducible factors for oxygen-dependent proteolysis. Nature 399, 271-275

Mayor S, Rothberg KG, Maxfield FR (1994): Sequestration of GPI-anchored proteins in caveolae triggered by cross-linking. Science 264, 1948-1951

Mayor S, Parton RG, Donaldson JG (2014): Clathrin-independent pathways of endocytosis. Cold Spring Harb Perspect Biol 6, pii a016758

Meister M, Tikkanen R (2014): Endocytic trafficking of membrane-bound cargo: a flotillin point of view. Membranes (Basel) 4, 356-371

Mellman I (1996): Endocytosis and molecular sorting. Annu Rev Cell Dev Biol 12, 575-625

Menard JA, Christianson HC, Kucharzewska P, Bourseau-Guilmain E, Svensson KJ, Lindqvist E, Indira Chandran V, Kjellen L, Welinder C, Bengzon J, et al. (2016): Metastasis Stimulation by Hypoxia and Acidosis-Induced Extracellular Lipid Uptake Is Mediated by Proteoglycan-Dependent Endocytosis. Cancer Res 76, 4828-4840

Metzen E, Berchner-Pfannschmidt U, Stengel P, Marxsen JH, Stolze I, Klinger M, Huang WQ, Wotzlaw C, Hellwig-Burgel T, Jelkmann W, et al. (2003): Intracellular localisation of human HIF-1 alpha hydroxylases: implications for oxygen sensing. J Cell Sci 116, 1319-1326

Miaczynska M (2013): Effects of membrane trafficking on signaling by receptor tyrosine kinases. Cold Spring Harb Perspect Biol 5, a009035

Mindell JA (2012): Lysosomal acidification mechanisms. Annu Rev Physiol 74, 69-86

Mole DR, Schlemminger I, McNeill LA, Hewitson KS, Pugh CW, Ratcliffe PJ, Schofield CJ (2003): 2-oxoglutarate analogue inhibitors of HIF prolyl hydroxylase. Bioorg Med Chem Lett 13, 2677-2680

Mooren OL, Galletta BJ, Cooper JA (2012): Roles for actin assembly in endocytosis. Annu Rev Biochem 81, 661-686

Morel E, Parton RG, Gruenberg J (2009): Annexin A2-dependent polymerization of actin mediates endosome biogenesis. Dev Cell 16, 445-457

Mosesson Y, Mills GB, Yarden Y (2008): Derailed endocytosis: an emerging feature of cancer. Nat Rev Cancer 8, 835-850

Mukherjee S, Soe TT, Maxfield FR (1999): Endocytic sorting of lipid analogues differing solely in the chemistry of their hydrophobic tails. J Cell Biol 144, 1271-1284

Mukhopadhyay S, Xu F, Sehgal PB (2007): Aberrant cytoplasmic sequestration of eNOS in endothelial cells after monocrotaline, hypoxia, and senescence: live-cell caveolar and cytoplasmic NO imaging. Am J Physiol Heart Circ Physiol 292, 1373-1389

Mullis KB, Faloona FA (1987): Specific synthesis of DNA in vitro via a polymerase-catalyzed chain reaction. Methods Enzymol 155, 335-350

Myllyharju J (2013): Prolyl 4-hydroxylases, master regulators of the hypoxia response. Acta Physiol (Oxf) 208, 148-165

Nakamura N, Rabouille C, Watson R, Nilsson T, Hui N, Slusarewicz P, Kreis TE, Warren G (1995): Characterization of a cis-Golgi matrix protein, GM130. J Cell Biol 131, 1715-1726

Olkkonen VM, Ikonen E (2006): When intracellular logistics fails-genetic defects in membrane trafficking. J Cell Sci 119, 5031-5045

Olson EN, Nordheim A (2010): Linking actin dynamics and gene transcription to drive cellular motile functions. Nat Rev Mol Cell Biol 11, 353-365

Palade GE (1953): Fine structure of blood capillaries. J Appl Phys 24, 1424

Park EC, Ghose P, Shao ZY, Ye Q, Kang LJ, Xu XZS, Powell-Coffman JA, Rongo C (2012): Hypoxia regulates glutamate receptor trafficking through an HIF-independent mechanism. EMBO J 31, 1379-1393

Park SK, Dadak AM, Haase VH, Fontana L, Giaccia AJ, Johnson RS (2003): Hypoxia-induced gene expression occurs solely through the action of hypoxia-inducible factor 1alpha (HIF-1alpha): role of cytoplasmic trapping of HIF-2alpha. Mol Cell Biol 23, 4959-4971

Parton RG, Simons K (2007): The multiple faces of caveolae. Nat Rev Mol Cell Biol 8, 185-194

Patel SA, Simon MC (2008): Biology of hypoxia-inducible factor-2alpha in development and disease. Cell Death Differ 15, 628-634

Pearse BM (1975): Coated vesicles from pig brain: purification and biochemical characterization. J Mol Biol 97, 93-98

Pelkmans L, Puntener D, Helenius A (2002): Local actin polymerization and dynamin recruitment in SV40-induced internalization of caveolae. Science 296, 535-539

Peng WJ, Yan JW, Wan YN, Wang BX, Tao JH, Yang GJ, Pan HF, Wang J (2012): Matrix metalloproteinases: a review of their structure and role in systemic sclerosis. J Clin Immunol 32, 1409-1414

Pfeffer SR (2001): Rab GTPases: specifying and deciphering organelle identity and function. Trends Cell Biol 11, 487-491

Pfeffer SR (2013): Rab GTPase regulation of membrane identity. Curr Opin Cell Biol 25, 414-419

Piper RC, Katzmann DJ (2007): Biogenesis and function of multivesicular bodies. Annu Rev Cell Dev Biol 23, 519-547

Pollard TD, Borisy GG (2003): Cellular motility driven by assembly and disassembly of actin filaments. Cell 112, 453-465

Pollard TD, Cooper JA (2009): Actin, a central player in cell shape and movement. Science 326, 1208-1212

Pugh CW, Ratcliffe PJ (2003): Regulation of angiogenesis by hypoxia: role of the HIF system. Nat Med 9, 677-684

Pugh CW, O'Rourke JF, Nagao M, Gleadle JM, Ratcliffe PJ (1997): Activation of hypoxia-inducible factor-1; definition of regulatory domains within the alpha subunit. J Biol Chem 272, 11205-11214

Ranftler C, Auinger P, Meisslitzer-Ruppitsch C, Ellinger A, Neumuller J, Pavelka M (2013): Electron microscopy of endocytic pathways. Methods Mol Biol 931, 437-447

Ratcliffe PJ (2013): Oxygen sensing and hypoxia signalling pathways in animals: the implications of physiology for cancer. J Physiol 591, 2027-2042

Ren M, Xu G, Zeng J, De Lemos-Chiarandini C, Adesnik M, Sabatini DD (1998): Hydrolysis of GTP on rab11 is required for the direct delivery of transferrin from the pericentriolar recycling compartment to the cell surface but not from sorting endosomes. Proc Natl Acad Sci U S A 95, 6187-6192

Revelo NH, Kamin D, Truckenbrodt S, Wong AB, Reuter-Jessen K, Reisinger E, Moser T, Rizzoli SO (2014): A new probe for super-resolution imaging of membranes elucidates trafficking pathways. J Cell Biol 205, 591-606

Revenu C, Ubelmann F, Hurbain I, El-Marjou F, Dingli F, Loew D, Delacour D, Gilet J, Brot-Laroche E, Rivero F, et al. (2012): A new role for the architecture of microvillar actin bundles in apical retention of membrane proteins. Mol Biol Cell 23, 324-336

Rio DC, Ares M, Jr., Hannon GJ, Nilsen TW (2010): Purification of RNA using TRIzol (TRI reagent). Cold Spring Harb Protoc 2010, 5439

Robinson MS (2015): Forty Years of Clathrin-coated Vesicles. Traffic 16, 1210-1238

Rodriguez-Boulan E, Musch A (2005): Protein sorting in the Golgi complex: shifting paradigms. Biochim Biophys Acta 1744, 455-464

Rohn WM, Rouille Y, Waguri S, Hoflack B (2000): Bi-directional trafficking between the trans-Golgi network and the endosomal/lysosomal system. J Cell Sci 113 (Pt 12), 2093-2101

Rothberg KG, Heuser JE, Donzell WC, Ying YS, Glenney JR, Anderson RG (1992): Caveolin, a protein component of caveolae membrane coats. Cell 68, 673-682

Ryan HE, Poloni M, McNulty W, Elson D, Gassmann M, Arbeit JM, Johnson RS (2000): Hypoxia-inducible factor-1alpha is a positive factor in solid tumor growth. Cancer Res 60, 4010-4015

Salceda S, Caro J (1997): Hypoxia-inducible factor 1alpha (HIF-1alpha) protein is rapidly degraded by the ubiquitin-proteasome system under normoxic conditions. Its stabilization by hypoxia depends on redox-induced changes. J Biol Chem 272, 22642-22647

Samstag Y, Klemke M (2007): Ectopic expression of L-plastin in human tumor cells: diagnostic and therapeutic implications. Adv Enzyme Regul 47, 118-126

Sandvig K, van Deurs B (2005): Delivery into cells: lessons learned from plant and bacterial toxins. Gene Ther 12, 865-872

Sbai O, Ferhat L, Bernard A, Gueye Y, Ould-Yahoui A, Thiolloy S, Charrat E, Charton G, Tremblay E, Risso JJ, et al. (2008): Vesicular trafficking and secretion of matrix metalloproteinases-2, -9 and tissue inhibitor of metalloproteinases-1 in neuronal cells. Mol Cell Neurosci 39, 549-568

Schofield CJ, Ratcliffe PJ (2004): Oxygen sensing by HIF hydroxylases. Nat Rev Mol Cell Biol 5, 343-354

Scott CC, Vacca F, Gruenberg J (2014): Endosome maturation, transport and functions. Semin Cell Dev Biol 31, 2-10

Semenza GL (2011): Oxygen sensing, homeostasis, and disease. N Engl J Med 365, 537-547

Semenza GL (2012): Hypoxia-inducible factors in physiology and medicine. Cell 148, 399-408

Semenza GL, Wang GL (1992): A nuclear factor induced by hypoxia via de novo protein synthesis binds to the human erythropoietin gene enhancer at a site required for transcriptional activation. Mol Cell Biol 12, 5447-5454

Shin JB, Krey JF, Hassan A, Metlagel Z, Tauscher AN, Pagana JM, Sherman NE, Jeffery ED, Spinelli KJ, Zhao H, et al. (2013): Molecular architecture of the chick vestibular hair bundle. Nat Neurosci 16, 365-374

Shinomiya H (2012): Plastin family of actin-bundling proteins: its functions in leukocytes, neurons, intestines, and cancer. Int J Cell Biol 2012, 213492

Shmuel M, Nodel-Berner E, Hyman T, Rouvinski A, Altschuler Y (2007): Caveolin 2 regulates endocytosis and trafficking of the M1 muscarinic receptor in MDCK epithelial cells. Mol Biol Cell 18, 1570-1585

Simon MC, Keith B (2008): The role of oxygen availability in embryonic development and stem cell function. Nat Rev Mol Cell Biol 9, 285-296

Simonsen A, Lippe R, Christoforidis S, Gaullier JM, Brech A, Callaghan J, Toh BH, Murphy C, Zerial M, Stenmark H (1998): EEA1 links PI(3)K function to Rab5 regulation of endosome fusion. Nature 394, 494-498

Skau CT, Courson DS, Bestul AJ, Winkelman JD, Rock RS, Sirotkin V, Kovar DR (2011): Actin filament bundling by fimbrin is important for endocytosis, cytokinesis, and polarization in fission yeast. J Biol Chem 286, 26964-26977

Smythe E, Ayscough KR (2006): Actin regulation in endocytosis. J Cell Sci 119, 4589-4598

Snapp EL, Lajoie P (2011): Imaging of membrane systems and membrane traffic in living cells. Cold Spring Harb Protoc 2011, 1295-1304

Sorkin A, Goh LK (2009): Endocytosis and intracellular trafficking of ErbBs. Exp Cell Res 315, 683-696

Stevenson RP, Veltman D, Machesky LM (2012): Actin-bundling proteins in cancer progression at a glance. J Cell Sci 125, 1073-1079

Stockmann C, Fandrey J (2006): Hypoxia-induced erythropoietin production: a paradigm for oxygen-regulated gene expression. Clin Exp Pharmacol Physiol 33, 968-979

Takeda K, Ho VC, Takeda H, Duan LJ, Nagy A, Fong GH (2006): Placental but not heart defects are associated with elevated hypoxia-inducible factor alpha levels in mice lacking prolyl hydroxylase domain protein 2. Mol Cell Biol 26, 8336-8346

Thomas CM, Smart EJ (2008): Caveolae structure and function. J Cell Mol Med 12, 796-809

Thomas G (2002): Furin at the cutting edge: from protein traffic to embryogenesis and disease. Nat Rev Mol Cell Biol 3, 753-766

Thomsen P, Roepstorff K, Stahlhut M, van Deurs B (2002): Caveolae are highly immobile plasma membrane microdomains, which are not involved in constitutive endocytic trafficking. Mol Biol Cell 13, 238-250

Towbin H, Staehelin T, Gordon J (1979): Electrophoretic transfer of proteins from polyacrylamide gels to nitrocellulose sheets: procedure and some applications. Proc Natl Acad Sci U S A 76, 4350-4354

Ungewickell E, Branton D (1981): Assembly units of clathrin coats. Nature 289, 420-422

van der Sluijs P, Hull M, Webster P, Male P, Goud B, Mellman I (1992): The small GTP-binding protein rab4 controls an early sorting event on the endocytic pathway. Cell 70, 729-740

van Renswoude J, Bridges KR, Harford JB, Klausner RD (1982): Receptor-mediated endocytosis of transferrin and the uptake of fe in K562 cells: identification of a nonlysosomal acidic compartment. Proc Natl Acad Sci USA 79, 6186-6190

Verma IM, Temple GF, Fan H, Baltimore D (1972): In vitro synthesis of DNA complementary to rabbit reticulocyte 10S RNA. Nat New Biol 235, 163-167

Vogler M, Vogel S, Krull S, Farhat K, Leisering P, Lutz S, Wuertz CM, Katschinski DM, Zieseniss A (2013): Hypoxia Modulates Fibroblastic Architecture, Adhesion and Migration: A Role for HIF-1 alpha in Cofilin Regulation and Cytoplasmic Actin Distribution. PLoS One 8, e69128

Wandinger-Ness A, Zerial M (2014): Rab proteins and the compartmentalization of the endosomal system. Cold Spring Harb Perspect Biol 6, a022616

Wang GL, Jiang BH, Rue EA, Semenza GL (1995): Hypoxia-inducible factor 1 is a basic-helix-loop-helix-PAS heterodimer regulated by cellular O2 tension. Proc Natl Acad Sci U S A 92, 5510-5514

Wang Y, Ohh M (2010): Oxygen-mediated endocytosis in cancer. J Cell Mol Med 14, 496-503

Wang Y, Roche O, Yan MS, Finak G, Evans AJ, Metcalf JL, Hast BE, Hanna SC, Wondergem B, Furge KA, et al. (2009): Regulation of endocytosis via the oxygen-sensing pathway. Nat Med 15, 319-324

Wang Y, Roche O, Xu C, Moriyama EH, Heir P, Chung J, Roos FC, Chen Y, Finak G, Milosevic M, et al. (2012): Hypoxia promotes ligand-independent EGF receptor signaling via hypoxia-inducible factor-mediated upregulation of caveolin-1. Proc Natl Acad Sci USA 109, 4892-4897

Wilner SE, Wengerter B, Maier K, de Lourdes Borba Magalhaes M, Del Amo DS, Pai S, Opazo F, Rizzoli SO, Yan A, Levy M (2012): An RNA alternative to human transferrin: a new tool for targeting human cells. Mol Ther Nucleic Acids 1, 21

Wottawa M, Naas S, Bottger J, van Belle GJ, Mobius W, Revelo NH, Heidenreich D, von Ahlen M, Zieseniss A, Krohnert K, et al. (2017): Hypoxia-stimulated membrane trafficking requires T-plastin. Acta Physiol (Oxf) 221, 59-73

Yamada E (1955): The fine structure of the gall bladder epithelium of the mouse. J Biophys Biochem Cytol 1, 445-458

Yamashiro DJ, Tycko B, Fluss SR, Maxfield FR (1984): Segregation of transferrin to a mildly acidic (pH 6.5) para-Golgi compartment in the recycling pathway. Cell 37, 789-800

Yoon SO, Shin S, Mercurio AM (2005): Hypoxia stimulates carcinoma invasion by stabilizing microtubules and promoting the Rab11 trafficking of the alpha6beta4 integrin. Cancer Res 65, 2761-2769

Yu F, White SB, Zhao Q, Lee FS (2001): HIF-1alpha binding to VHL is regulated by stimulus-sensitive proline hydroxylation. Proc Natl Acad Sci USA 98, 9630-9635

Yu W, Wang Z, Li Y, Liu L, Liu J, Ding F, Zhang X, Cheng Z, Chen P, Dou J (2016): Endocytosis mediated by Caveolin-1 inhibits activity of matrix metalloproteinase-2 in human renal proximal tubular cells under hypoxia. Int J Clin Exp Path 9(2), 1276-1284

Zhang AS (2010): Control of systemic iron homeostasis by the hemojuvelin-hepcidin axis. Adv Nutr 1, 38-45

Zhou D, Mooseker MS, Galan JE (1999): An invasion-associated Salmonella protein modulates the actin-bundling activity of plastin. Proc Natl Acad Sci USA 96, 10176-10181

Zieseniss A (2014): Hypoxia and the modulation of the actin cytoskeleton - emerging interrelations. Hypoxia (Auckl) 2, 11-21

Danksagung

Mein besonderer Dank gilt Frau Prof. Dr. Dörthe Katschinski, die es mir ermöglicht hat, an diesem interessanten Forschungsprojekt zu arbeiten und damit einen umfangreichen Einblick in wissenschaftliches Arbeiten zu erhalten. Vielen Dank für die exzellente Betreuung, die konstante Unterstützung in der Fertigstellung dieser Doktorarbeit und das Interesse sowie die Förderung hinsichtlich meiner beruflichen Zukunft.

Außerdem bedanke ich mich bei meiner Betreuerin Frau Dr. rer. nat. Marieke Wottawa, die mich mit dauerhafter Hilfsbereitschaft und großer Kompetenz im Labor ausgebildet hat und einen entscheidenden Beitrag zu dieser Arbeit geleistet hat.

Ich möchte mich ganz herzlich bei Herrn Prof. Silvio O. Rizzoli für die Bereitstellung der Mikroskope, weiterer Materialien sowie der Auswertungstools bedanken. Danke auch für unzählige Ideen und Ratschläge, die dieses Projekt bereichert haben. Außerdem gilt mein Dank Frau Katharina Kröhnert und Frau Dr. rer. nat. Natalia Revelo für ihre technische sowie methodische Unterstützung und Beratung.

Darüber hinaus möchte ich allen Mitarbeiterinnen und Mitarbeitern der Arbeitsgruppe von Frau Prof. Katschinski für die produktive Arbeitsatmosphäre, die Unterstützung und ihren Beitrag zu dieser Arbeit danken: Insbesondere Frau Dr. rer. nat. Anke Zieseniß und Herrn Dr. Gijsbert van Belle für Korrekturen und Anregungen in der Fertigstellung der Arbeit; Frau Melanie von Ahlen und Frau Doris Heidenreich für die Hilfe im Labor.

Furthermore, I would like to express my gratitude to Prof. Ajay Shah. I appreciated the opportunity to visit your laboratory and the time you took to discuss my work. Many thanks go to Dr. Ioannis Smyrnias and Dr. Celio X. Santos for their kind supervision during my stay in the Shah lab.

I would like to thank all organizers and members of the International Research Training Group 1816 for providing a stimulating environment and great possibilities to experience science and research beyond the own project.